Table of Contents

General methods and instrumentation

Commercial reagents were used without further purification. Solvents were freshly distilled from the appropriate drying agents or purified under nitrogen with the mBraun MBSPS-800 before use. The analytical TLCs were performed with silica gel 60 F254 plates. Column chromatography was performed by using silica gel 60 (200-300 mesh ASTM). The NMR spectra were recorded on a Bruker Avance II spectrometer, operating at 500 MHz for ^{1}H and 125 MHz for ^{13}C or a Bruker Avance II spectrometer operating at 600 MHz for ^{1}H and 150 MHz for ^{13}C. TMS was used as an internal reference for ^{1}H and ^{13}C chemical shifts and $CDCl_3$ was used as solvent. Standard pulse programs from the Bruker library were used for 2D experiments. Mass spectrometry measurements were conducted by using the electrospray ionization technique on a Bruker Daltonics microTOF-Q or Finnigan LCQ Advantage MAX mass spectrometer. MALDI mass spectrometry was performed using Bruker ultrafleXtreme spectrometer with trans-2-[3-(4-tert-Butylphenyl)-2-methyl-2-propenylidene]malononitrile (DCTB) matrix and potassium trifluoroacetate. Absorption UV/Vis/NIR spectra were recorded by using a Varian Cary 50 Bio and Jasco V-770 spectrophotometers. The applied dichloromethane was freshly distilled over calcium hydride. Electrochemical measurements were performed by means of Autolab (Metrohm) potentiostat/galvanostat system for dichloromethane solutions with a glassy carbon, a platinum wire, and Ag/AgCl as the working, auxiliary, and reference electrodes, respectively. Tetrabutylammonium hexafluorophosphate was used as a supporting electrolyte. The potentials were referenced with the ferrocene/ferrocenium couple used as an internal standard. Crystals were obtained by slow diffusion of the dichloromethane solution into hexane. Crystal data for was collected at low temperature using Oxford Cryosystem device on Xcalibur Onyx four-circle diffractometer with graphite-monochromated Cu Kα radiation (λ = 1.54184 Å). Data reduction and analysis were carried out with the CrysAlisPRO programs[1]. The structures were solved by using the SHELXT[2] and refined by the full-matrix least-squares method on all F^2 data using the SHELXL.[3] All hydrogen atoms, including those located in the difference density map, were placed in calculated positions and refined as the riding model. The symmetry-independent unit of **2e** contains a half of a molecule which is disordered by the inversion center. See Tables S1and S2 for detailed data. The full structures and diffraction data are available in Cambridge Crystallographic Data Center under the CCDC numbers 1957894 and 1977696.

Table S1 Crystal data for **2e**

Crystal data	
Chemical formula	$C_{54}H_{47}N_5O_8 \cdot C_6H_{14}$
M_r	980.13
Crystal system, space group	Triclinic, *P*-1
Temperature (K)	100
***a*, *b*, *c* (Å)**	8.915 (1), 9.991(1), 14.328(2)
α, β, γ (°)	98.93(1), 91.79(1), 92.21(1)
***V* (Å^3)**	1259.0(3)
Z	1
Radiation type	Cu *K*α
μ (mm^{-1})	0.69
Crystal size (mm)	0.49 × 0.17 × 0.09
Data collection	
Diffractometer	Xcalibur, Onyx
Absorption correction	–
No. of measured, independent and observed [*I* > 2σ(*I*)] reflections	6859, 3952, 2398
R_{int}	0.095
(sin θ/λ)$_{max}$ (Å^{-1})	0.575
Refinement	
R*[*F*^{2} > 2σ(*F*^{2})], *wR*(*F*^{2}), *S	0.099, 0.293, 1.00
No. of reflections	3952
No. of parameters	347
Δρ$_{max}$, Δρ$_{min}$ (e Å^{-3})	0.39, −0.42

Table S2 Crystal data for **5a**

Crystal data	
Chemical formula	$C_{48.50}H_{33}AgAuCl_4N_5$
M_r	1132.43
Crystal system, space group	Triclinic, *P*-1
Temperature (K)	100
***a*, *b*, *c* (Å)**	9.9193 (5), 13.7034 (8), 15.7321 (8)
α, β, γ (°)	75.013 (5), 84.724 (4), 78.550 (4)
***V* (Å^3)**	2022.72 (19)
Z	2
Radiation type	Cu Kα
μ (mm^{-1})	13.38
Crystal size (mm)	0.34 × 0.03 × 0.03
Data collection	
Diffractometer	Xcalibur, Ruby, Gemini ultra
Absorption correction	Analytical
Tmin, Tmax	0.212, 0.736
No. of measured, independent and observed [I > 2σ(I)] reflections	13937, 6395, 5470
Rint	0.069
(sin θ/λ)$_{max}$ (Å^{-1})	0.575
Refinement	
R[F2 > 2σ(F2)], wR(F2), S	0.045, 0.118, 1.02
No. of reflections	6395
No. of parameters	552
H-atom treatment	H-atom parameters constrained
Δρ$_{max}$, Δρ$_{min}$ (e Å^{-3})	1.74, −1.47

Synthesis and characterization

Synthesis of the precursor. Starting porphyrins **1a** -**1h** were obtained as described previously.[4]

Scheme S1. Synthesis of imidazole fused-21-carbachlorin derivatives **2a-h**

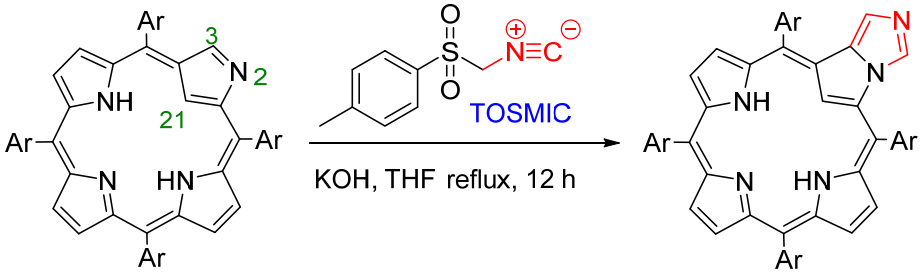

1a-h **2a-h**

2a: Ar = Ph, yield 69%; **2b**: Ar = 4-$CH_3C_6H_4$, yield 74%;
2c: Ar = 3,5-$(CH_3)_2C_6H_3$, yield 65%; **2d**: Ar = 4-$CH_3OC_6H_4$, yield 70%;
2e: Ar = 3,5-$(CH_3O)_2C_6H_3$, yield 71%; **2f**: Ar = 3,4,5-$(CH_3O)_3C_6H_2$, yield 76%;
2g: Ar = 4-FC_6H_4, yield 68%; **2h**: Ar = 4-$CO_2CH_3C_6H_4$, yield 69%;

General procedure for synthesis of Imidazole fused-21-carbachlorin:

A solution of 2-aza-21-carbaporphyrin **1** (0.1 mmol), toluenesulphonylmethyl isocyanide (0.3 mmol) and KOH (1 mmol) in THF (20 ml) was stirred at reflux temperature for 12 hr. The solvent was then evaporated under vacuum. The residue was chromatographed on a silica gel column with dichloromethane/ethyl acetate (*V*/*V* = 100:3) as eluent. The first red fraction was collected, followed by removal of solvent to afford imidazole fused-21-carbachlorin derivative **2.**

Selected data for 2a-h

2a: yield 69%. ^{1}H NMR (500MHz, $CDCl_3$, 298K) δ = –5.58 (s, 1H, -HC=), –2.48 (br, 2H, -NH), 6.24 (s, 1H, -HC=), 6.84 (s, 1H, -HC=), 7.69-7.73 (m, 6H, ArH), 7.75-7.78 (m, 3H, ArH), 7.79-7.84 (m, 3H, ArH), 8.08-8.10 (m, 2H, ArH), 8.11-8.13 (m, 6H, ArH), 8.52-8.53 (m, 5H, pyrrH), 8.56 (d, *J* = 5.0 Hz, 1H, pyrrH); ^{13}C NMR (125MHz, $CDCl_3$, 298 K) δ_C = 104.2, 104.3, 110.9, 118.2, 120.3, 120.5, 121.4, 125.3, 125.7, 126.1, 126.5, 126.9, 127.8, 127.9, 128.56, 128.66, 128.74, 129.4, 129.8, 131.0, 132.8, 132.9, 133.2, 133.63, 133.65, 134.3, 137.1, 137.3, 137.4, 138.6, 139.0, 139.2, 140.9, 141.8, 141.9, 154.7, 154.8. UV-vis (CH_2Cl_2) λ_{max}/nm (logε): 451 (5.22), 533 (4.38), 645 (3.67). ESI-HRMS calc. for $[C_{46}H_{32}N_5]^+$ $(M+H)^+$: 654.2652, Found: 654.2650.

2b: yield 74%. ^{1}H NMR (500MHz, $CDCl_3$, 298K) δ = –5.55 (s, 1H, -HC=), –2.35 (br, 2H, -NH), 2.67 (s, 12H, H_3C-), 6.28 (s, 1H, -HC=), 6.89 (s, 1H, -HC=), 7.52 (d, *J* = 8.0 Hz, 4H, ArH), 7.58 (d, *J* = 7.5 Hz, 2H, ArH), 7.64 (d, *J* = 7.5 Hz, 2H, ArH), 7.98-8.01 (m, 8H, ArH), 8.54-8.55 (m, 5H, pyrrH), 8.59 (d, *J* = 5.0 Hz, 1H, pyrrH); ^{13}C NMR (125MHz, $CDCl_3$, 298 K) δ_C = 21.53, 21.58, 21.6, 104.2, 110.9, 118.1, 120.2, 120.3, 121.2, 125.2, 125.6, 126.29, 126.34, 127.6, 128.8, 129.3, 130.5, 130.9, 132.7, 132.9, 133.1, 133.49, 133.52, 134.3, 136.2, 137.2, 137.4, 137.5, 138.2, 138.3, 138.7, 138.9, 139.0, 139.2, 139.3, 154.7, 154.8. UV-vis (CH_2Cl_2) λ_{max}/nm (logε): 452 (5.25), 540 (4.39), 642 (3.62). ESI-HRMS calc. for $[C_{50}H_{40}N_5]^+$ $(M+H)^+$: 710.3278, Found: 710.3277.

2c: yield 65%. ^{1}H NMR (500MHz, $CDCl_3$, 298K) δ = –5.60 (s, 1H, -HC=), –2.37 (br, 2H, -NH), 2.58 (s, 24H, H_3C-), 6.33 (s, 1H, -HC=), 6.92 (s, 1H, -HC=), 7.37 (s, 2H, ArH), 7.40 (s, 1H, ArH), 7.44 (s, 1H, ArH), 7.73 (s, 4H, ArH), 7.76 (s, 4H, ArH), 8.57-8.59 (m, 5H, pyrrH), 8.65 (d, *J* = 5.0 Hz, 1H, pyrrH); ^{13}C NMR (125MHz, $CDCl_3$, 298 K) δ_C = 21.5, 21.6, 104.2, 111.2, 118.4, 120.4, 120.6, 125.3, 125.7, 126.3, 129.4, 130.0, 130.5, 130.9, 131.0, 132.6, 132.7, 133.5, 133.6, 136.1, 137.2, 137.4, 138.0, 139.0, 139.2, 139.4,

141.0, 141.77, 141.81, 154.6, 154.8. UV-vis (CH_2Cl_2) λ_{max}/nm (logε): 451 (5.21), 535 (4.40), 641 (3.75). ESI-HRMS calc. for $[C_{54}H_{48}N_5]^+$ $(M+H)^+$: 766.3904, Found: 766.3903.

2d: yield 70%. ^{1}H NMR (500MHz, $CDCl_3$, 298K) δ = –5.58 (s, 1H, -HC=), –2.23 (br, 2H, -NH), 4.06 (s, 12H, $-CH_3O$), 6.34 (s, 1H, -HC=), 6.95 (s, 1H, -HC=), 7.26 (d, *J* = 8.0 Hz, 4H, ArH), 7.29 (d, *J* = 8.5 Hz, 2H, ArH), 7.35 (d, *J* = 8.5 Hz, 2H, ArH), 7.99-8.03 (m, 8H, ArH), 8.50-8.52 (m, 6H, pyrrH); ^{13}C NMR (125MHz, $CDCl_3$, 298 K) δ_C = 55.58, 55.62, 104.2, 110.5, 112.4, 113.1, 114.0, 115.2, 117.8, 119.79, 119.82, 120.9, 125.1, 125.4, 126.2, 126.3, 128.9, 130.7, 131.5, 133.0, 133.4, 133.5, 133.7, 134.1, 134.3, 134.4, 134.5, 135.5, 137.4, 137.5, 137.6, 138.8, 139.2, 154.95, 154.97, 159.5, 160.0, 160.5. UV-vis (CH_2Cl_2) λ_{max}/nm (logε): 454 (5.22), 539 (4.37), 644 (3.73). ESI-HRMS calc. for $[C_{50}H_{40}N_5O_4]^+$ $(M+H)^+$: 774.3075, Found: 774.3074.

2e: yield 71%. ^{1}H NMR (500MHz, $CDCl_3$, 298K) δ = –5.62 (s, 1H, -HC=), –2.41 (br, 2H, -NH), 3.95 (s, 18H, H_3CO-), 3.96 (s, 6H, H_3CO-), 6.53 (s, 1H, -HC=), 6.87 (t, *J* = 2.5 Hz , 2H, ArH), 6.89 (t, *J* = 2.5 Hz , 1H, ArH), 6.91 (t, *J* = 2.5 Hz , 1H, ArH), 7.12 (s, 1H, ArH), 7.24 (d, *J* = 2.0 Hz, 2H, ArH), 7.25 (d, *J* = 2.0 Hz, 2H, ArH), 7.34 (d, *J* = 2.0 Hz, 4H, ArH), 8.66-8.70 (m, 5H, pyrrH), 8.73 (d, *J* = 5.0 Hz, 1H, pyrrH); ^{13}C NMR (125MHz, $CDCl_3$, 298 K) δ_C = 55.6, 55.7, 55.8, 100.1, 100.8, 101.4, 110.76, 110.79, 111.5, 113.5, 117.9, 119.9, 120.1, 121.7, 125.5, 125.9, 126.40, 126.42, 128.5, 131.4, 132.6, 133.7, 136.9, 134.3, 137.2, 137.3, 138.5, 138.8, 140.7, 142.8, 143.68, 143.72, 154.4, 154.6, 159.1, 160.8, 161.8. UV-vis (CH_2Cl_2) λ_{max}/nm (logε): 449 (5.31), 535 (4.50), 638 (3.85). ESI-HRMS calc. for $[C_{54}H_{48}N_5O_8]^+$ $(M+H)^+$: 894.3497, Found: 894.3497.

2f: yield 76%. ^{1}H NMR (500MHz, $CDCl_3$, 298K) δ = –5.58 (s, 1H, -HC=), –1.95 (br, 2H, -NH), 3.98 (s, 18H, $-CH_3O$), 3.99 (s, 6H, $-CH_3O$), 4.17 (s, 12H, $-CH_3O$), 6.55 (s, 1H, -HC=), 7.12 (s, 1H, -HC=), 7.33 (s, 2H, ArH), 7.36 (s, 2H, ArH), 7.41 (s, 2H, ArH), 7.42 (s, 2H, ArH), 8.69-8.70 (m, 3H, pyrrH), 8.73 (d, *J* = 5.0 Hz, 2H, pyrrH), 8.76 (d, *J* = 5.0 Hz, 1H, pyrrH); ^{13}C NMR (125MHz, $CDCl_3$, 298 K) δ_C = 56.4, 56.55, 56.58, 61.3, 61.5, 61.6, 104.2, 109.8, 110.7, 110.9, 112.4, 118.1, 120.2, 120.4, 121.6, 125.5, 125.6, 126.1, 126.5, 128.8, 131.2, 132.9, 133.7, 134.4, 135.8, 136.5, 137.2, 137.3, 137.4, 137.5, 138.0, 138.7, 138.8, 138.9, 139.3, 151.7, 153.3, 154.4, 154.7, 154.8. UV-vis (CH_2Cl_2) λ_{max}/nm (logε): 452 (5.16), 534 (4.35), 642 (3.71). ESI-HRMS calc. for $[C_{58}H_{56}N_5O_{12}]^+$ $(M+H)^+$: 1014.3920, Found: 1014.3919.

2g: yield 68%. ^{1}H NMR (500MHz, $CDCl_3$, 298K) δ = –5.61 (s, 1H, -HC=), –2.53 (br, 2H, -NH), 6.31 (s, 1H, -HC=), 6.92 (s, 1H, -HC=), 7.43 (t, *J* = 8.5 Hz , 4H, ArH), 7.49 (t, *J* = 8.5 Hz , 2H, ArH), 7.56 (t, *J* = 8.5 Hz , 2H, ArH), 8.06-8.11 (m, 8H, ArH), 8.49-8.52 (m, 6H, pyrrH); ^{13}C NMR (125MHz, $CDCl_3$, 298 K) δ_C = 104.2, 109.8, 113.9 (d, ^2J = 21 Hz), 115.8 (d, ^2J = 21 Hz), 116.9 (d, ^2J = 21 Hz), 117.0, 119.2, 119.4, 121.4, 125.2, 125.6, 126.4, 126.5, 128.9, 130.8, 132.9, 133.61, 133.63, 134.58, 134.65, 134.78, 134.8, 134.90, 134.93, 135.5, 135.6, 136.83, 136.86, 137.2, 137.4, 137.54, 137.57, 137.6, 138.7, 139.1, 154.8, 154.9, 162.9 (d, ^1J = 250 Hz), 163.3 (d, ^1J = 250 Hz), 163.7 (d, ^1J = 250 Hz). UV-vis (CH_2Cl_2) λ_{max}/nm (logε): 450 (5.28), 535 (4.46), 644 (3.79). ESI-HRMS calc. for $[C_{46}H_{28}F_4N_5]^+$ $(M+H)^+$: 726.2275, Found: 726.2273.

2h: yield 69%. ^{1}H NMR (500MHz, $CDCl_3$, 298K) δ = –5.84 (s, 1H, -HC=), –1.96 (br, 2H, -NH), 4.11 (s, 6H, $-H_3C$-), 4.12 (s, 3H, $-H_3C$-), 4.13 (s, 3H, $-H_3C$-), 6.16 (s, 1H, -HC=), 6.78 (s, 1H, -HC=), 8.04 (d, *J* = 8.0 Hz, 2H, ArH), 8.10-8.15 (m, 6H, ArH), 8.28 (d, *J* = 4.5 Hz, 1H, pyrrH), 8.33 (d, *J* = 4.5 Hz, 1H, pyrrH), 8.35 (d, *J* = 4.5 Hz, 1H, pyrrH), 8.40-8.44 (m, 9H), 8.49 (d, *J* = 8.0 Hz, 2H, ArH); ^{13}C NMR (125MHz, $CDCl_3$, 298 K) δ_C = 52.5, 52.6, 104.2, 104.3, 110.0, 117.1, 119.6, 119.7, 121.5, 125.3, 125.5, 126.3, 126.5, 128.3, 129.87, 129.88, 129.9, 130.3, 130.9, 131.0, 131.1, 132.2, 133.0, 133.2, 133.7, 134.3, 136.6, 136.8, 137.0, 138.1, 138.7, 142.9, 144.8, 146.1. UV-vis (CH_2Cl_2) λ_{max}/nm (logε): 454 (5.29), 537 (4.47), 644 (3.80). ESI-HRMS calc. for $[C_{54}H_{40}N_5O_8]^+$ $(M+H)^+$: 886.2871, Found: 886.2869.

Scheme S2. Synthesis of Ag^{III} complexes of imidazole fused-21-carbachlorin derivatives **3**

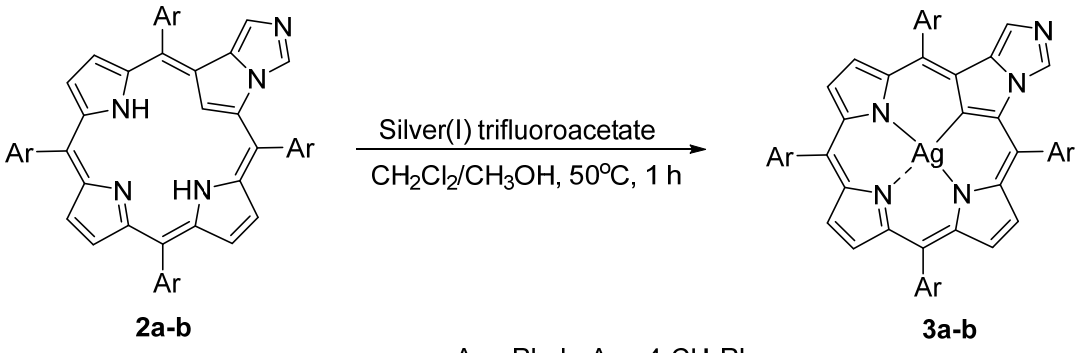

2a-b **3a-b**

a: Ar = Ph; b: Ar = 4-CH_3Ph

General procedure for synthesis of Ag^{III} complex of imidazole fused-21-carbachlorin 3:

A 20 mg (0.028 mmol) sample of imidazole fused-21-carbachlorin **2** was dissolved in 12 mL of CH_2Cl_2, and 24 mg (0.11 mmol, 4 equiv) of silver(I) trifluoroacetate dissolved in 0.5 mL of MeOH was added. The reaction mixture was protected from light and stirred for 1 h at 50°C. The solvent was removed under vacuum and the crude compound was loaded on a silica column and eluted with CH_2Cl_2. The first fraction was collected, followed by removal of solvent to afford silver(III) complex of imidazole fused-21-carbachlorin derivative **3.**

Selected data for 3a-b

3a: yield 85%. ^{1}H NMR (500MHz, $CDCl_3$, 298K) δ = 6.36 (s, 1H, -HC=), 6.89 (s, 1H, -HC=), 7.70-7.79 (m, 9H, ArH), 7.83-7.85 (m, 3H, ArH), 7.97-8.01 (m, 4H, ArH), 8.11-8.12 (m, 4H, ArH), 8.62-8.64 (m, 3H, pyrrH), 8.67-8.70 (m, 2H, pyrrH), 8.75-8.76 (m, 1H, pyrrH); ^{13}C NMR (125MHz, $CDCl_3$, 298 K) δ_C = 114.37, 118.21, 121.13, 121.15, 121.60, 122.11, 122.45, 124.72, 126.27, 126.30, 126.73, 126.75, 127.09, 128.05, 128.07, 128.51, 128.62, 128.79, 128.93, 128.95, 129.31, 129.39, 129.73, 130.04, 130.06, 131.31, 131.59, 132.11, 133.73, 133.77, 136.88, 137.06, 137.59, 137.61, 137.89, 137.98, 138.94, 138.99, 139.02, 139.15, 141.13, 141.61. UV-vis (CH_2Cl_2) λ_{max}/nm (logε): 389 (4.42), 449 (5.30), 523 (4.29), 555 (4.06), 575 (4.09), 629 (3.85). ESI-HRMS calc. for $[C_{46}H_{29}AgN_5]^+$ $(M+H)^+$: 758.1468, Found: 758.1473.

3b: yield 81%. ^{1}H NMR (500MHz, $CDCl_3$, 298K) δ = 2.68 (s, 12H, -CH_3), 6.40 (s, 1H, -HC=), 6.94 (s, 1H, -HC=), 7.53 (d, *J* = 7.5 Hz, 4H, ArH), 7.58 (d, *J* = 8.0 Hz, 2H, ArH), 7.64 (d, *J* = 8.0 Hz, 2H, ArH), 7.84-7.88 (m, 4H, ArH), 7.99 (d, *J* = 8.0 Hz, 4H, ArH), 8.63-8.66 (m, 3H, pyrrH), 8.69-8.72 (m, 2H, pyrrH), 8.76-8.78 (m, 1H, pyrrH); ^{13}C NMR (125MHz, $CDCl_3$, 298 K) δ_C = 21.56, 21.63, 21.67, 114.35, 118.20, 121.15, 121.55, 122.06, 124.76, 126.13, 126.16, 126.59, 126.62, 127.77, 128.69, 128.80, 129.21, 129.29, 129.96, 130.42, 131.07, 131.41, 132.06, 133.63, 133.67, 136.14, 136.94, 137.15, 137.68, 137.71, 137.98, 138.07, 138.15. UV-vis (CH_2Cl_2) λ_{max}/nm (logε): 387 (4.31), 453 (5.17), 524 (4.21), 558 (3.94), 574 (3.94), 627 (3.71). ESI-HRMS calc. for $[C_{50}H_{37}AgN_5]^+$ $(M+H)^+$: 814.2094, Found: 814.2098.

Scheme 3. Synthesis of 3'-methyl- imidazole fused-21-carbachlorin silver(III) Derivatives **4**

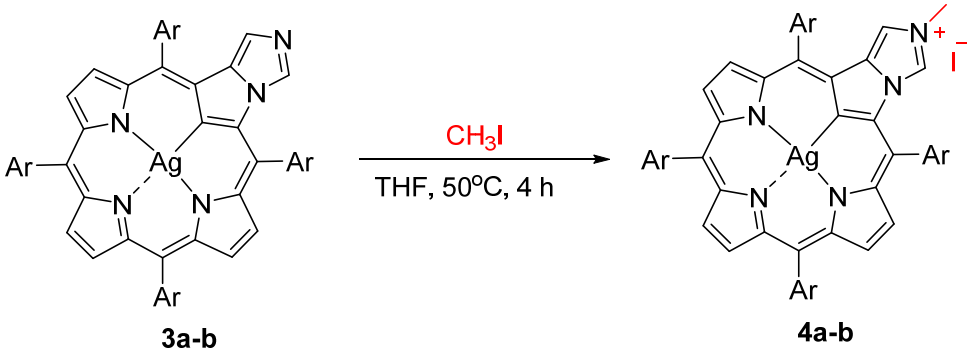

3a-b **4a-b**

3a: Ar = Ph; **3b**: Ar = 4-CH_3Ph

General procedure for synthesis of *N*-methylated Ag-imidazole fused-21-carbachlorin 4:

A 20 mg (0.028 mmol) sample of Ag^{III} complex of imidazole fused-21-carbachlorin **3** was dissolved in 3 mL of THF, and 100 µL of CH_3I was added. The reaction mixture was stirred for 4 h at 50°C. The solvent was removed under vacuum and the crude compound was loaded on a silica column and eluted with CH_2Cl_2/CH_3OH(*V*:*V* = 95:5). The last fraction was collected, followed by removal of solvent to afford 3'-methylated Ag-imidazole fused-21-carbachlorin derivative **4.**

Selected data for [4a-b]I.

[4a]I: yield 68%. ^{1}H NMR (500MHz, $CDCl_3$, 298K) δ = 4.18 (s, 3H, -CH_3), 6.37 (s, 1H, -HC=), 7.57 (s, 1H, -HC=), 7.76-7.82 (m, 6H, ArH), 7.88-7.89 (m, 3H, ArH), 7.99-8.05 (m, 5H, ArH), 8.08-8.10 (m, 2H, ArH), 8.13-8.15 (m, 4H, ArH), 8.76-8.77 (m, 3H, pyrrH), 8.80 (d, *J* = 5.0 Hz, 1H, pyrrH), 8.82 (d, *J* = 5.0 Hz, 1H, pyrrH), 8.87 (d, *J* = 4.5 Hz, 1H, pyrrH); ^{13}C NMR (125MHz, $CDCl_3$, 298 K) δ_C = 39.53, 113.33, 114.35, 116.44, 121.54, 122.77, 122.99, 123.39, 127.28, 127.85, 127.99, 128.49, 128.99, 129.53, 129.71, 130.34, 130.57, 130.62, 130.78, 131.22, 131.51, 133.82, 136.76, 137.25, 137.93, 138.59, 138.69, 138.77, 138.85, 139.62, 139.68; UV-vis (CH_2Cl_2) λ_{max}/nm (logε): 438 (5.54), 518 (4.38), 558 (4.30). ESI-HRMS calc. for $[C_{47}H_{31}AgN_5]^+$ $(M\text{-}I)^+$: 772.1625, Found: 772.1627.

[4b]I: yield 65%. ^{1}H NMR (500MHz, $CDCl_3$, 298K) δ = 2.70 (s, 6H, -CH_3), 2.70 (s, 3H, -CH_3), 2.77 (s, 3H, -CH_3), 4.24 (s, 3H, -CH_3), 6.47 (s, 1H, -HC=), 7.57 (d, *J* = 7.5 Hz, 4H, ArH), 7.63 (s, 1H, -HC=), 7.67 (d, *J* = 7.5 Hz, 2H, ArH), 7.80 (d, *J* = 7.5 Hz, 2H, ArH), 7.89 (d, *J* = 7.5 Hz, 2H, ArH), 7.93 (d, *J* = 7.5 Hz, 2H, ArH), 8.01 (d, *J* = 7.5 Hz, 4H, ArH), 8.74-8.87 (m, 6H, pyrrH); ^{13}C NMR (125MHz, $CDCl_3$, 298 K) δ_C = 21.57, 21.81, 22.03, 39.88, 113.33, 114.30, 116.49, 121.60, 122.79, 123.03, 123.50, 127.82, 127.98, 129.60, 130.24, 130.69, 130.95, 131.27, 131.38, 133.75, 136.70, 137.44, 137.94, 137.97, 138.04, 138.23, 138.25, 138.71, 138.85, 139.44, 139.72, 140.77. UV-vis (CH_2Cl_2) λ_{max}/nm (logε): 442 (5.52), 518 (4.42), 558 (4.31). ESI-HRMS calc. for $[C_{51}H_{39}AgN_5]^+$ $(M\text{-}I)^+$: 828.2251, Found: 828.2251.

Iodide counteranion was exchanged into BF_4^- by addition of 10 mg of silver(I) tetrafluoroborate in 1 mL of ethanol into the solution of **[4a]**I (15 mg) in dichloromethane (5 mL) and stirring for 10 min at room temperature. The solvent was then removed by evaporation, and the compound was extracted with CH_2Cl_2, solution was filtered, and passed down a short silica gel column with dichloromethane/ethanol solution (99/1). Substitution of I^- with chloride was accomplished by stirring of a sample of **[4a]**I (10 mg) in chloroform with brine for 1 h. The organic layer was then separated and washed with three portion of water, evaporated and passed down a short silica gel column.

Iodide counteranion was exchanged into Cl^- by stirring a sample of **[4a]**I or **[4b]**I (10 mg) in dichloromethane (5 mL) with brine (2 mL) for 20 h at room temperature. The organic layer was then

separated and washed with four portion of water, dried in vacuo and crystallized from chloroform/hexane.

[4a]BF_4: yield 85%. ^{1}H NMR (500MHz, $CDCl_3$, 300K) δ = 4.03 (m, 3H, 3'-CH_3), 6.31, (dq, J_d= 1.2 Hz, J_q = 0.4 Hz, 1H, 4'), 7.51 (dq, J_d= 1.2 Hz, J_q = 0.6 Hz, 1H, 2'), 7.77 (m, 6H, meta+para Ph), 7.87 (m, 3H, meta Ph), 8.00 (m, 5H, meta+ortho Ph), 8.01 (m, 2, ortho Ph), 8.12 (m, 4H, ortho Ph), 8.74 (dd, $^3J_{HH}$ = 4.8 Hz, $^4J_{AgH}$ = 0.4 Hz, 1H, pyrrH), 8.75 (dd, $^3J_{HH}$ = 4.9 Hz, $^4J_{AgH}$ = 0.3 Hz, 1H, pyrrH), 8.75 (dd, $^3J_{HH}$ = 4.8 Hz, $^4J_{AgH}$ = 0.3 Hz, 1H, pyrrH), 8.79 (dd, $^3J_{HH}$ = 4.9 Hz, $^4J_{AgH}$ = 1.1 Hz, 1H, pyrrH), 8.81 (dd, $^3J_{HH}$ = 4.9 Hz, $^4J_{AgH}$ = 1.2 Hz, 1H, pyrrH), 8.86 (dd, $^3J_{HH}$ = 4.9 Hz, $^4J_{AgH}$ = 1.6 Hz, 1H, pyrrH).

[4a]Cl: yield 90%. ^{1}H NMR (500MHz, $CDCl_3$, 300K) δ = 4.25 (s, 3H, 3'-CH_3), 6.36, (d, ^4J = 0.9 Hz, 1H, 4'), 7.77 (m, 6H, meta+para Ph), 7.87 (m, 3H, meta Ph), 7.92 (b, 1H, 2'), 7.99 (m, 5H, meta+ortho Ph), 8.02 (m, 2H, ortho Ph), 8.11 (m, 4H, ortho Ph), 8.72 (dd, $^3J_{HH}$ = 5.0 Hz, $^4J_{AgH}$ = 1.4 Hz, 1H, pyrrH), 8.73 (d, $^3J_{HH}$ = 4.6 Hz, 1H, pyrrH), 8.75 (d, $^3J_{HH}$ = 4.6 Hz, 1H, pyrrH), 8.78 (dd, $^3J_{HH}$ = 5.0 Hz, $^4J_{AgH}$ = 1.0 Hz, 1H, pyrrH), 8.81 (dd, $^3J_{HH}$ = 4.8 Hz, $^4J_{AgH}$ = 1.1 Hz, 1H, pyrrH), 8.85 (dd, $^3J_{HH}$ = 4.8 Hz, $^4J_{AgH}$ = 1.5 Hz, 1H, pyrrH).

[4b]Cl: yield 93%. ^{1}H NMR (500MHz, $CDCl_3$, 300K) δ = 2.69 (s, 6H, Tol(CH_3)x2), 2.77 (s, 3H, Tol(CH_3)), 2.73 (s, 3H, Tol(CH_3)), 4.30 (s, 3H, 3'-CH_3), 6.46 (d, ^4J = 1.1 Hz, 1H, 4'), 7.55 (m, 4H, meta Tol), 7.65 (m, 2H, meta Tol), 7.77 (m, 2H, meta Tol), 7.83 (m, 1H, 2'), 7.87 (m, 2H, ortho Tol), 7.89 (m, 2H, ortho Tol), 7.99 (m, 4H, ortho Tol), 8.72 (dd, $^3J_{HH}$ = 5.0 Hz, $^4J_{AgH}$ = 1.5 Hz, 1H, pyrrH), 8.74 (d, $^3J_{HH}$ = 4.9 Hz, 1H, pyrrH), 8.76 (d, $^3J_{HH}$ = 4.9 Hz, 1H, pyrrH), 8.79 (dd, $^3J_{HH}$ = 5.0 Hz, $^4J_{AgH}$ = 1.0 Hz, 1H, pyrrH), 8.81 (dd, $^3J_{HH}$ = 5.0 Hz, $^4J_{AgH}$ = 1.1 Hz, 1H, pyrrH), 8.85 (dd, $^3J_{HH}$ = 5.0 Hz, $^4J_{AgH}$ = 1.4 Hz, 1H, pyrrH),

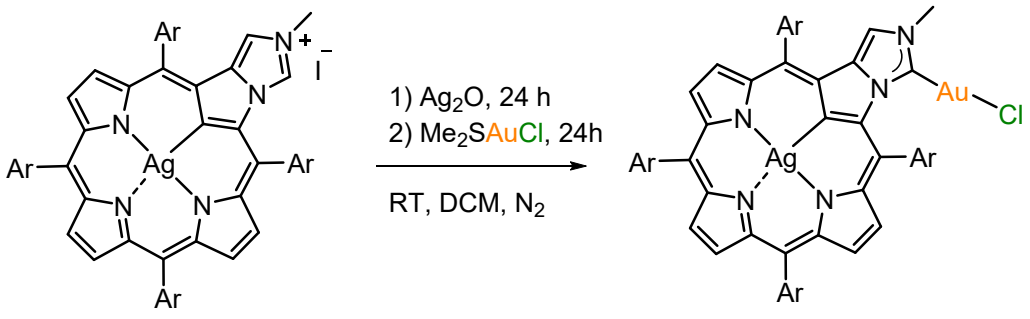

4a-b **5a-b**

Ar = **5a:** Ph, **5b:** *p*-Tol

General procedure for synthesis of chlorogold(I) carbene complex of methylated Ag-imidazole fused-21-carbachlorin 5:

A sample of [**4a**]I or [**4b**]I (20 mg, 0.025 mmol) was dissolved in10 mL of dichloromethane, and Ag_2O (0.05 mmol, 12 mg) was added. The slurry was deaerated for 20 min by a stream of N_2. The reaction mixture was then stirred for 24 h at room temperature under inert atmosphere. After that time 0.05 mmol of $AuClSMe_2$ (15 mg) was added and the reaction mixture was stirred for further 24 h. The mixture was then filtered, the solvent was evaporated and the product was redissolved in a small amount of dichloromethane and charged on the silica gel column. The fastest moving brown fraction migrating with dichloromethane was collected. The product **5a** or **5b** was recrystallized with dichloromethane/hexane and dried on air.

Selected data for 5a-b.

5a: yield 72%. ^{1}H NMR (500MHz, $CDCl_3$, 300K) δ = 8.74 (dd, $^3J_{HH}$ = 4.9 Hz, $^4J_{AgH}$ = 1.5 Hz, 1H, pyrrH), 8.69 (dd, $^3J_{HH}$ = 4.9 Hz, $^4J_{AgH}$ = 1.1 Hz, 1H, pyrrH), 8.65 (d, $^3J_{HH}$ = 4.8 Hz, 1H, pyrrH), 8.6 (dd, $^3J_{HH}$ = 5.0 Hz, $^4J_{AgH}$ = 1.2 Hz, 1H, pyrrH), 8.63(d, $^3J_{HH}$ = 4.8 Hz, 1H, pyrrH), 8.61 (dd, $^3J_{HH}$ = 4.9 Hz, $^4J_{AgH}$ = 1.5 Hz, 1H, pyrrH), 8.13 (dd, $^3J_{HH}$ = 7.6 Hz, $^4J_{HH}$ = 1.5 Hz, 2H, ortho ArH), 8.10 (m, 4H, ortho ArH), 8.00 (m, 2H, ortho ArH), 7.83 (m, 6H, meta+para ArH), 7.73 (m, 6H, meta+para ArH), 6.00 (s, 1H, 4'-H), 3.92 (s, 3H, 3'-CH_3). ^{13}C NMR (125MHz, $CDCl_3$, 298 K) δ_C = 170.1, 142.0, 141.3, 141., 140.9, 139.6, 139.5, 139.3, 138.9, 138.6, 137.7, 137.1, 133.9, 133.8, 133.7, 131.6, 130.2, 129.9, 129.6, 129.5, 129.3, 129.0, 128.9, 128.8, 128.3, 128.2, 127.2, 127.1, 126.2, 122., 121.7, 120.2, 117.4, 113.0, 40.2. UV-vis (CH_2Cl_2) λ_{max}/nm (logε): 266 (4.57), 303 sh, 363 (4.06), 384 (4.08), 427 sh, 452 (5.23), 491 sh, 530 (4.19), 572 (4.06), 620 (3.36). MALDI-TOF-HRMS calc. for $[C_{47}H_{30}AgAuClN_5]^+$ $(M)^+$: 1003.0906, Found: 1003.093; calc. for $[C_{47}H_{30}AgAuClKN_5]^+$ $(M+K)^+$: 1042.0538, Found: 1042.056.

5b: yield 60%. ^{1}H NMR (500MHz, $CDCl_3$, 300K) δ = 8.71 (dd, $^3J_{HH}$ = 4.9 Hz, $^4J_{AgH}$ = 1.4 Hz, 1H, pyrrH), 8.69 (dd, $^3J_{HH}$ = 4.9 Hz, $^4J_{AgH}$ = 1.1 Hz, 1H, pyrrH), 8.65 (d, $^3J_{HH}$ = 4.8 Hz, 1H, pyrrH), 8.64 (dd, $^3J_{HH}$ = 4.9 Hz, $^4J_{AgH}$ = 1.5 Hz, 1H, pyrrH), 8.637 (d, $^3J_{HH}$ = 4.8 Hz, 1H, pyrrH), 8.59 (dd, $^3J_{HH}$ = 4.9 Hz, $^4J_{AgH}$ = 1.4 Hz, 1H, pyrrH), 7.99 (m, 3H, ortho ArH), 7.98 (m, 3H, ortho ArH), 7.86 (m, 2H, ortho ArH), 7.63 (m, 2H, meta ArH), 7.61 (m, 2H, meta ArH), 7.53 (m, 4H, meta ArH), 6.07 (s, 1H, 4'-H), 3.95 (s, 3H, 3'-CH_3), 2.71 (s, 3H, *p*-CH_3), 2.70 (s, 3H, *p*-CH_3), 2.67 (s, 6H, *p*-CH_3). ^{13}C NMR (125MHz, $CDCl_3$, 298 K) δ_C = 169.8, 142.3, 140.0, 139.8, 139.6, 139.1, 138.6, 138.4. 138.4, 138.0, 137.9, 137.8, 137.3, 136.5, 133.9, 133.8, 133.3, 131.5, 130.4, 130.2, 129.8, 129.5, 129.1, 129.0, 128.8, 127.9, 127.0, 126.4, 122.7, 121.6, 120.2, 117.5, 115.6, 112.9, 40.3, 22.0, 21.7, 21.5. UV-vis (CH_2Cl_2) λ_{max}/nm (logε): 266 (4.56), 303 sh, 361 (4.07), 381

(4.11), 427 sh, 453 (5.23), 491 sh, 531 (4.22), 572 (4.06), 618 (3.31). MALDI-TOF-HRMS calc. for $[C_{51}H_{38}AgAuClN_5]^+$ $(M)^+$: 1059.1532, Found: 1059.190; calc. for $[C_{51}H_{38}AgAuClKN_5]^+$ $(M+K)^+$: 1098.1164, Found: 1098.157.

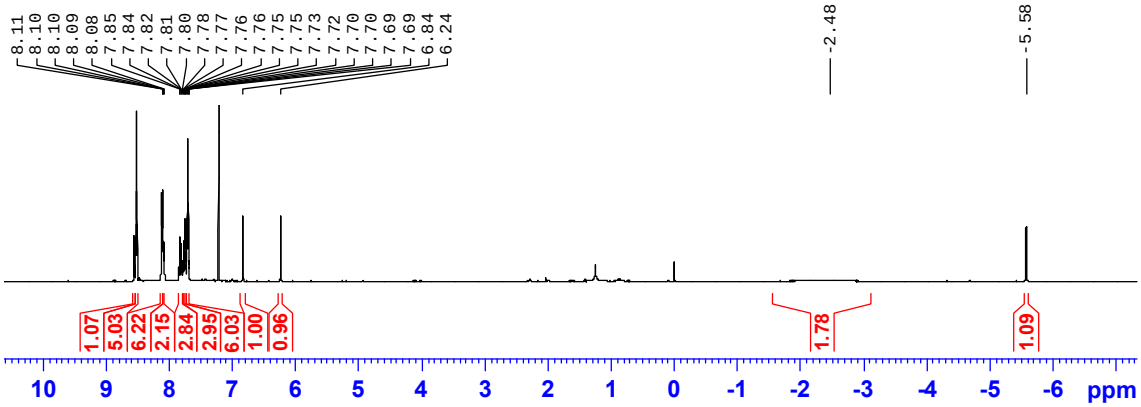

Figure S1. ^{1}H NMR spectrum of **2a**, 298 K, $CDCl_3$.

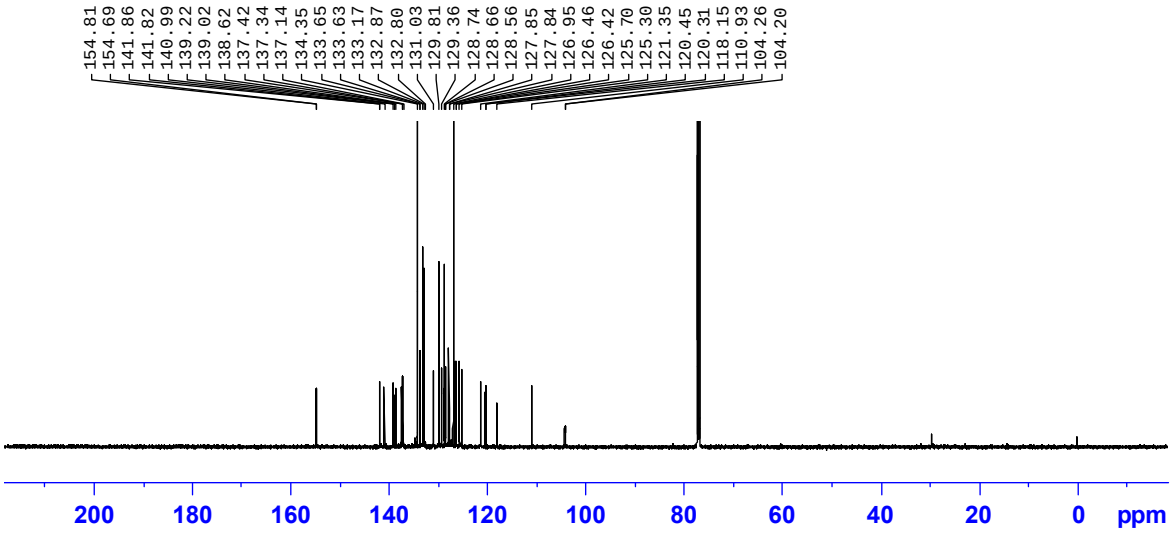

Figure S2. ^{13}C NMR spectrum of **2a**, 298 K, $CDCl_3$.

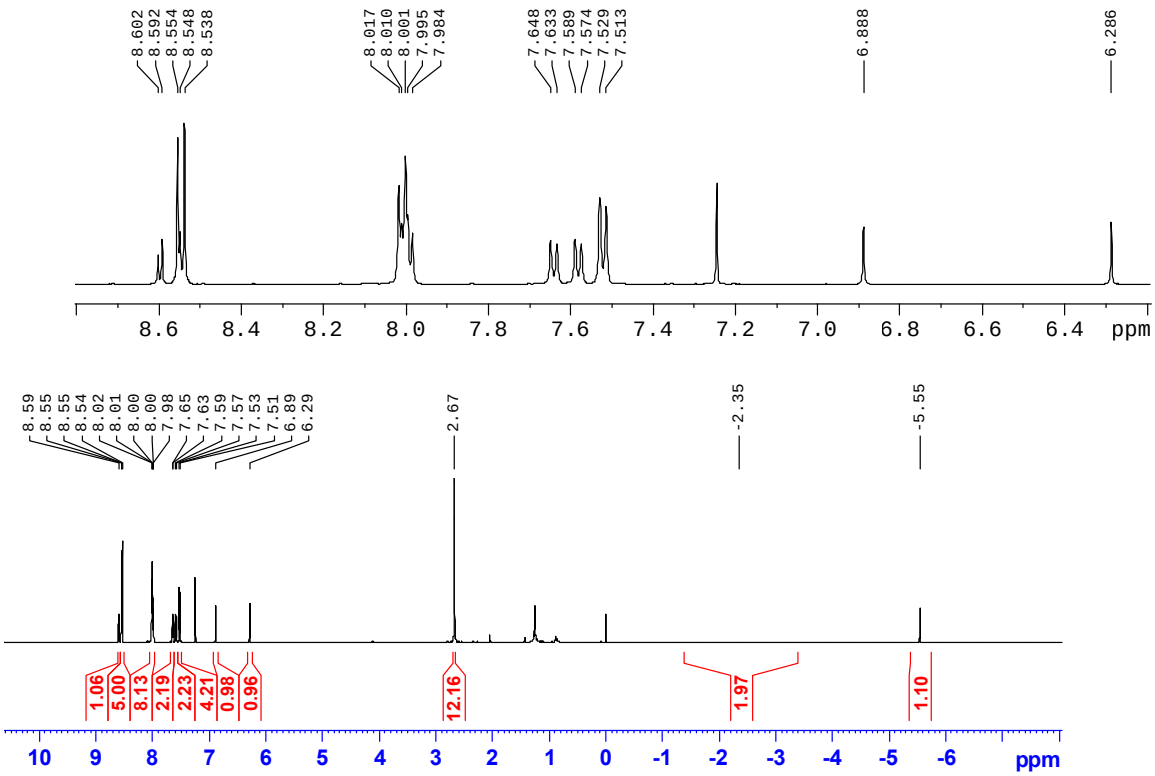

Figure S3. ^{1}H NMR spectrum of **2b**, 298 K, $CDCl_3$

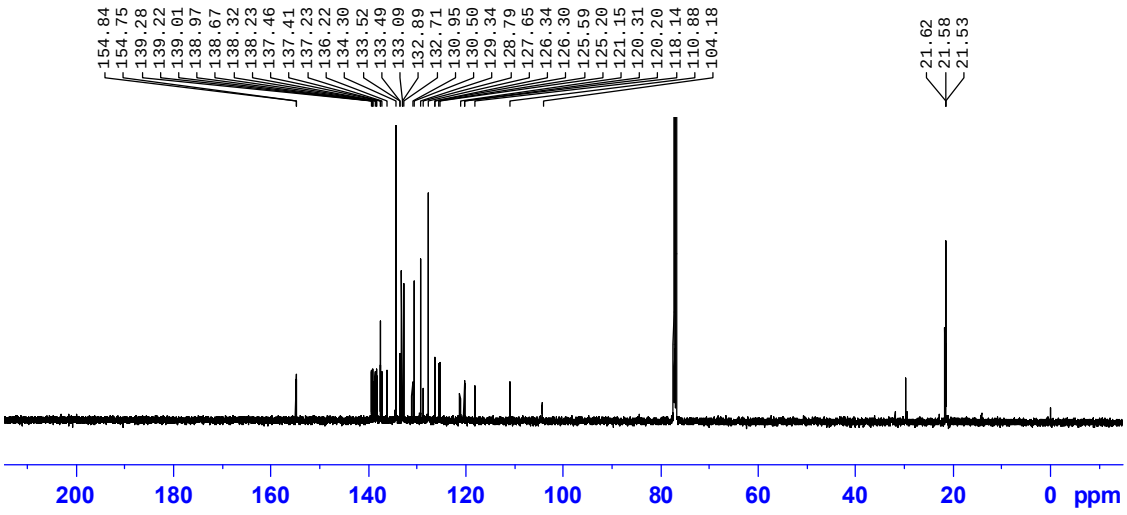

Figure S4. ^{13}C NMR spectrum of **2b**, 298 K, $CDCl_3$.

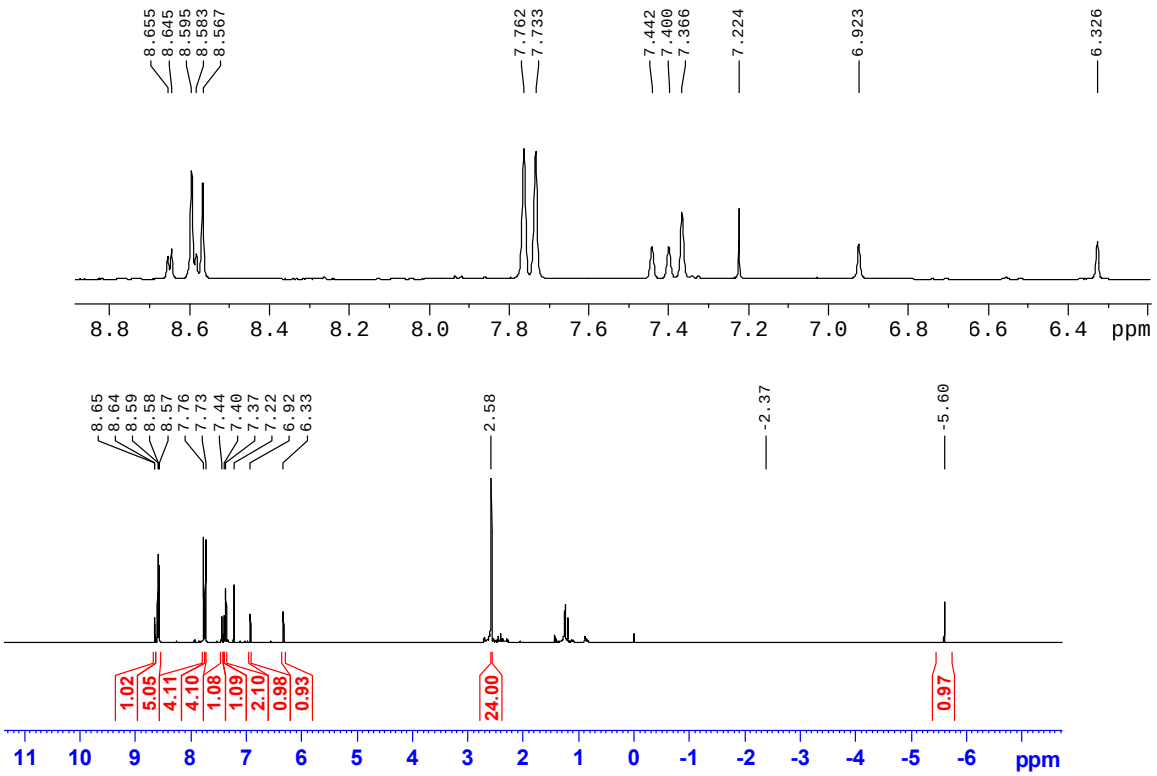

Figure S5. ^{1}H NMR spectrum of **2c**, 298 K, $CDCl_3$.

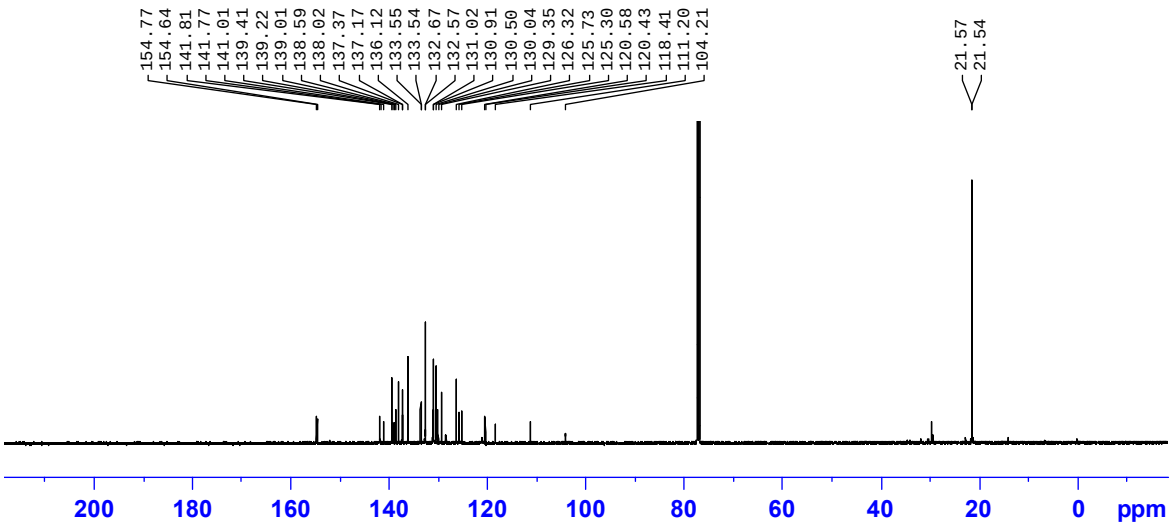

Figure S6. ^{13}C NMR spectrum of **2c**, 298 K, $CDCl_3$.

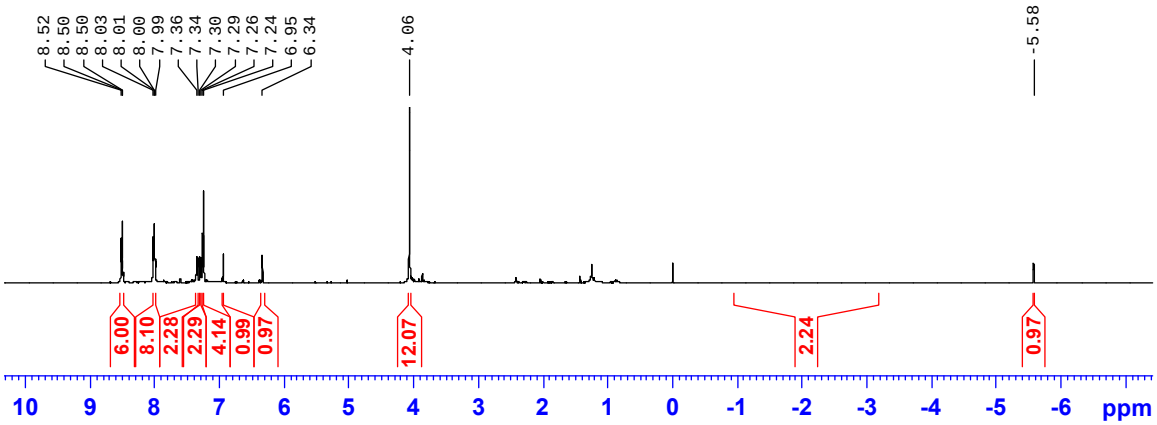

Figure S7. ^{1}H NMR spectrum of **2d**, 298 K, $CDCl_3$.

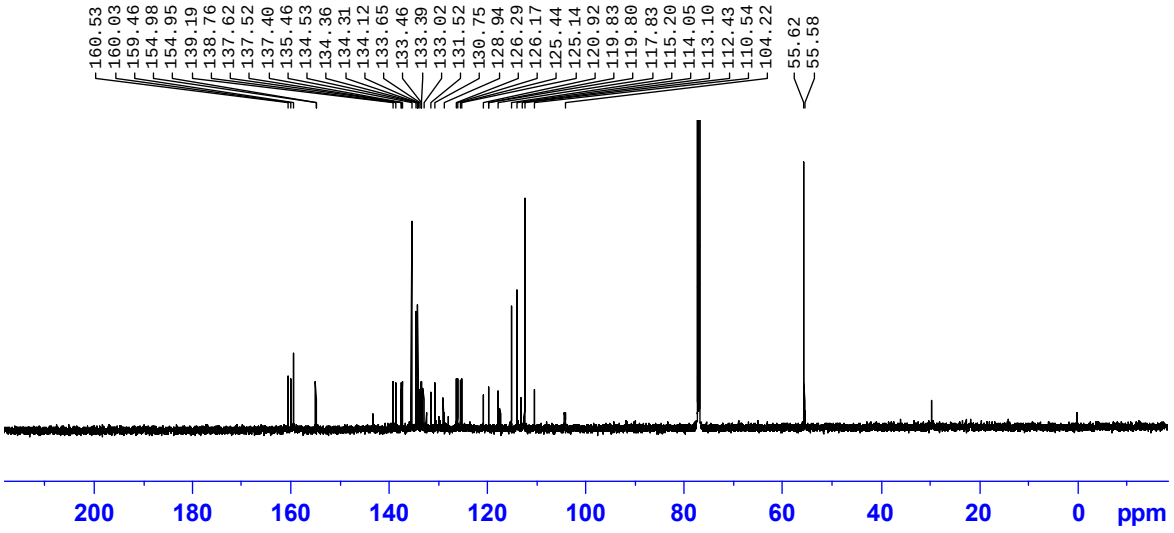

Figure S8. ^{13}C NMR spectrum of **2d**, 298 K, $CDCl_3$.

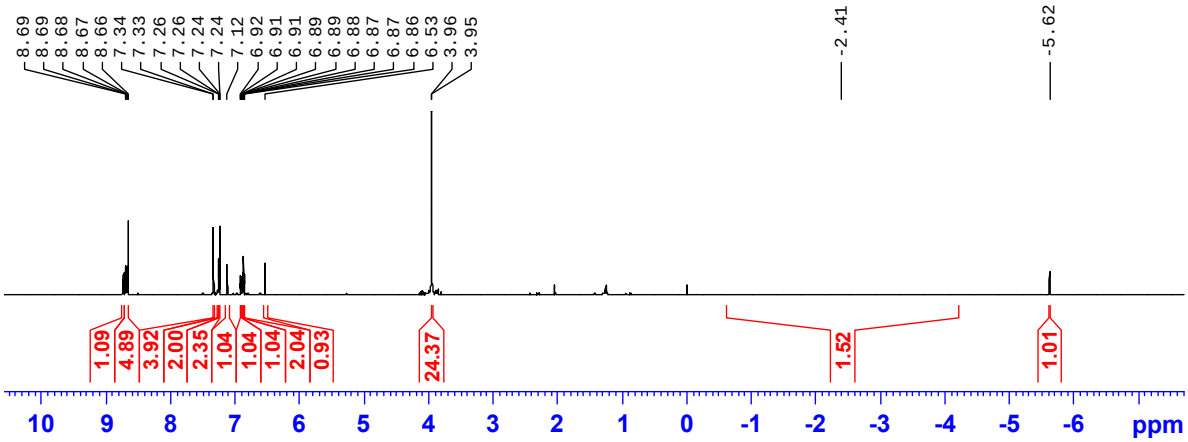

Figure S9. ^{1}H NMR spectrum of **2e**, 298 K, $CDCl_3$.

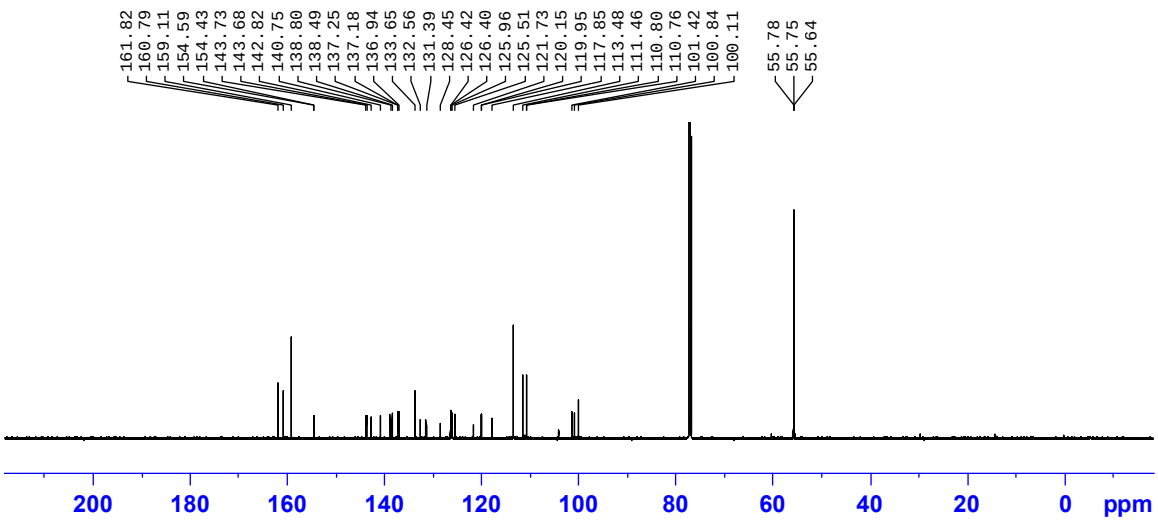

Figure S10. ^{13}C NMR spectrum of **2e**, 298 K, $CDCl_3$.

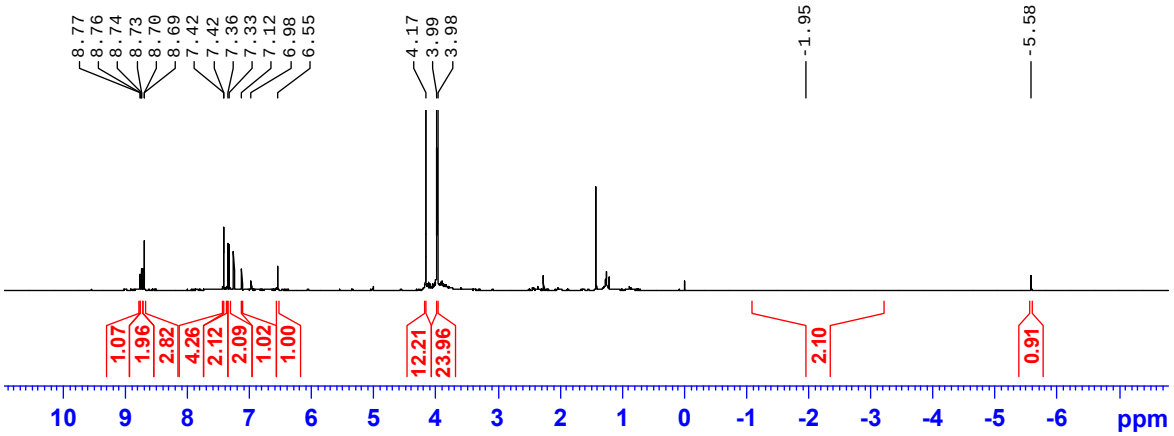

Figure S11. ^{1}H NMR spectrum of **2f**, 298 K, $CDCl_3$.

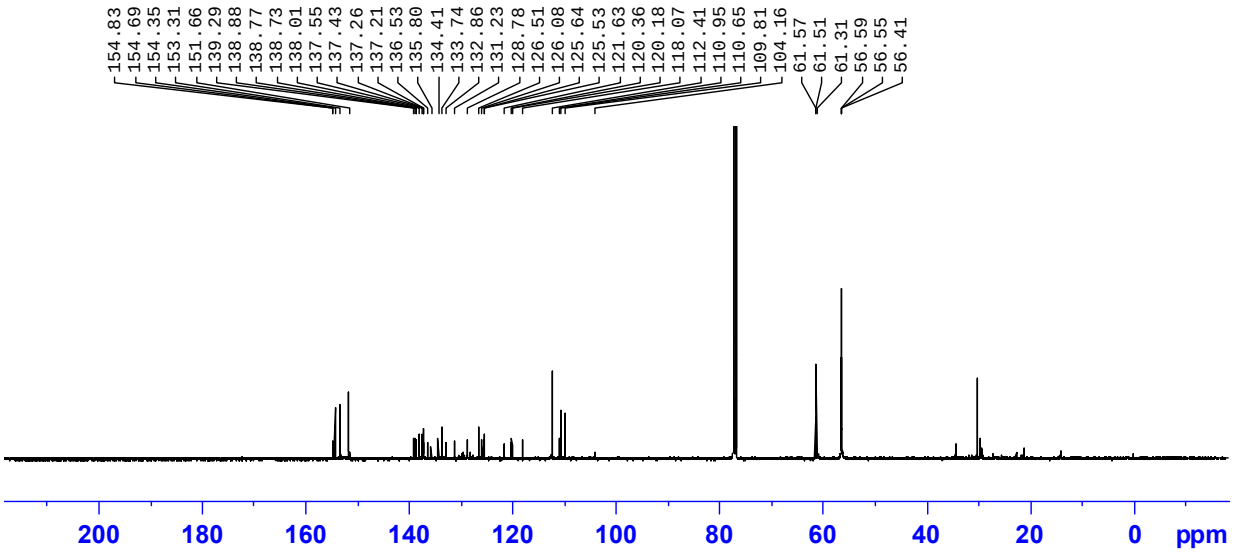

Figure S12. ^{13}C NMR spectrum of **2f**, 298 K, $CDCl_3$.

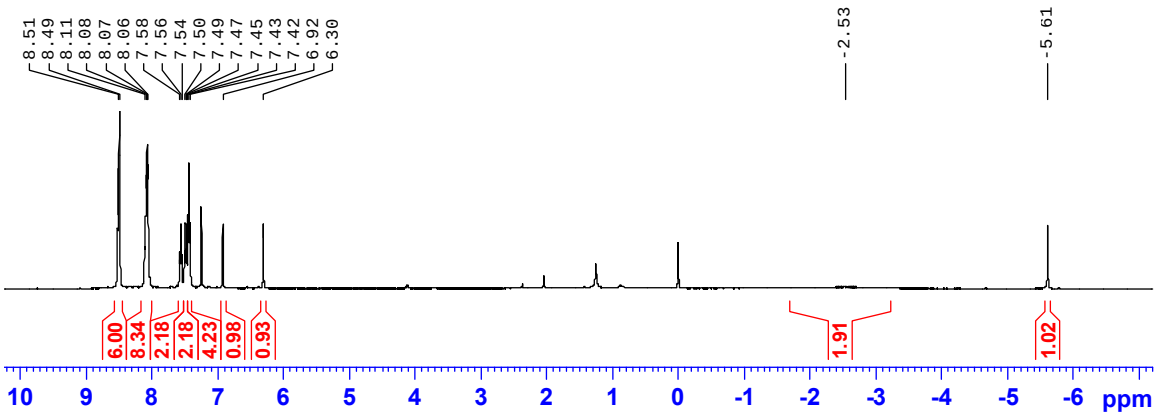

Figure S13. ^{1}H NMR spectrum of **2g**, 298 K, $CDCl_3$.

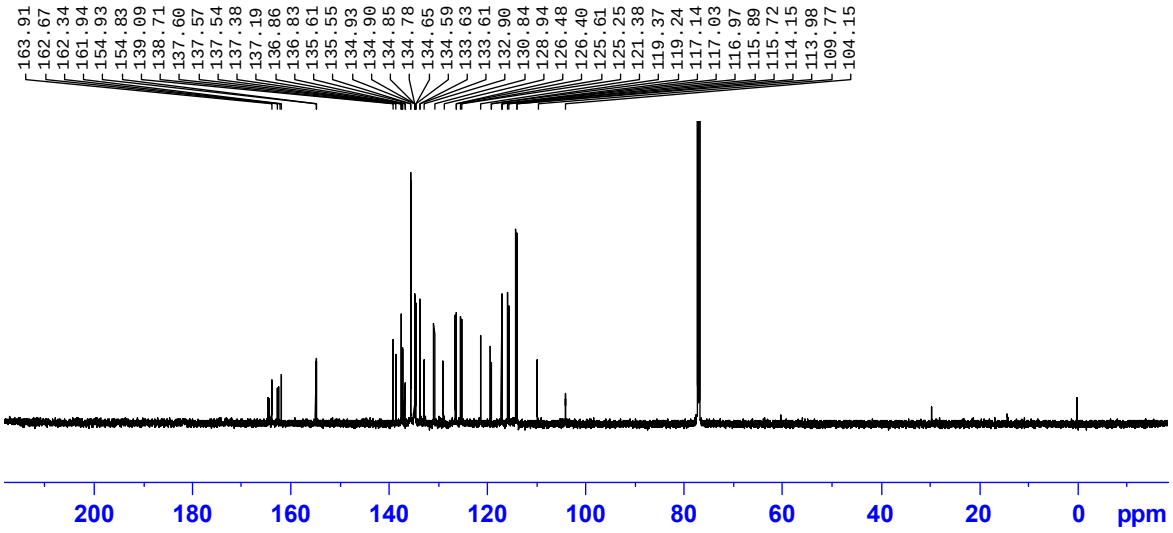

Figure S14. ^{13}C NMR spectrum of **2g**, 298 K, $CDCl_3$.

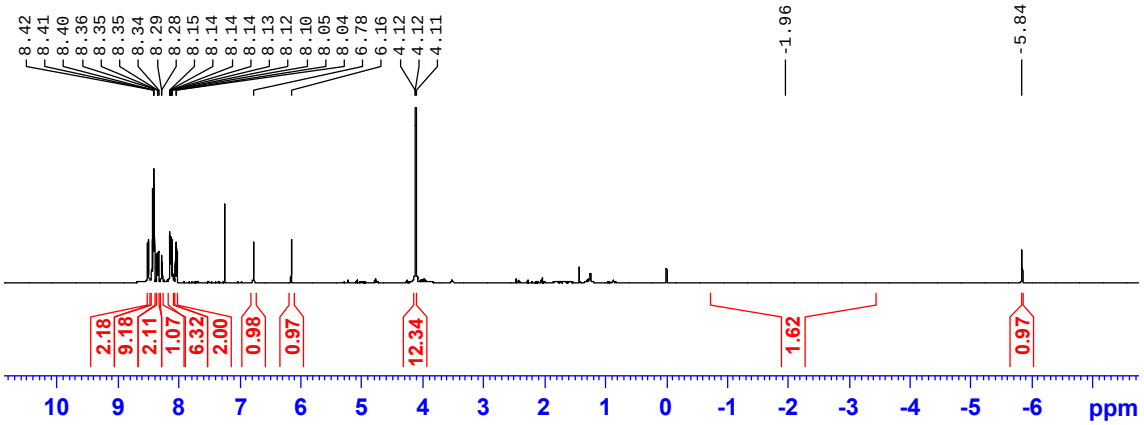

Figure S15. ^{1}H NMR spectrum of **2h**, 298 K, $CDCl_3$.

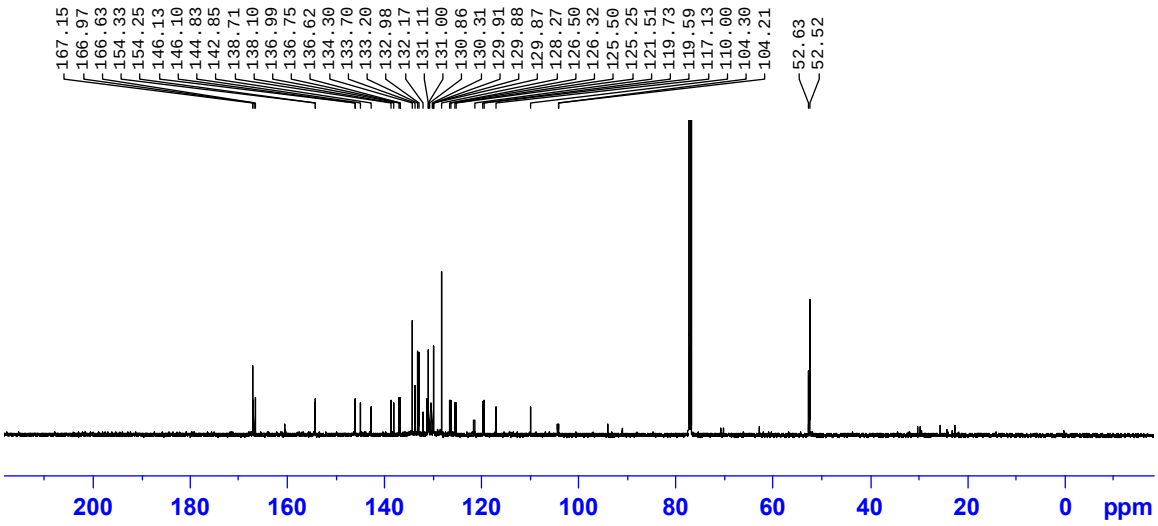

Figure S16. ^{13}C NMR spectrum of **2h**, 298 K, $CDCl_3$.

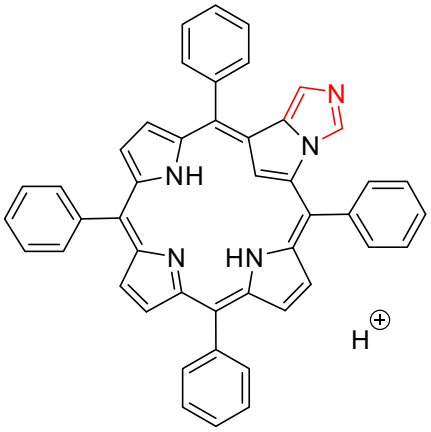

Chemical Formula: $C_{46}H_{32}N_5^+$
Exact Mass: 654.2652

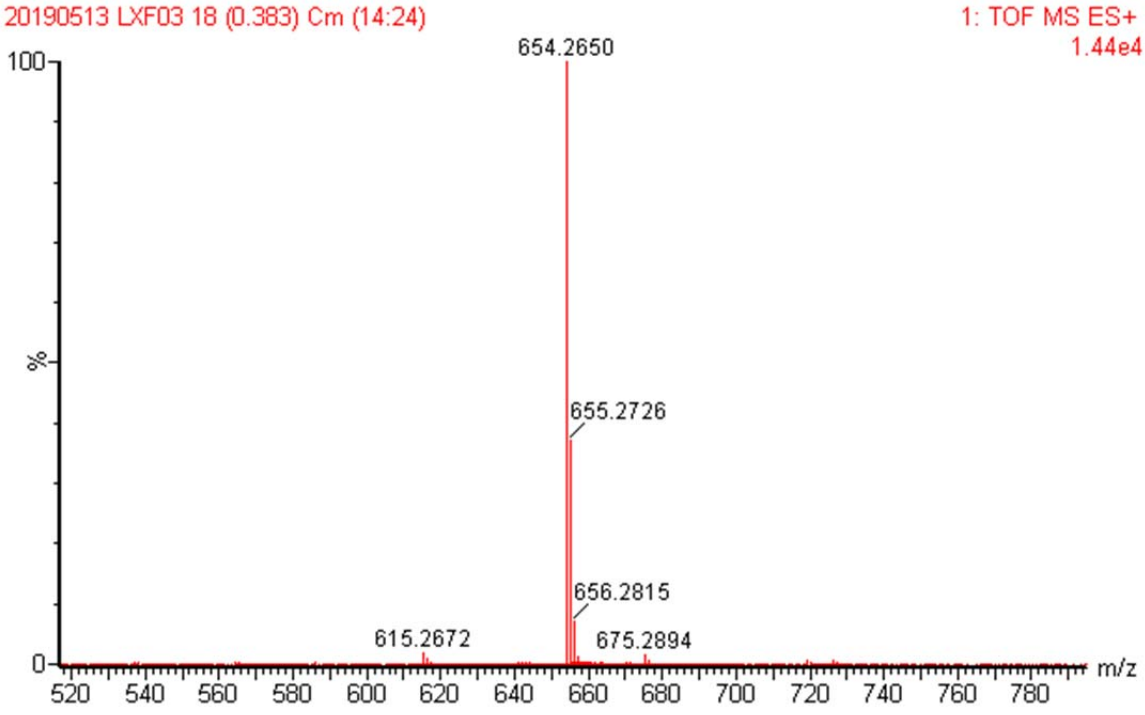

Figure S17. HRMS spectrum of **2a**.

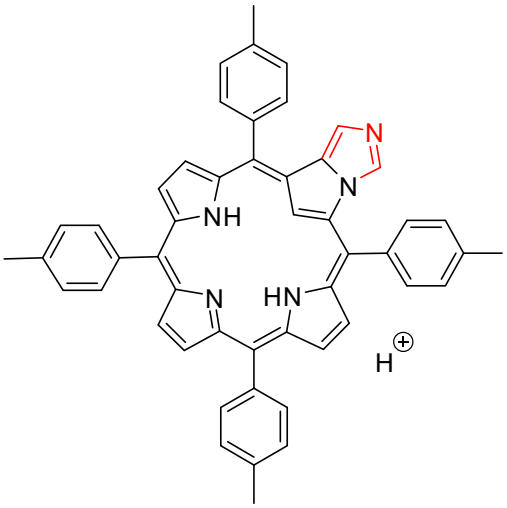

Chemical Formula: $C_{50}H_{40}N_5^+$
Exact Mass: 710.3278

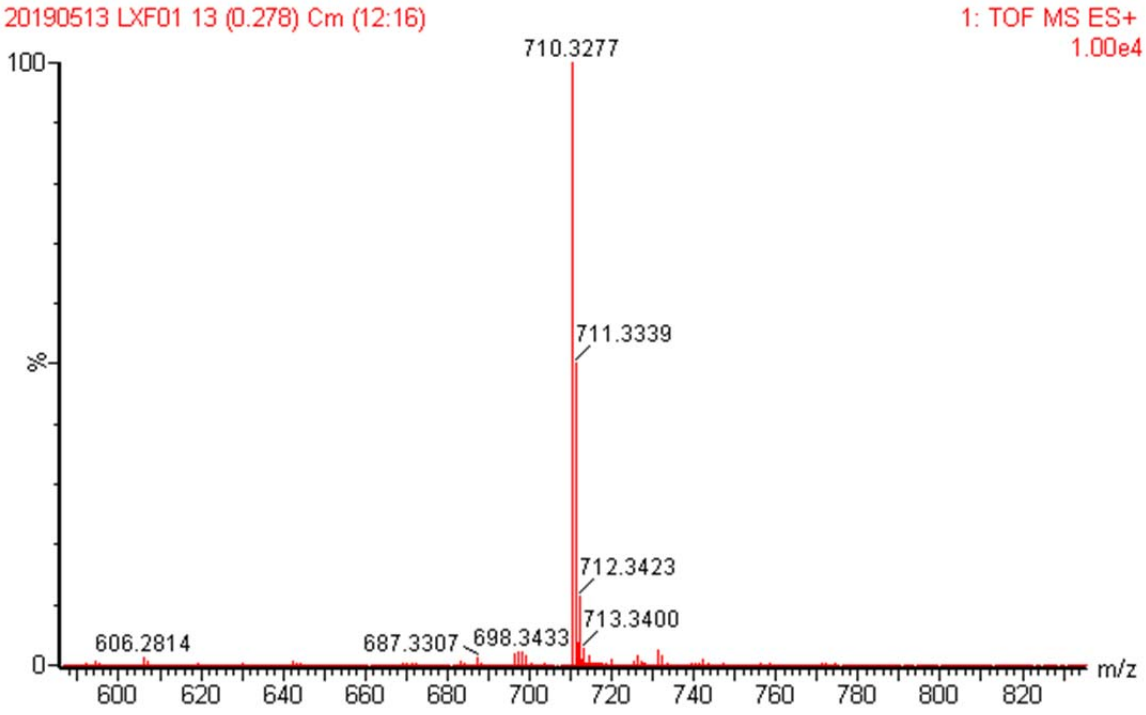

Figure S18. HRMS spectrum of **2b**.

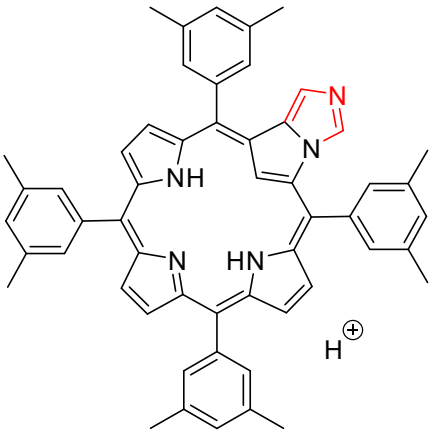

Chemical Formula: $C_{54}H_{48}N_5^+$
Exact Mass: 766.3904

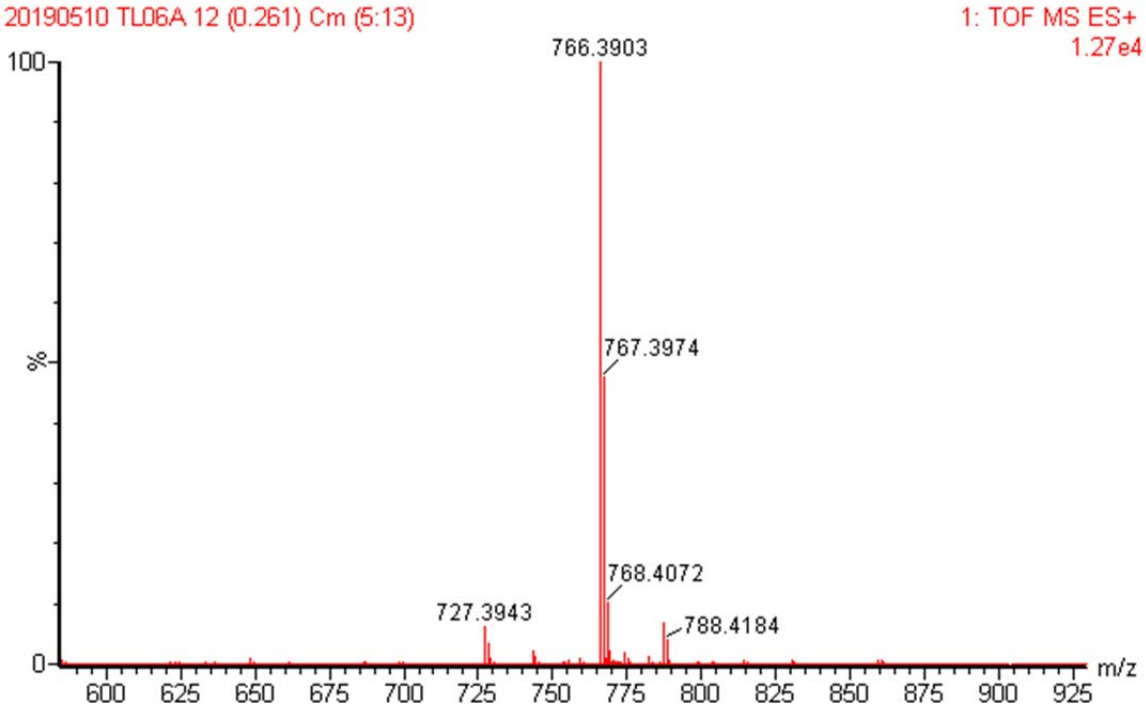

Figure S19. HRMS spectrum of **2c**.

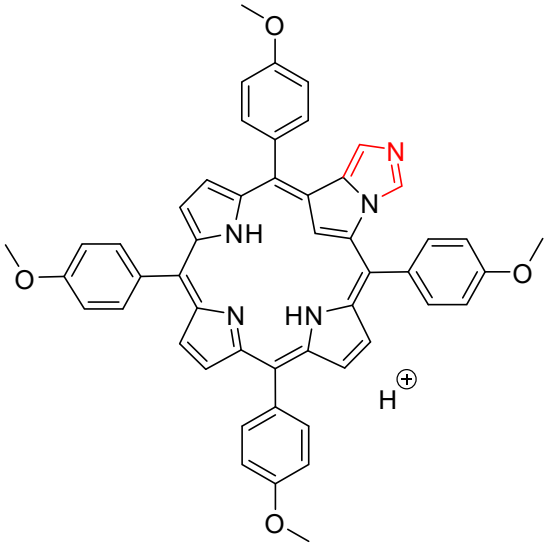

Chemical Formula: $C_{50}H_{40}N_5O_4^+$
Exact Mass: 774.3075

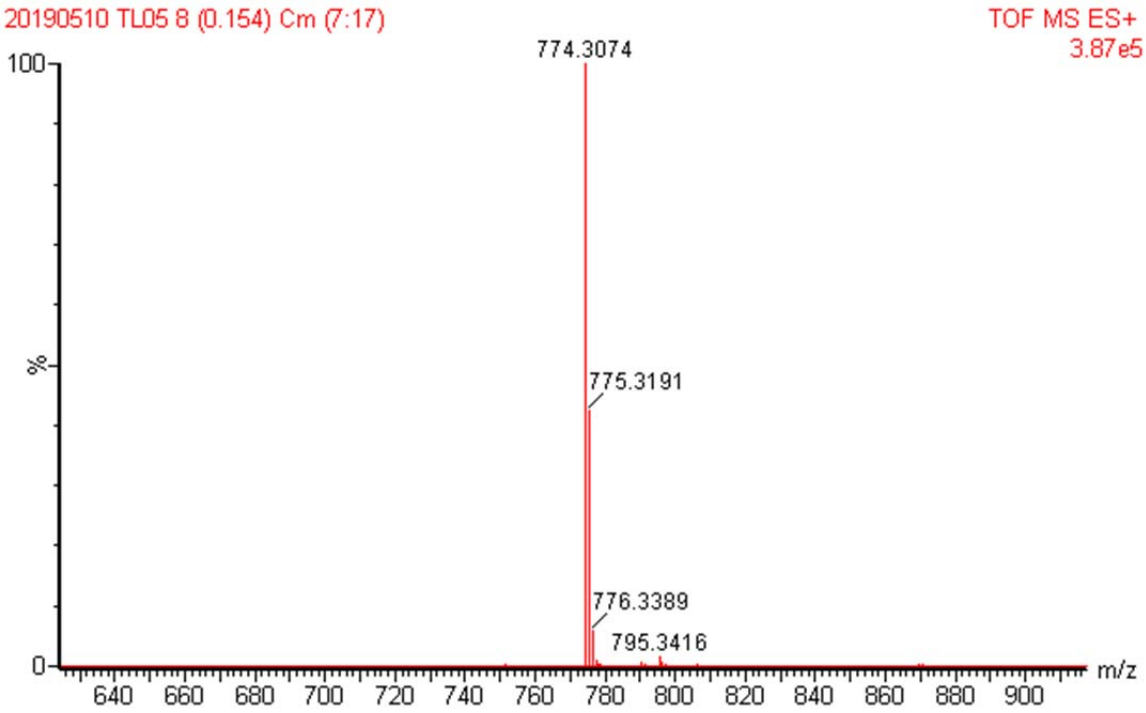

Figure S20. HRMS spectrum of **2d**.

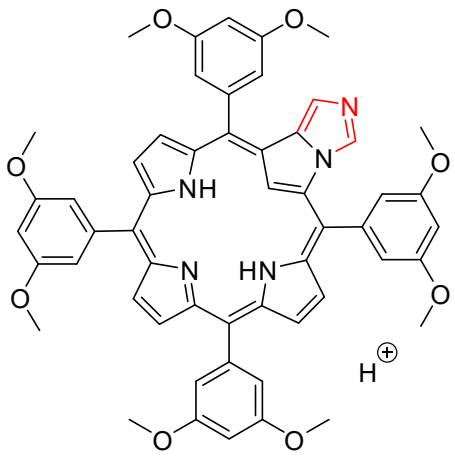

Chemical Formula: $C_{54}H_{48}N_5O_8^+$
Exact Mass: 894.3497

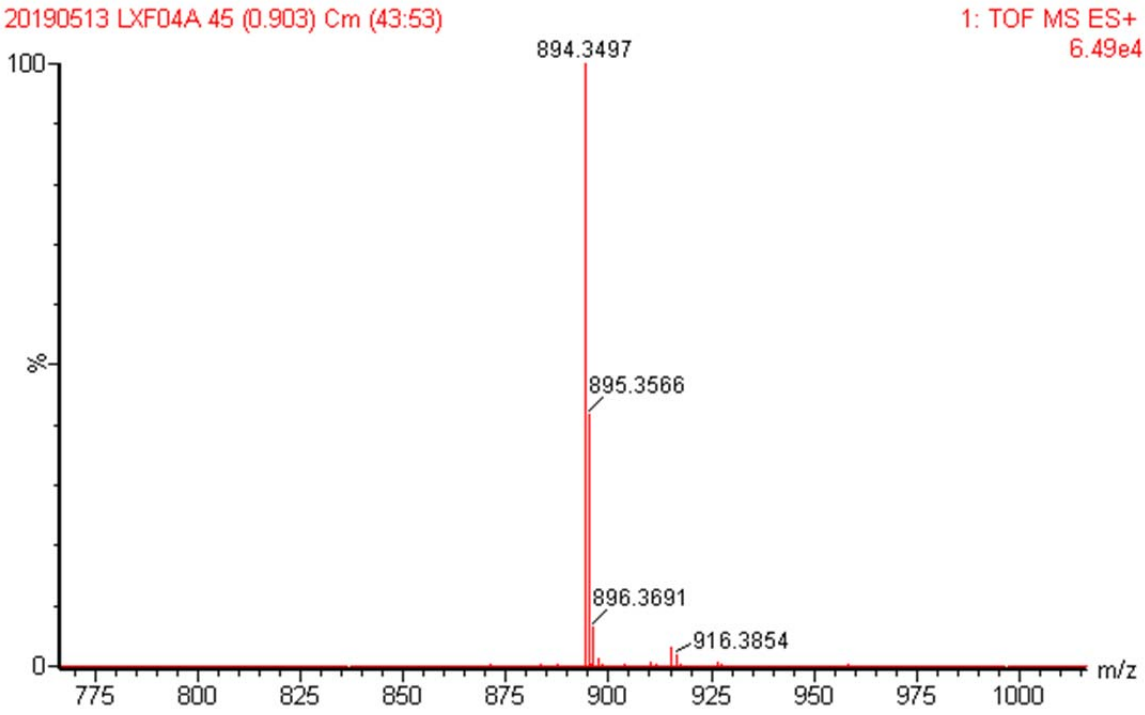

Figure S21. HRMS spectrum of **2e**.

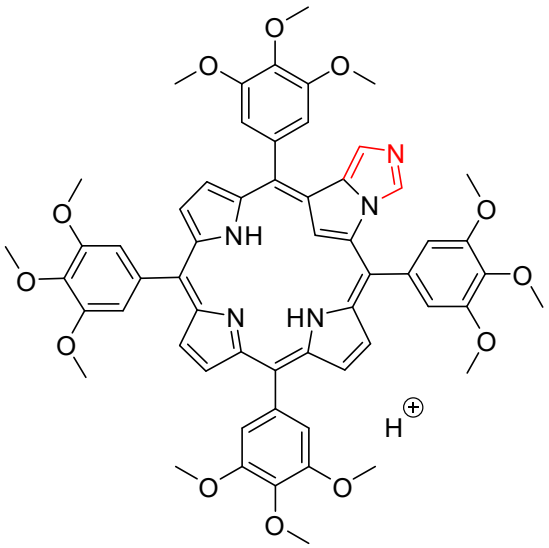

Chemical Formula: $C_{58}H_{56}N_5O_{12}^+$
Exact Mass: 1014.3920

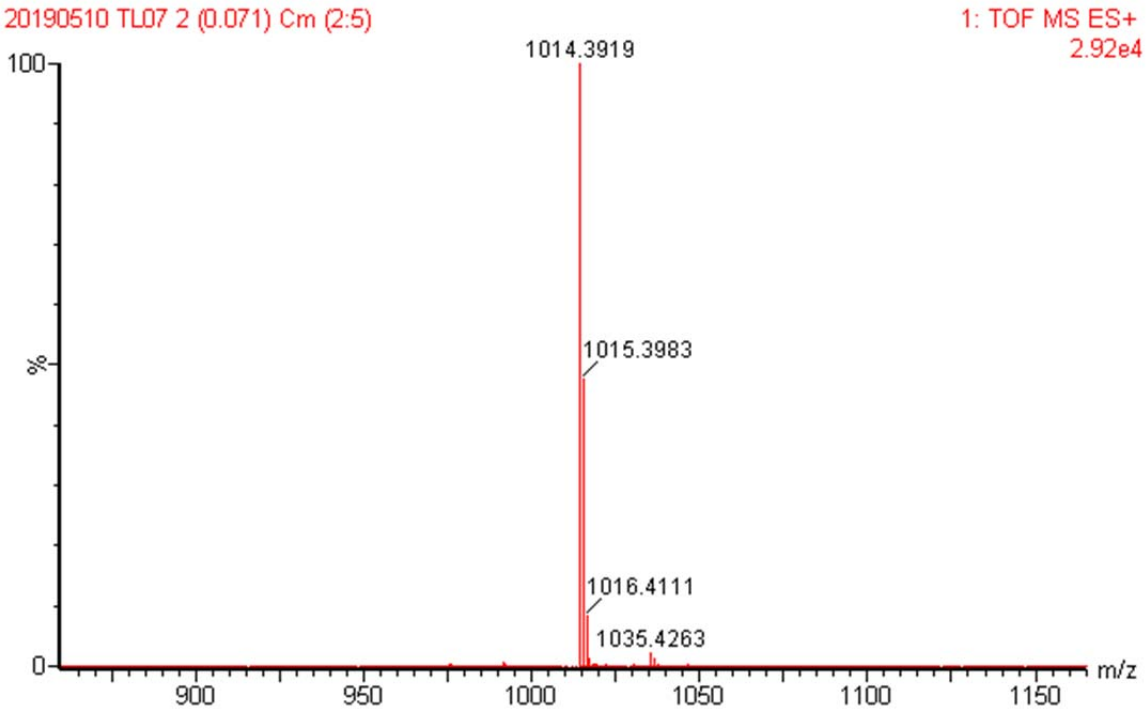

Figure S22. HRMS spectrum of **2f**.

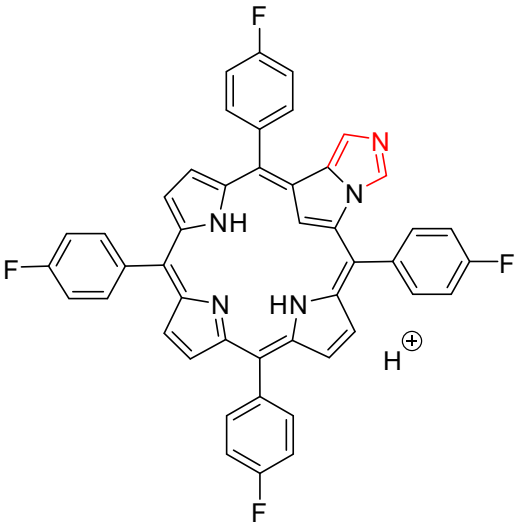

Chemical Formula: $C_{46}H_{28}F_4N_5^+$
Exact Mass: 726.2275

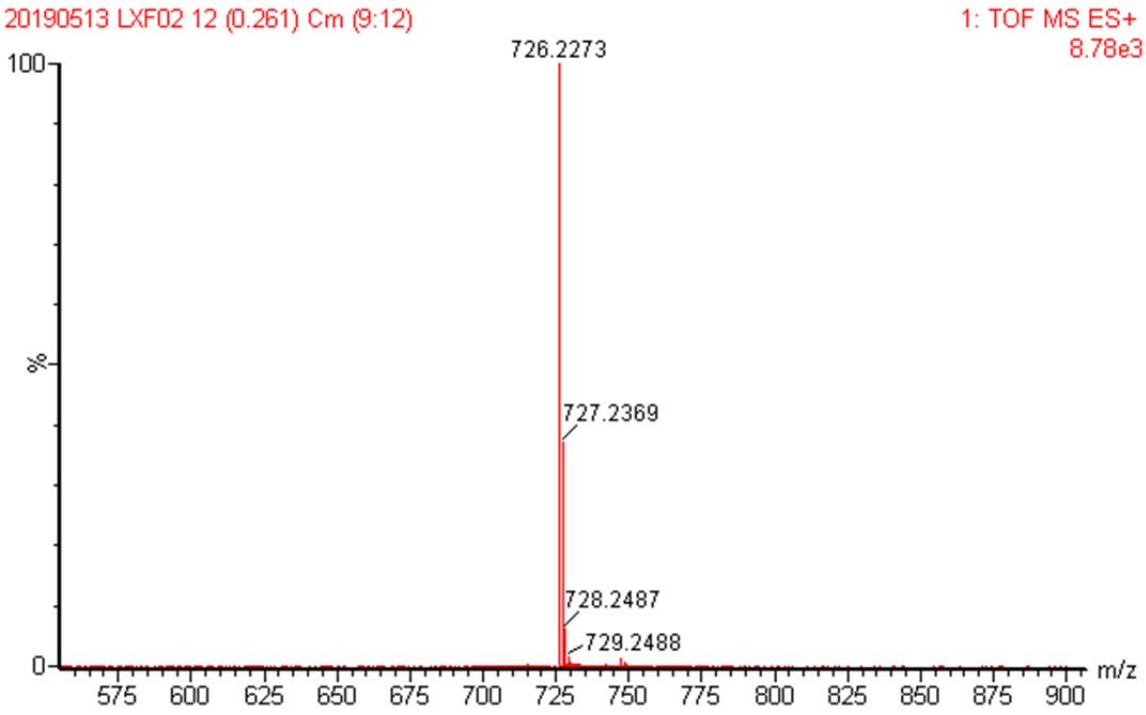

Figure S23. HRMS spectrum of **2g**.

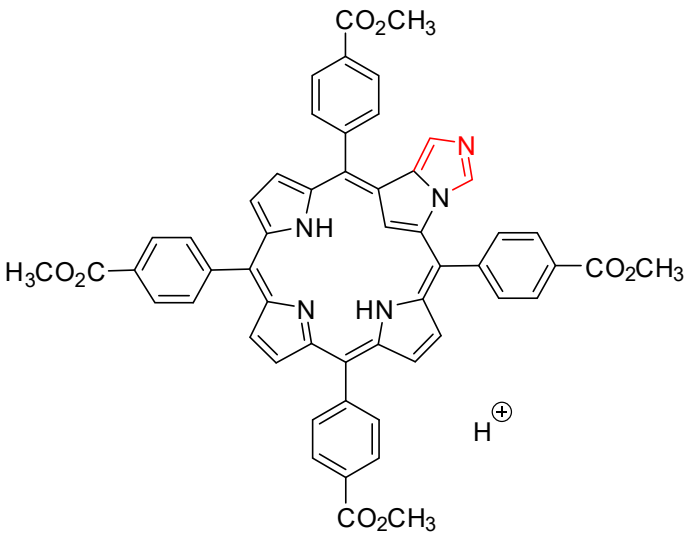

Chemical Formula: $C_{54}H_{40}N_5O_8^+$
Exact Mass: 886.2871

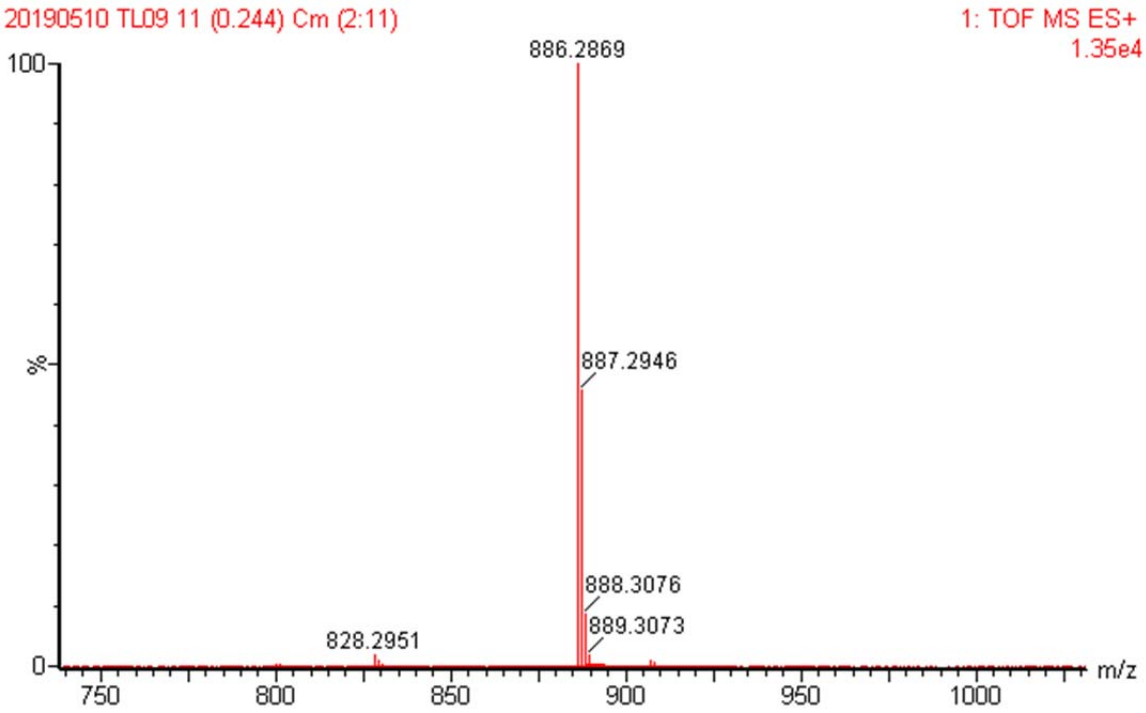

Figure S24. HRMS spectrum of **2h**.

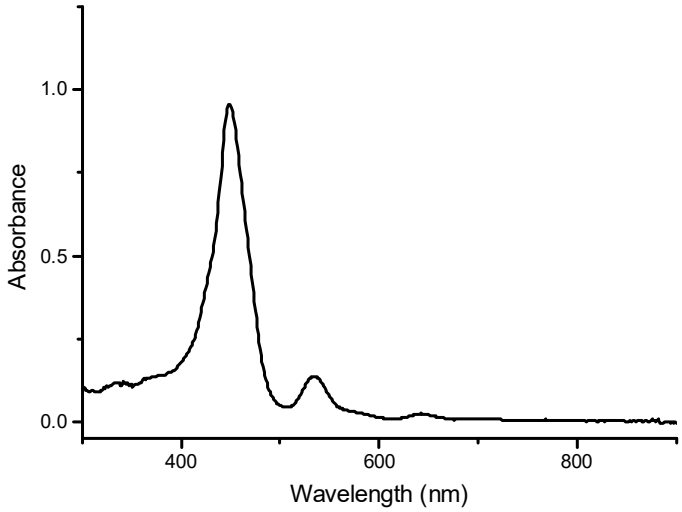

Figure S25. UV-vis spectra of **2a** (CH_2Cl_2, $5.67*10^{-6}$).

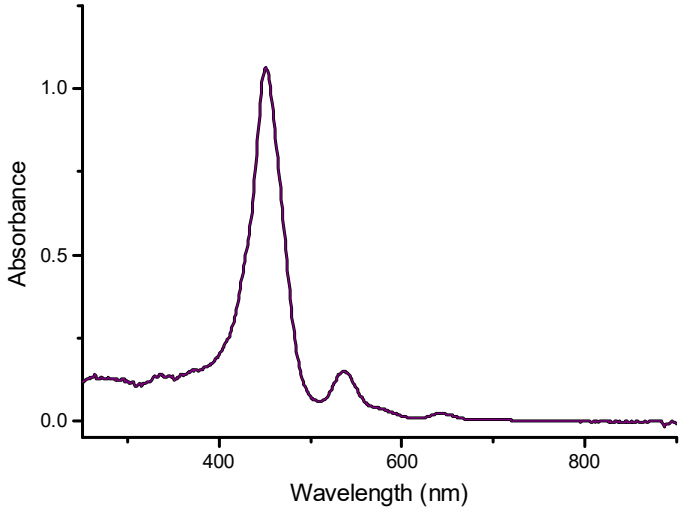

Figure S26. UV-vis spectra of **2b** (CH_2Cl_2, $6.01*10^{-6}$).

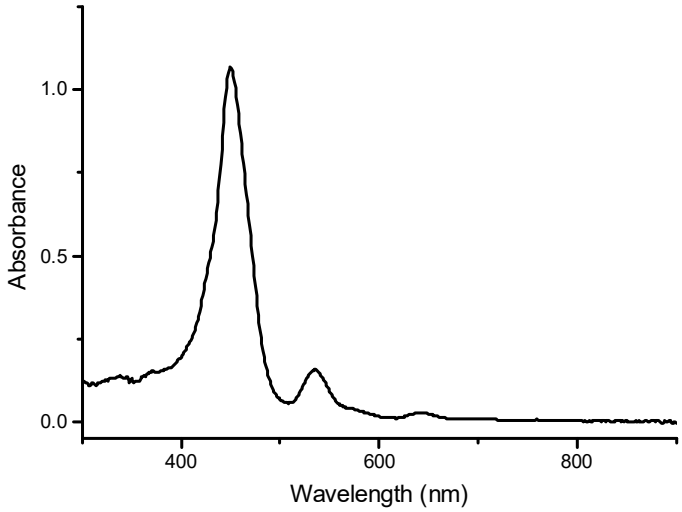

Figure S27. UV-vis spectra of **2c** (CH_2Cl_2, $6.45*10^{-6}$)

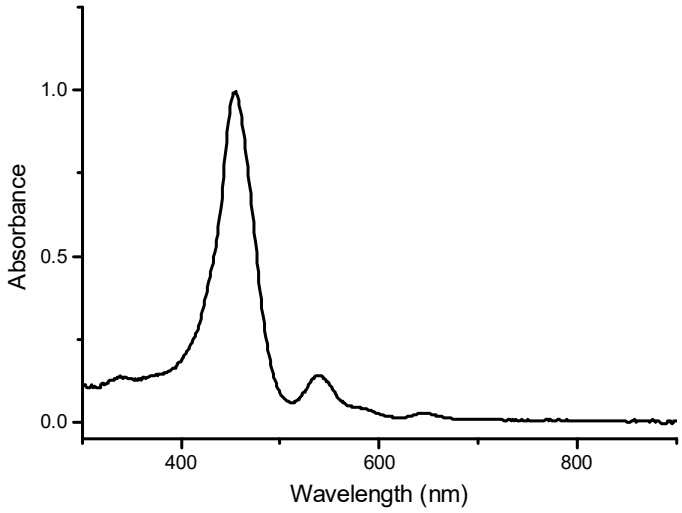

Figure S28. UV-vis spectra of **2d** (CH_2Cl_2, $5.99*10^{-6}$).

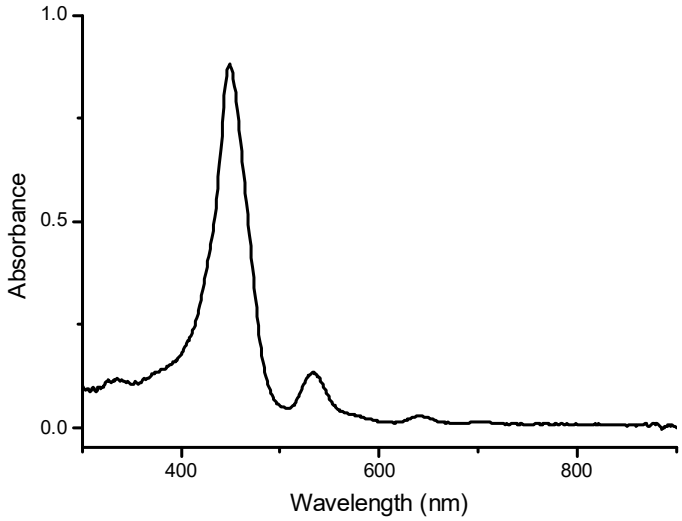

Figure S29. UV-vis spectra of **2e** (CH_2Cl_2, $4.29*10^{-6}$).

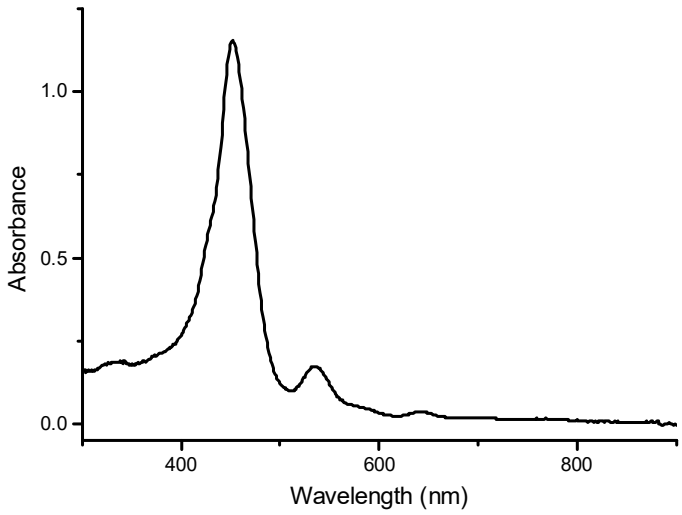

Figure S30. UV-vis spectra of **2f** (CH_2Cl_2, $7.96*10^{-6}$).

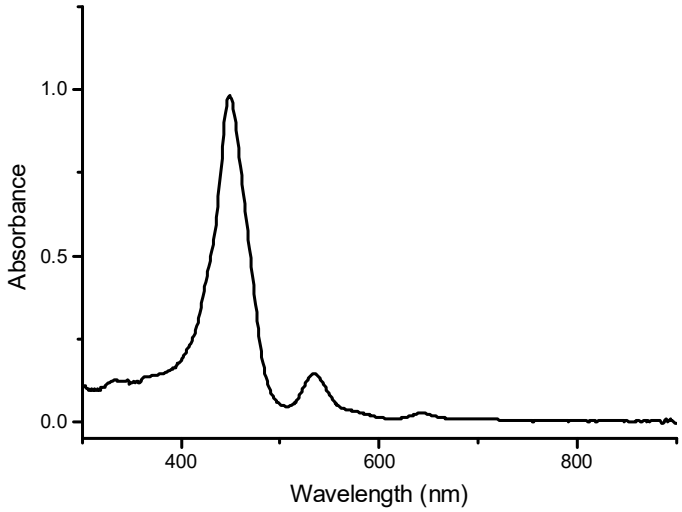

Figure S31. UV-vis spectra of **2g** (CH_2Cl_2, $5.15*10^{-6}$).

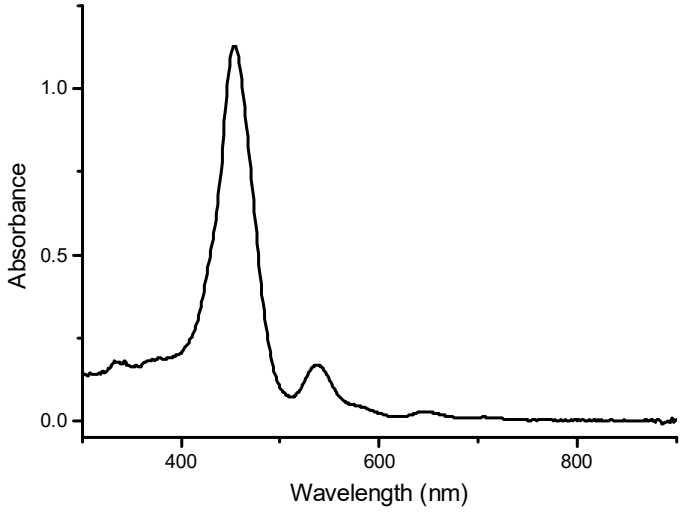

Figure S32. UV-vis spectra of **2h** (CH_2Cl_2, $5.76*10^{-6}$).

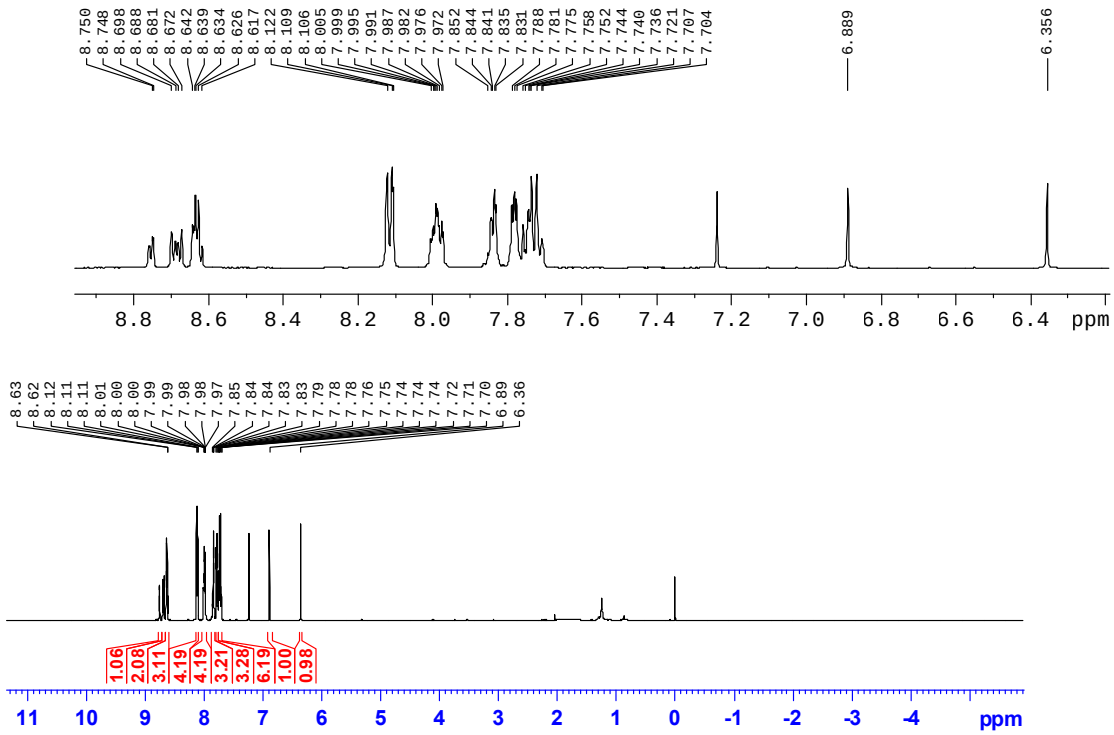

Figure S33. ^{1}H NMR spectrum of **3a**, 298 K, $CDCl_3$.

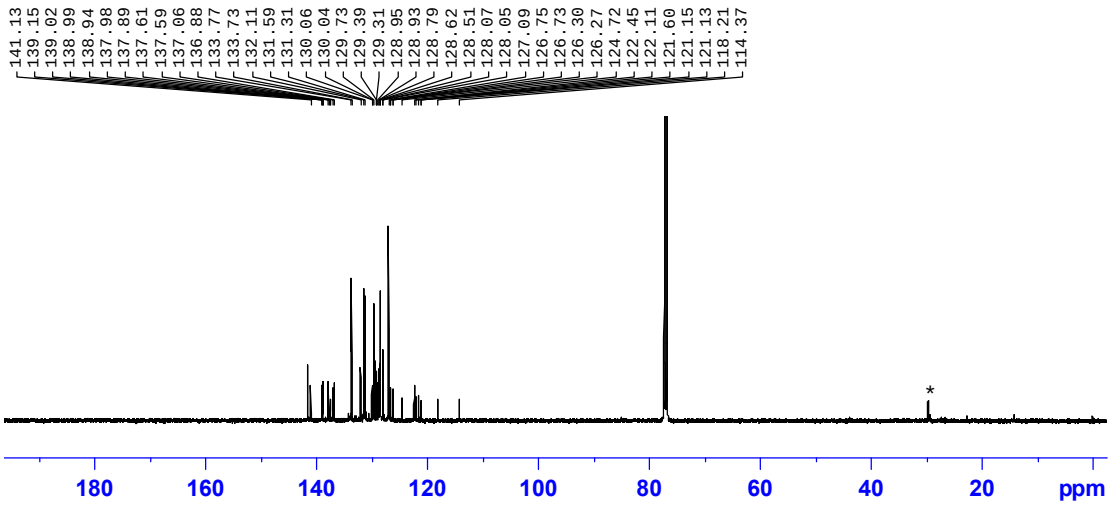

Figure S34. ^{13}C NMR spectrum of **3a**, 298 K, $CDCl_3$.

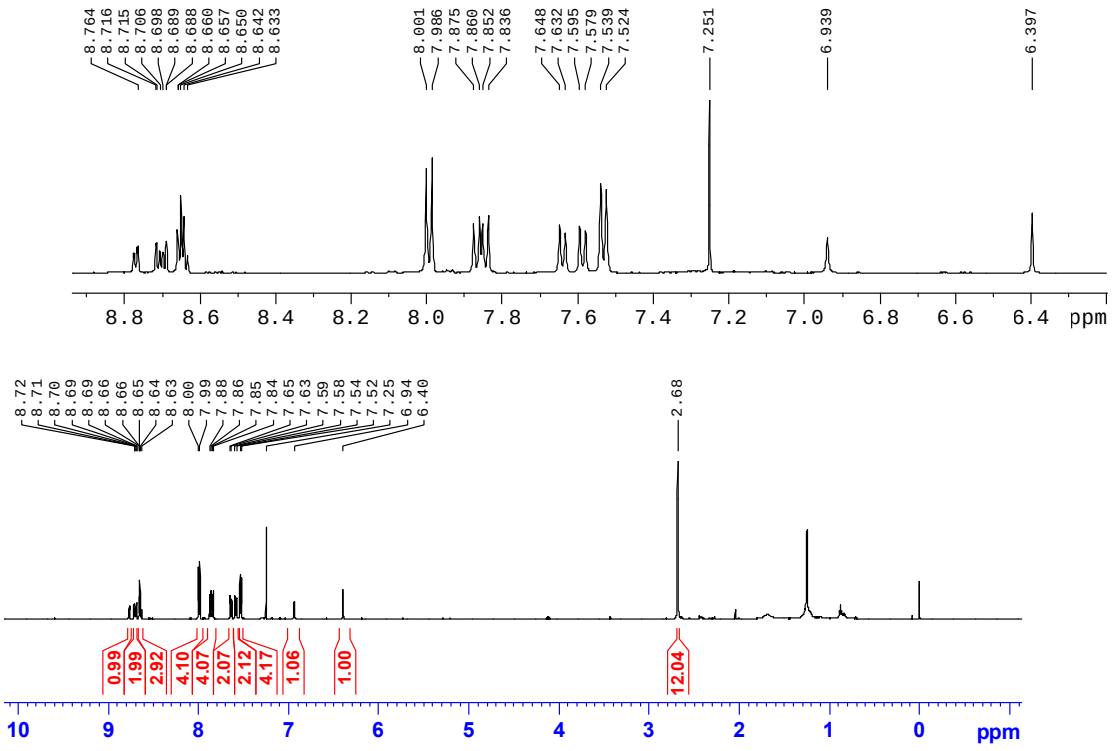

Figure S35. ^{1}H NMR spectrum of **3b**, 298 K, $CDCl_3$

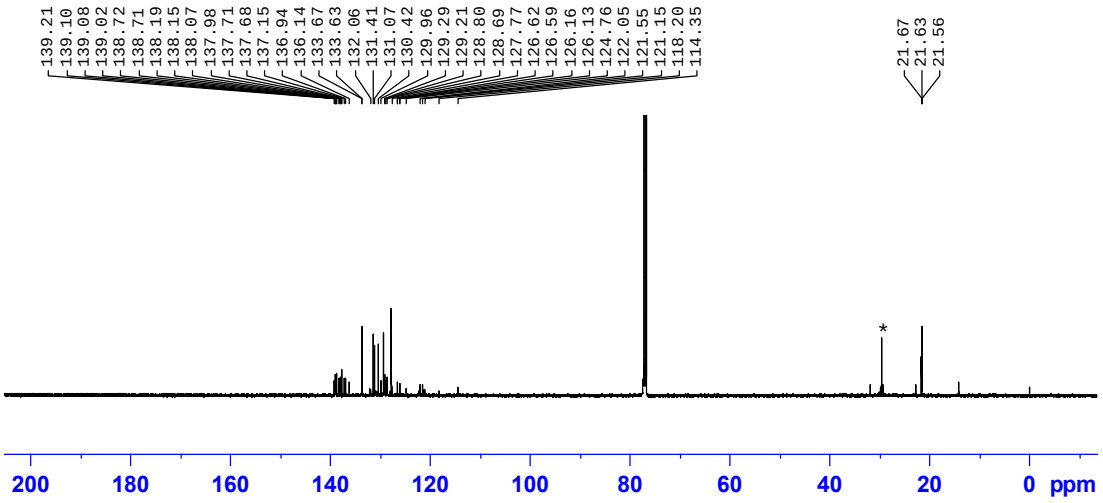

Figure S36. ^{13}C NMR spectrum of **3b**, 298 K, $CDCl_3$.

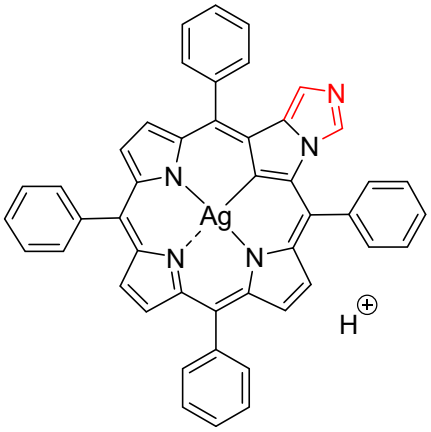

Chemical Formula: $C_{46}H_{29}AgN_5^+$
Exact Mass: 758.1468

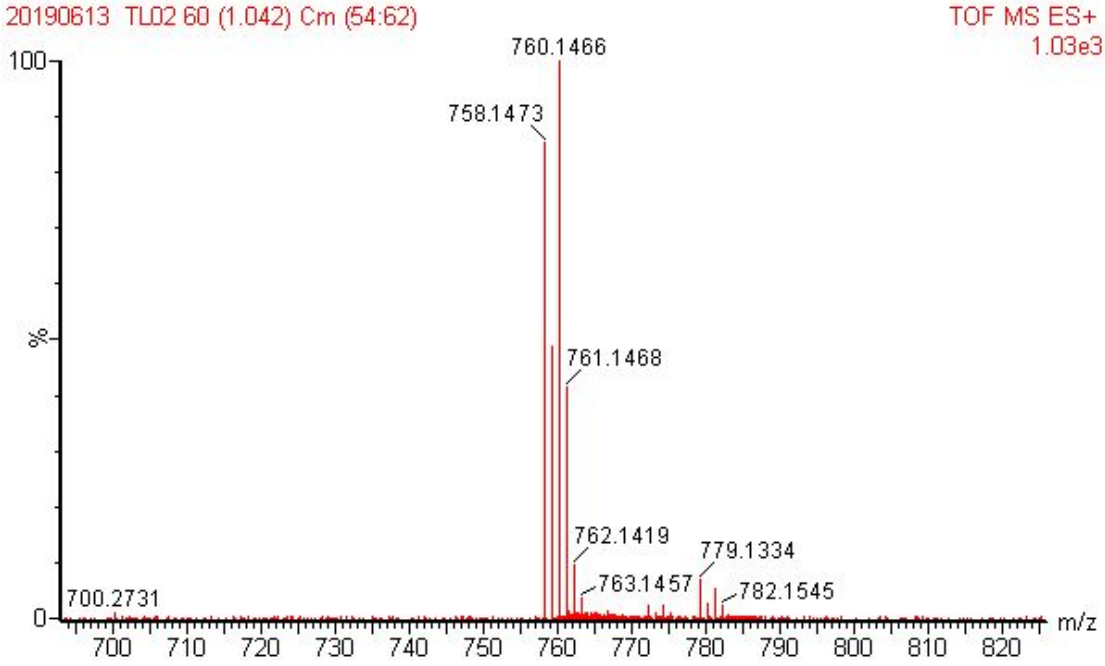

Figure S37. HRMS spectrum of **3a**.

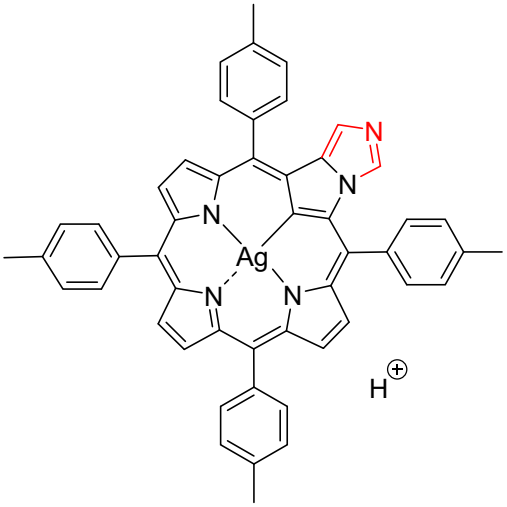

Chemical Formula: $C_{50}H_{37}AgN_5^+$
Exact Mass: 814.2094

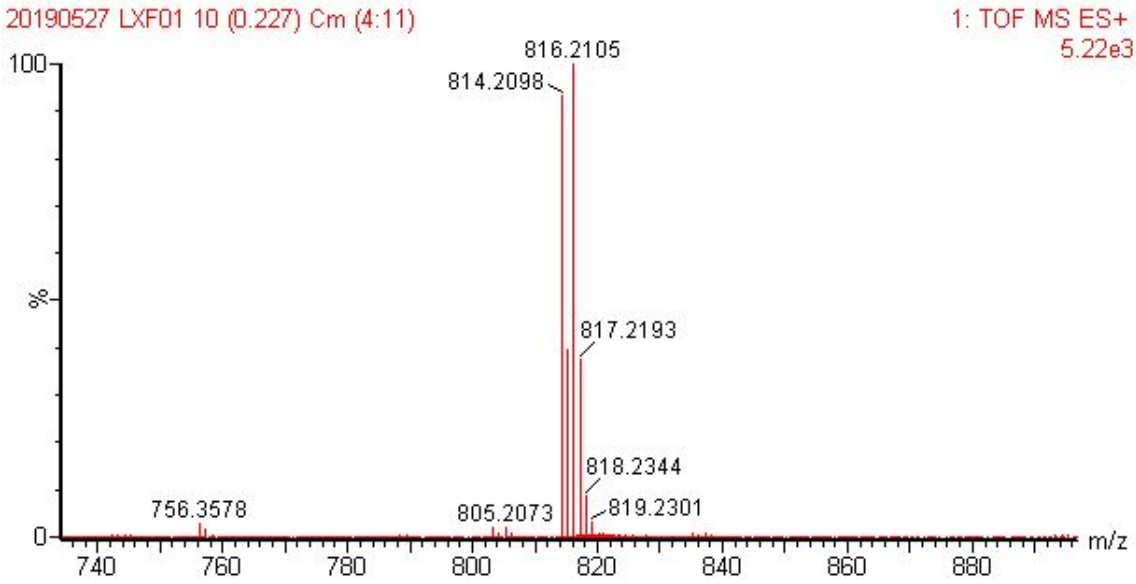

Figure S38. HRMS spectrum of **3b**.

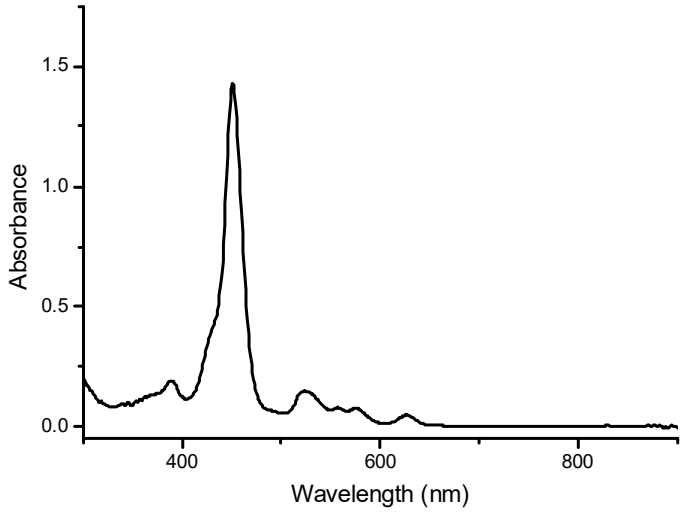

Figure S39. UV-vis spectra of **3a** (CH_2Cl_2, $7.13*10^{-6}$)

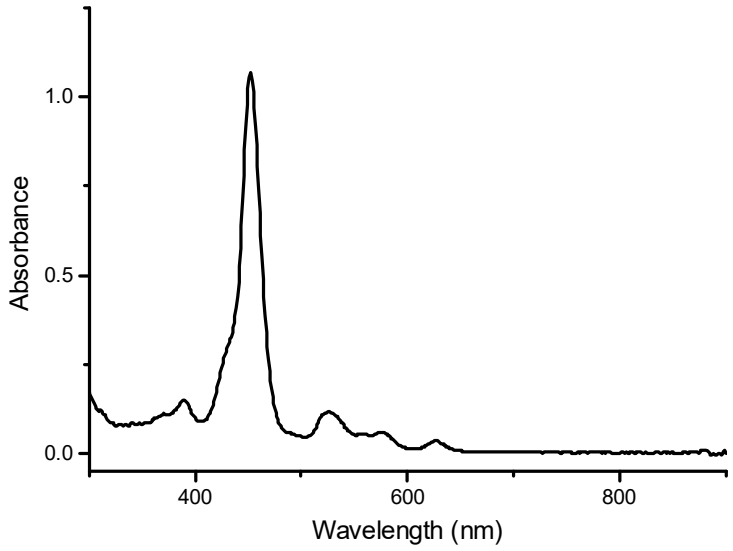

Figure S40. UV-vis spectra of **3b** (CH_2Cl_2, $7.22*10^{-6}$).

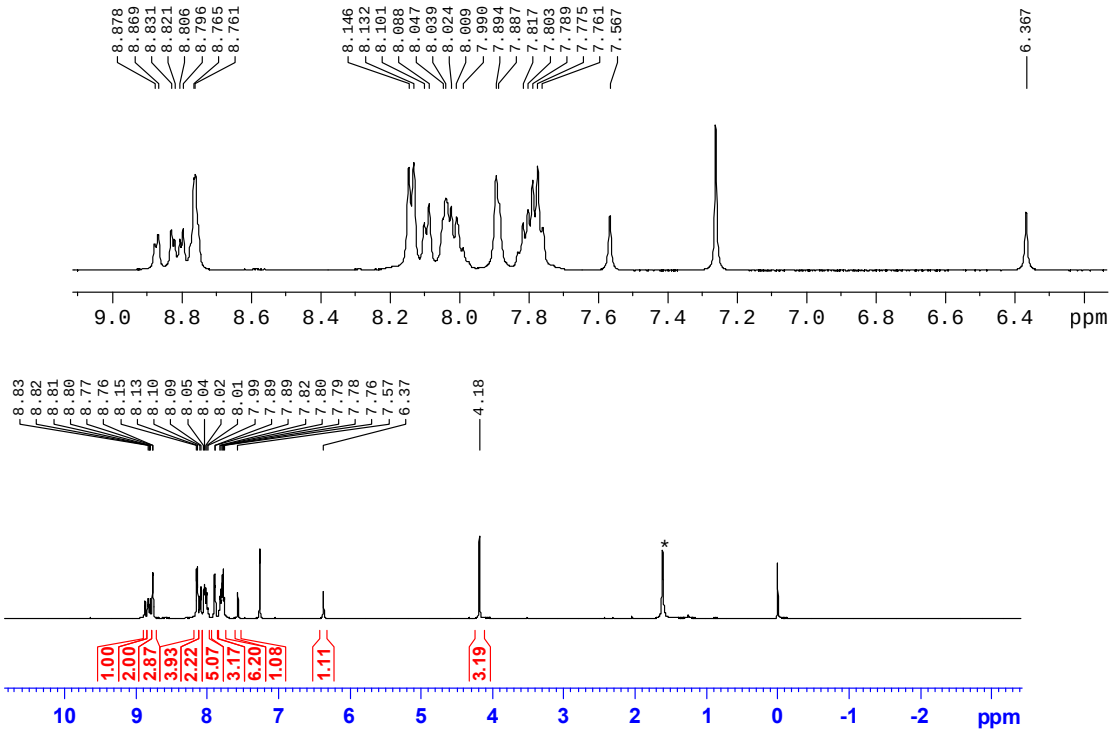

Figure S41. ^{1}H NMR spectrum of [**4a**]I, 298 K, $CDCl_3$.

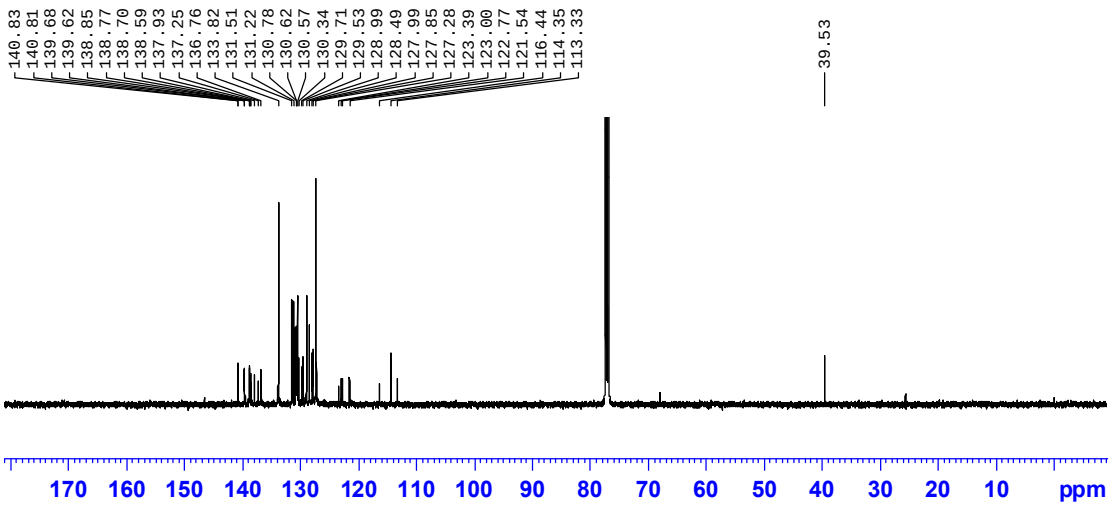

Figure S42. ^{13}C NMR spectrum of [**4a**]I, 298 K, $CDCl_3$.

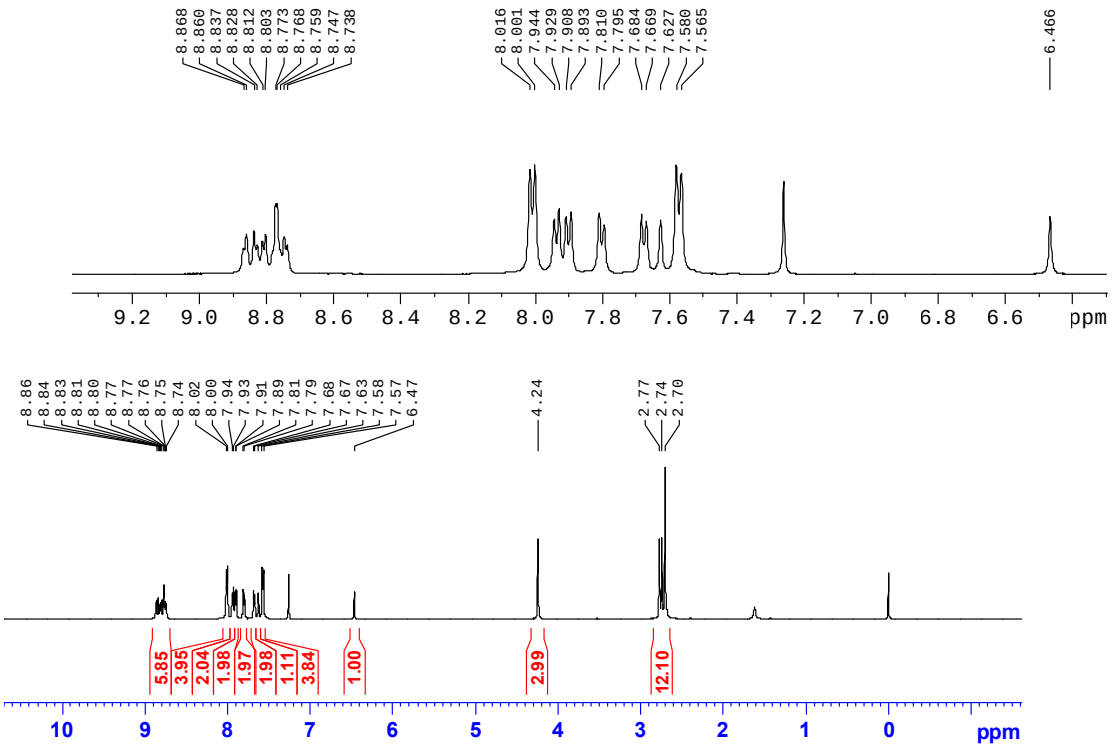

Figure S43. ^{1}H NMR spectrum of [**4b**]I, 298 K, $CDCl_3$

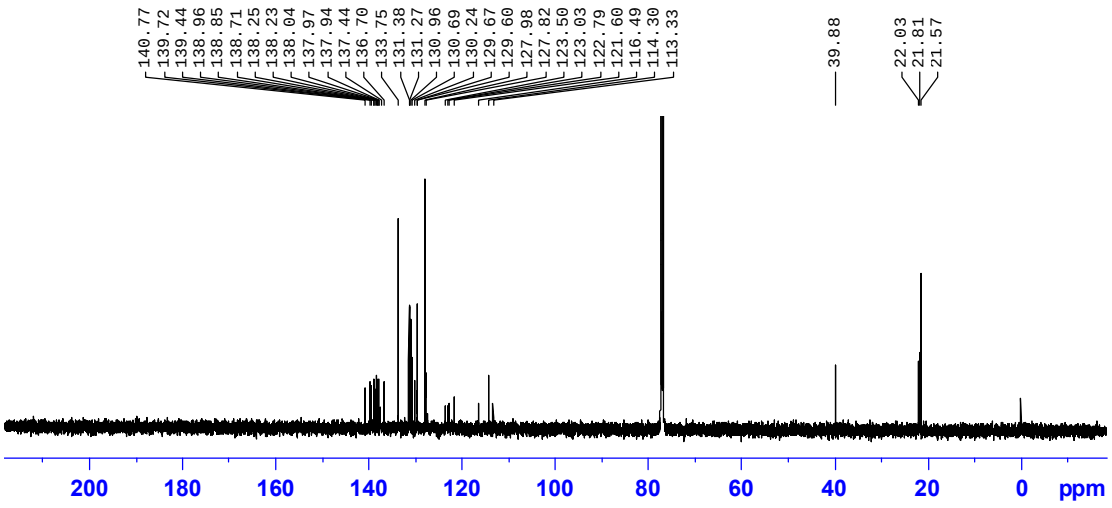

Figure S44. ^{13}C NMR spectrum of [**4b**]I, 298 K, $CDCl_3$.

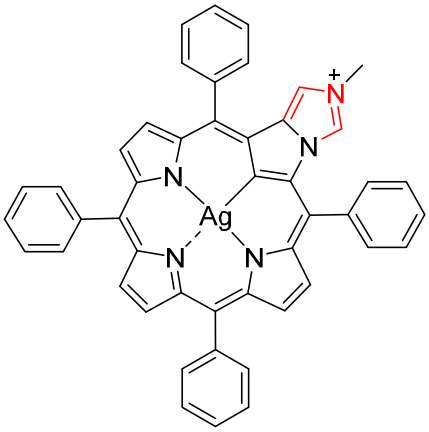

Chemical Formula: $C_{47}H_{31}AgN_5^+$
Exact Mass: 772.1625

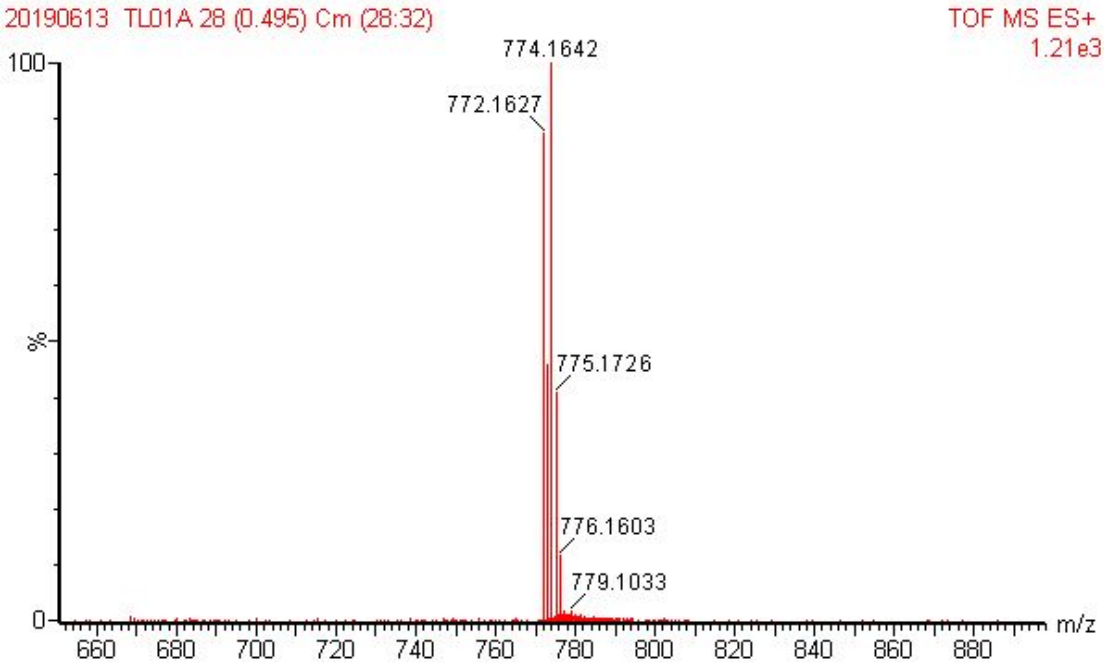

Figure S45. HRMS spectrum of [**4a**]I**.**

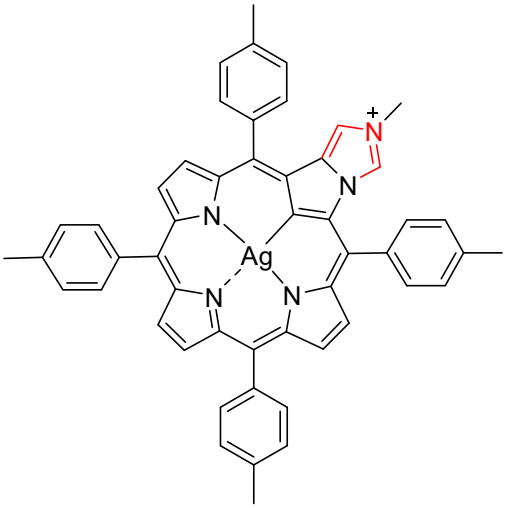

Chemical Formula: $C_{51}H_{39}AgN_5^+$
Exact Mass: 828.2251

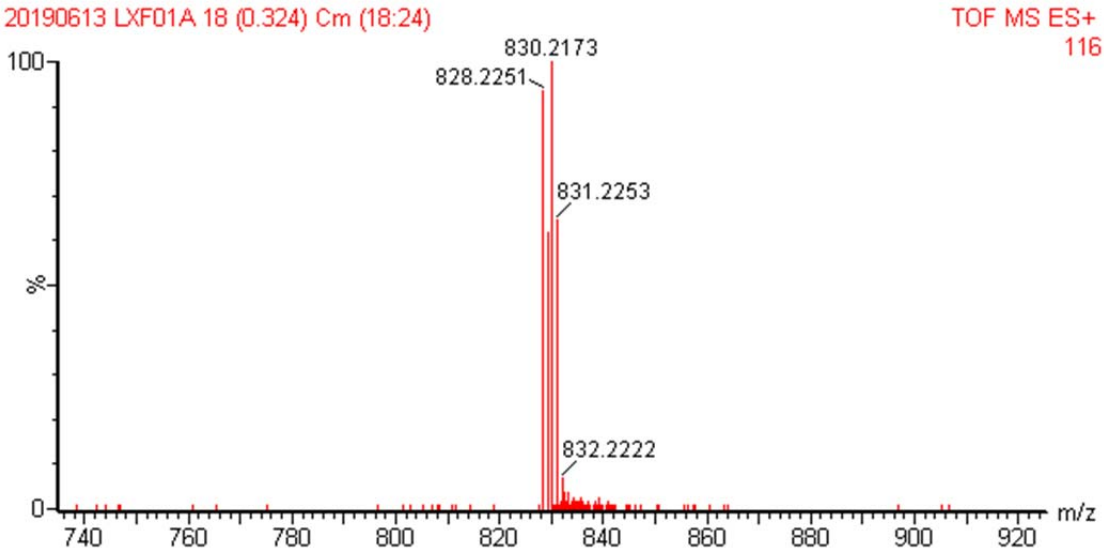

Figure S46. HRMS spectrum of [**4b**]I**.**

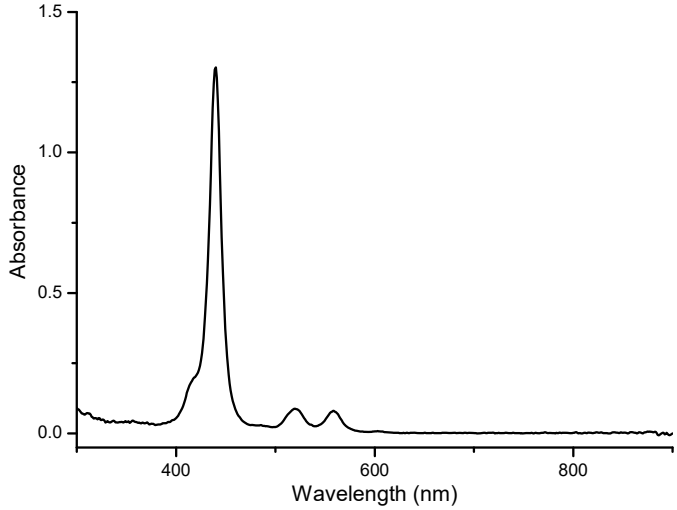

Figure S47. UV-vis spectra of [**4a**]I (CH_2Cl_2, $3.74*10^{-6}$).

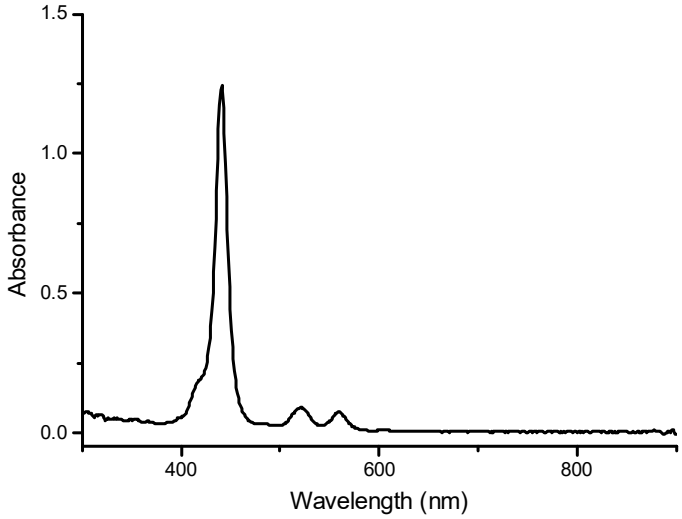

Figure S48. UV-vis spectra of [**4b**]I (CH_2Cl_2, $3.66*10^{-6}$).

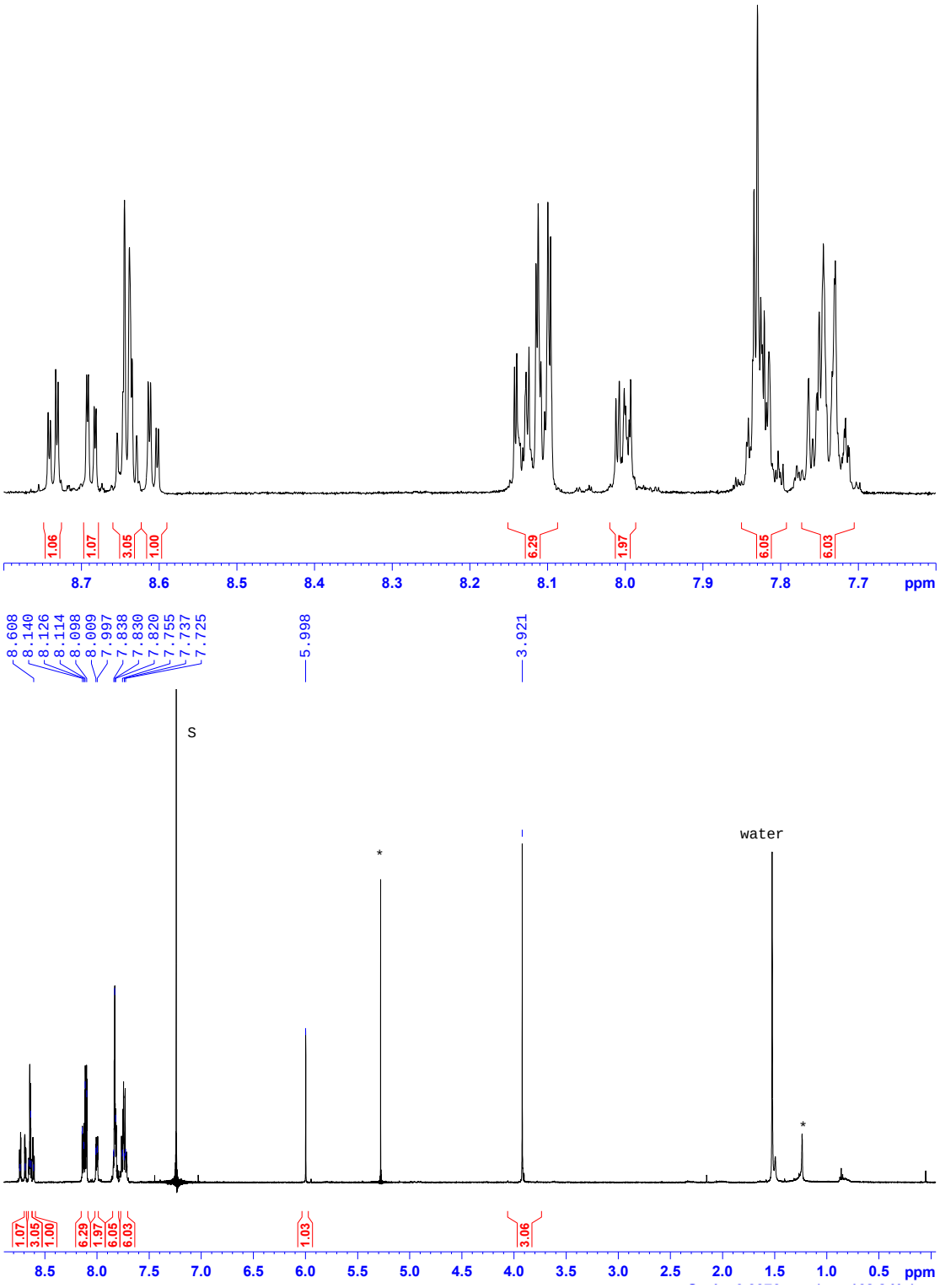

Figure S49. ^{1}H NMR spectrum of **5a**, 300 K, $CDCl_3$

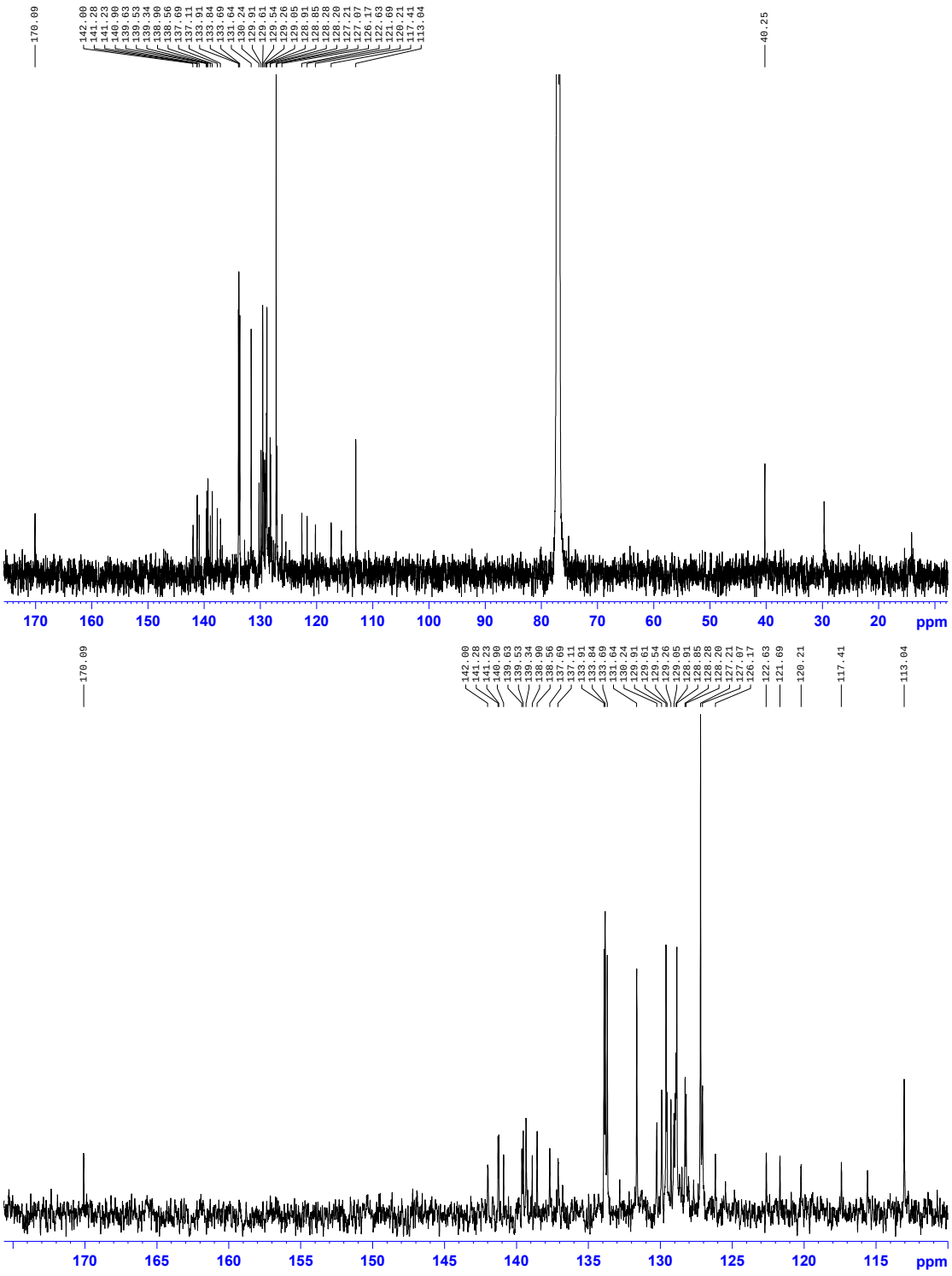

Figure S50. ^{13}C NMR spectrum of **5a**, 300 K, $CDCl_3$.

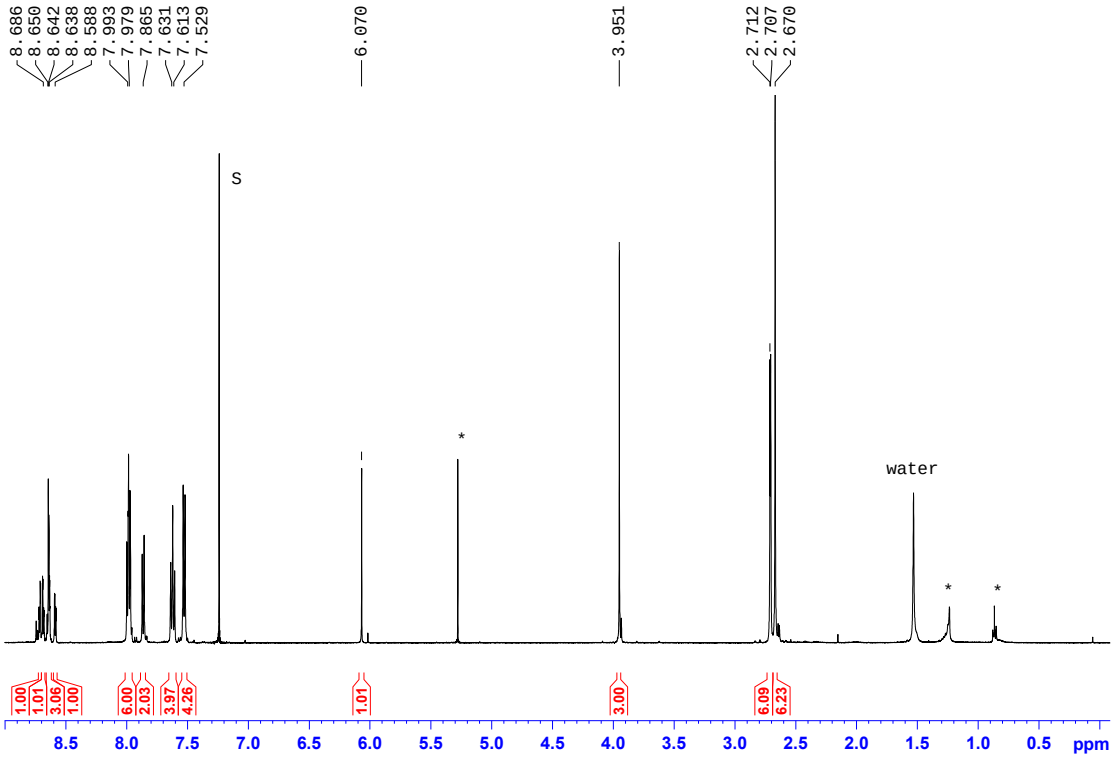

Figure S51. ^{1}H NMR spectrum of **5b**, 300 K, $CDCl_3$.

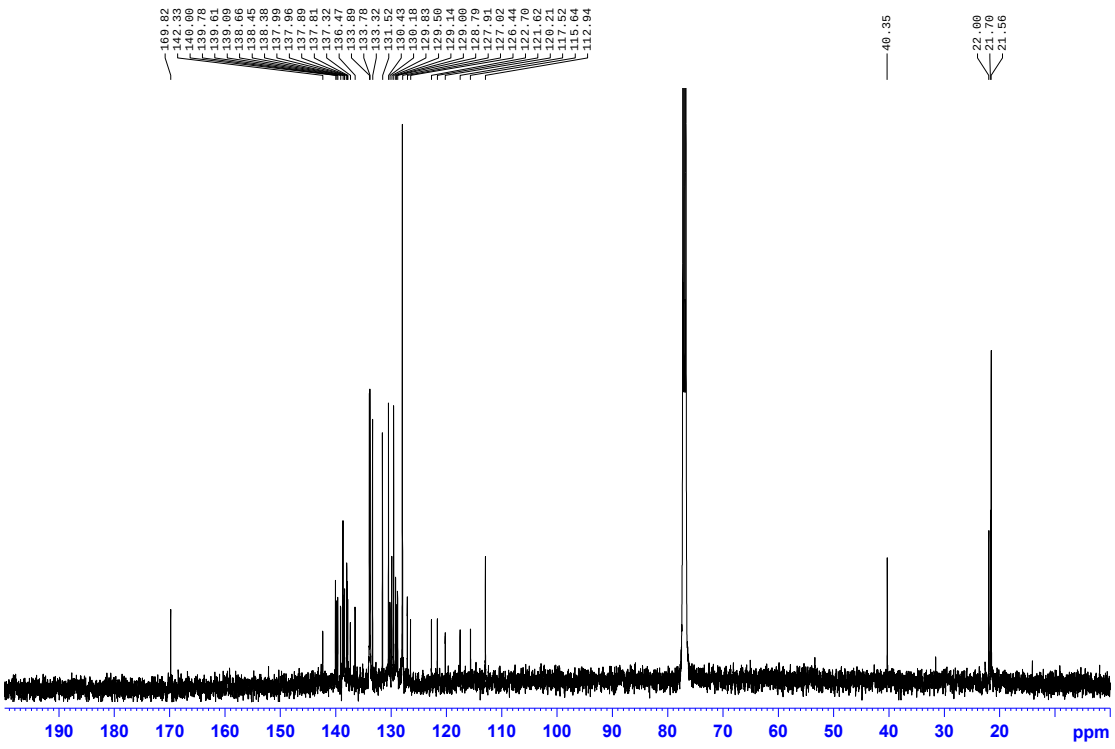

Figure S52. ^{13}C NMR spectrum of **5b**, 300 K, $CDCl_3$.

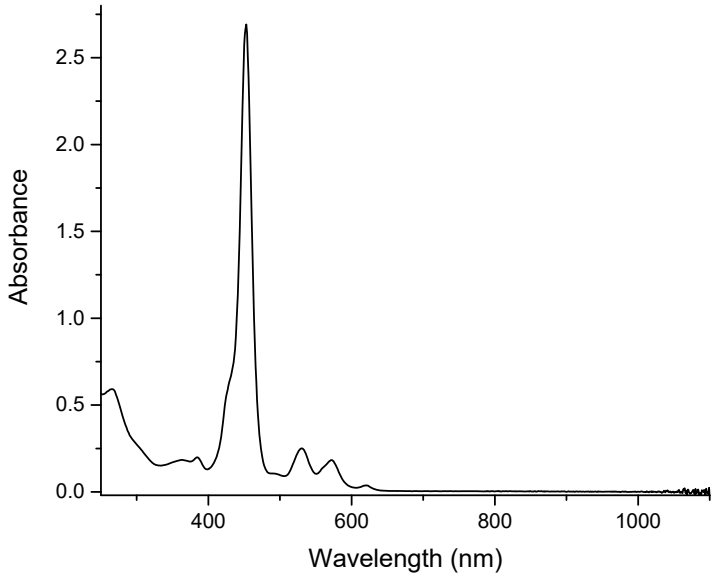

Figure S53. UV-vis spectrum of **5a** (CH_2Cl_2, 1.51*10^{-5} M, 1 cm).

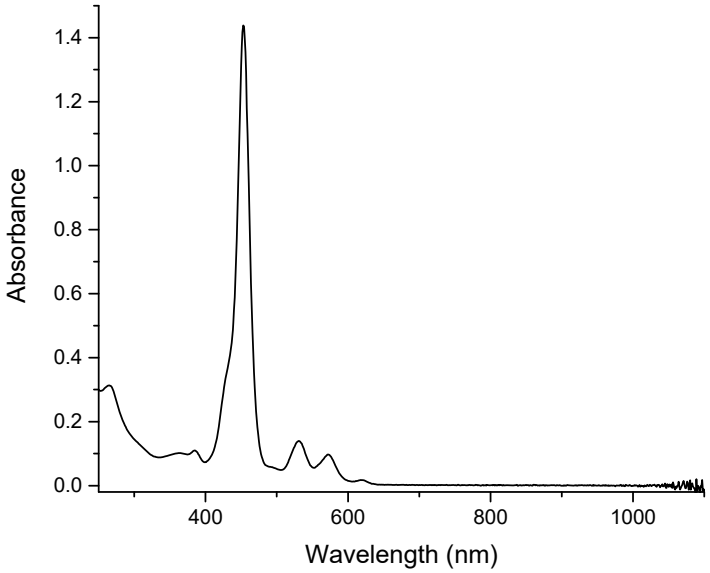

Figure S54. UV-vis spectrum of **5b** (CH_2Cl_2, 8.47*10^{-6} M, 1 cm).

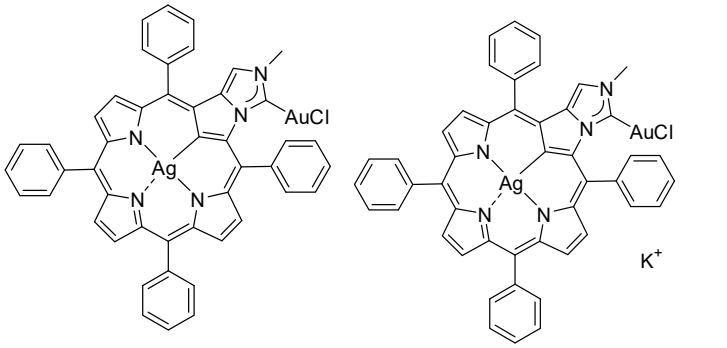

Chemical Formula: $C_{47}H_{30}AgAuClN_5$
Exact Mass: 1003.0906

Chemical Formula: $C_{47}H_{30}AgAuClKN_5^+$
Exact Mass: 1042.0538

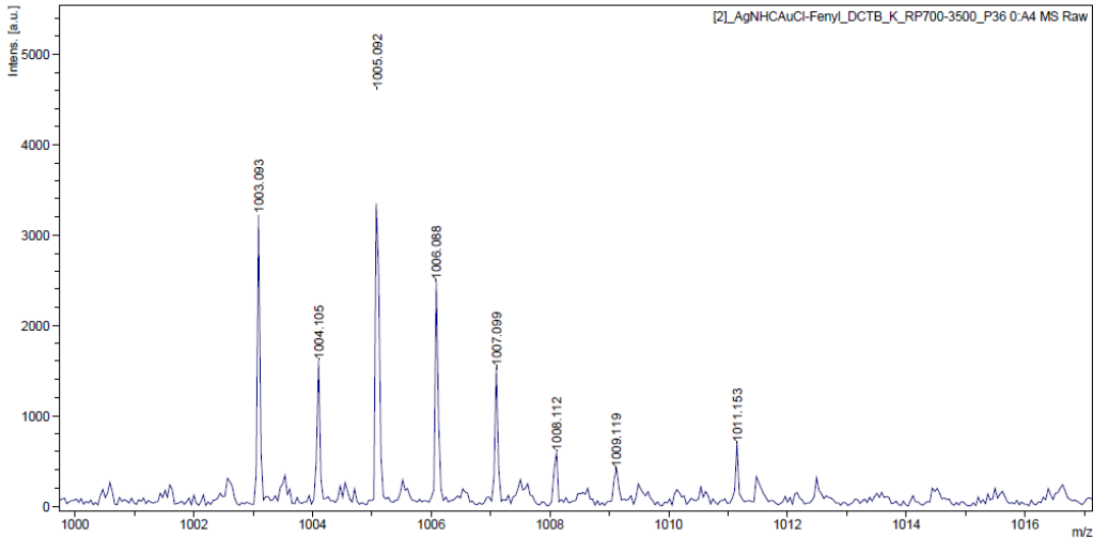

Figure S55. MALDI HRMS spectrum of **5a** (molecular ion).

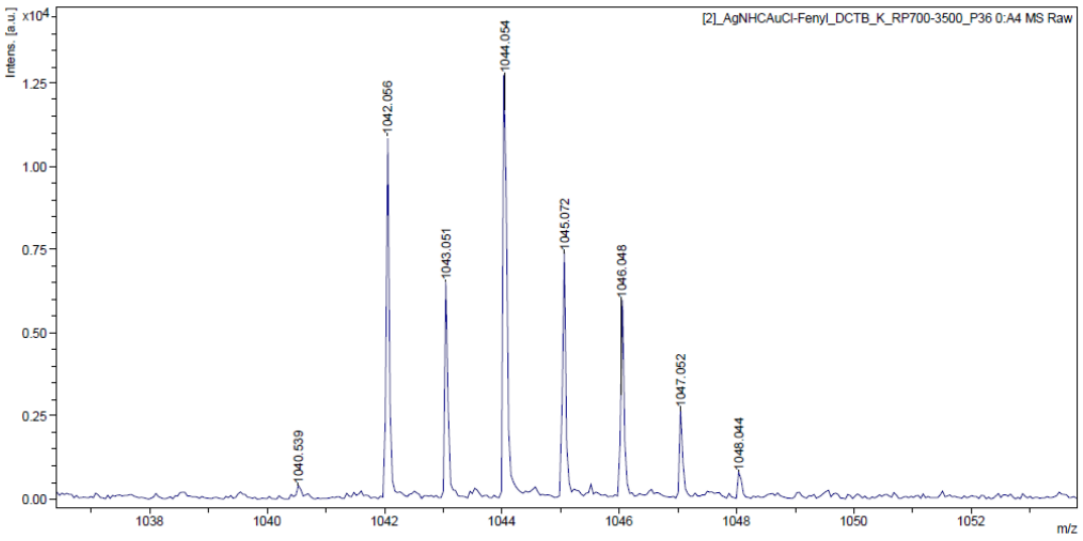

Figure S56. MALDI HRMS spectrum of **5a** ($[\mathbf{5a}+K]^+$).

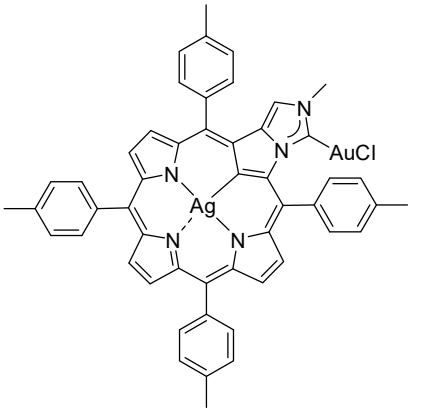

Chemical Formula: $C_{51}H_{38}AgAuClN_5$
Exact Mass: 1059.1532

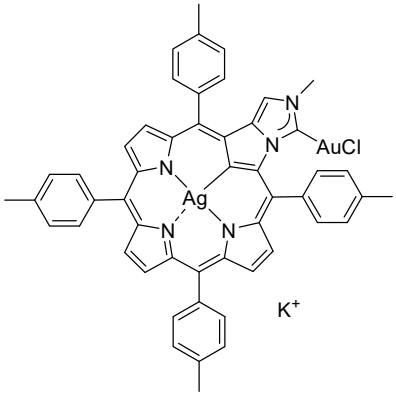

Chemical Formula: $C_{51}H_{38}AgAuClKN_5^+$
Exact Mass: 1098.1164

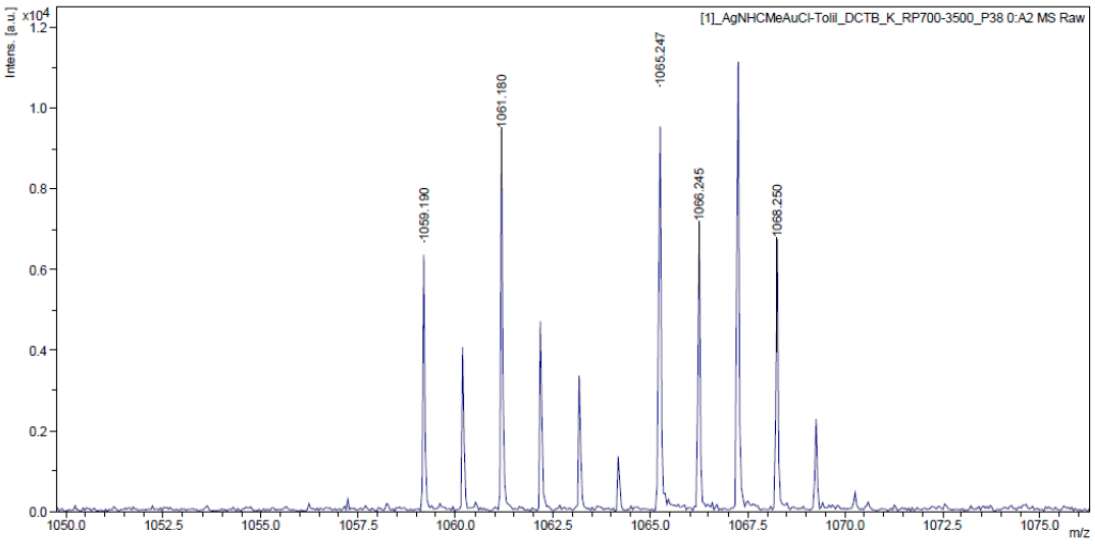

Figure S57. MALDI HRMS spectrum of **5b** (molecular ion).

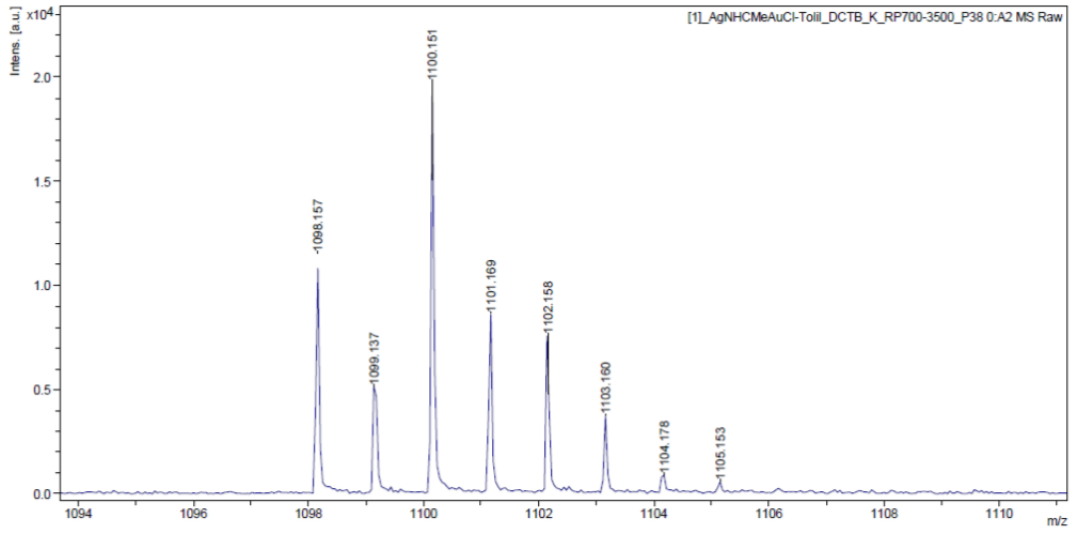

Figure S58. MALDI HRMS spectrum of **5b** ($[\mathbf{5b}+K]^+$).

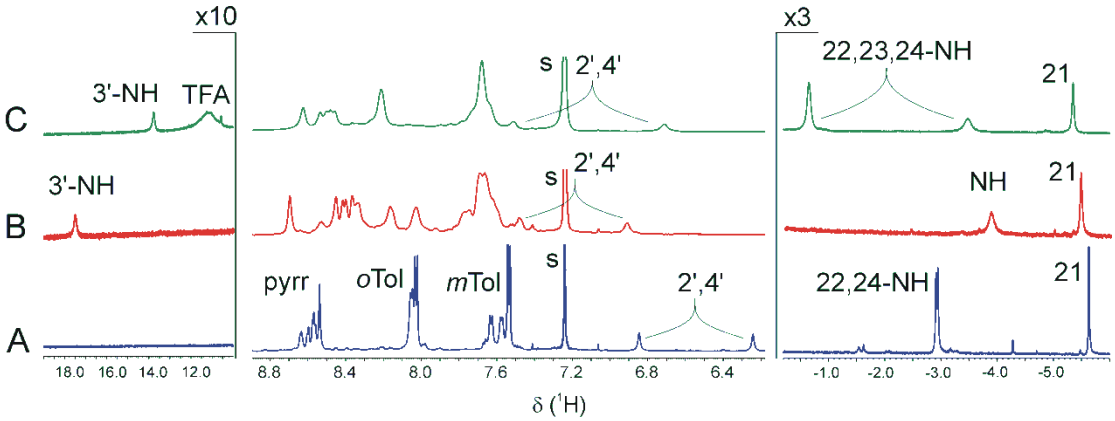

Figure S59. Protonation scheme of **2b** and selected regions of ^{1}H NMR spectra (600 MHz, $CDCl_3$, 213 K) of **2b** (A) and the same solution after addition of 1.1 equiv. (B) and 4 equiv. (C) of trifluoroacetic acid (TFA).

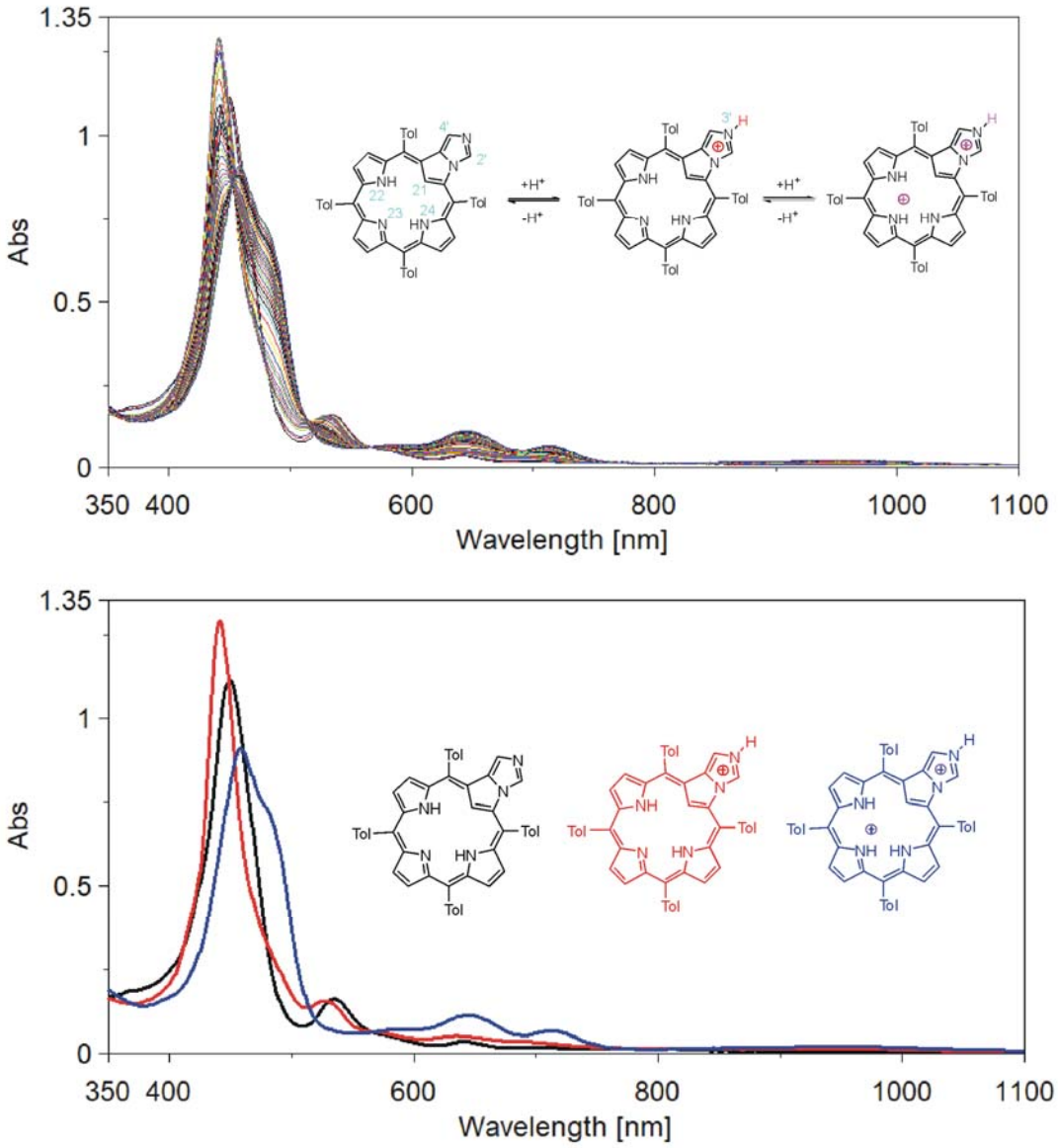

Figure S60. Top, spectrophotometric titration of **2b** with TFA ($CHCl_3$, 298 K); bottom, selected spectra recorded after addition of 0 equiv. (black trace), 1.5 equiv. (red trace), and 6 equiv. (blue) of the acid.

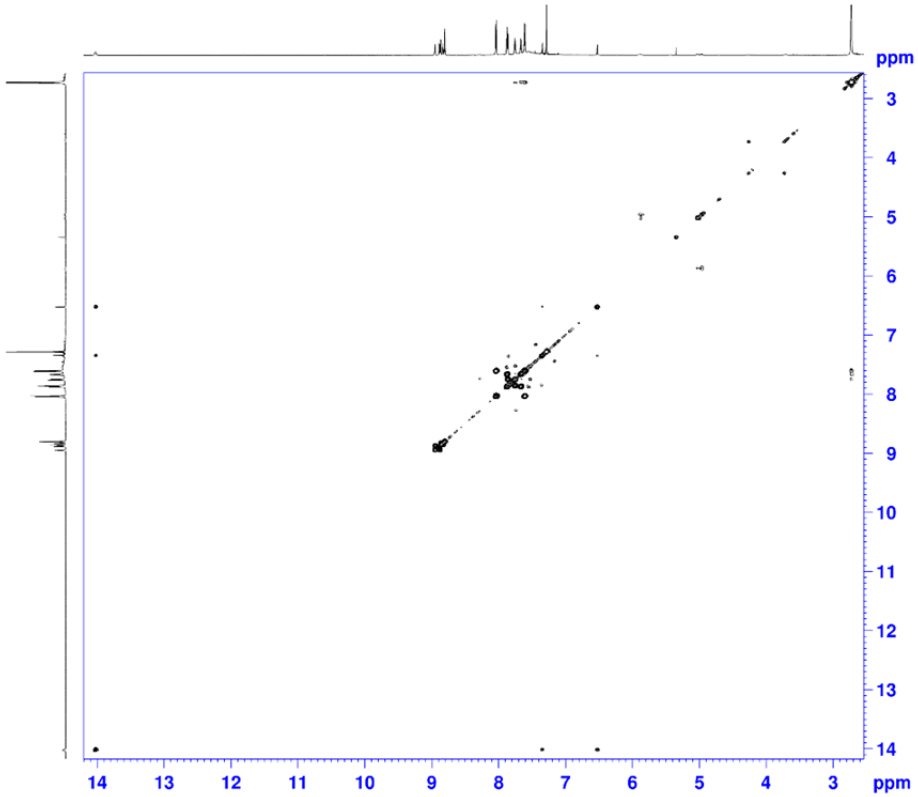

Figure S61. ^{1}H,^{1}H COSY spectrum of [**3b**H]$^{+}$ (600 MHz, 233 K, $CDCl_3$).

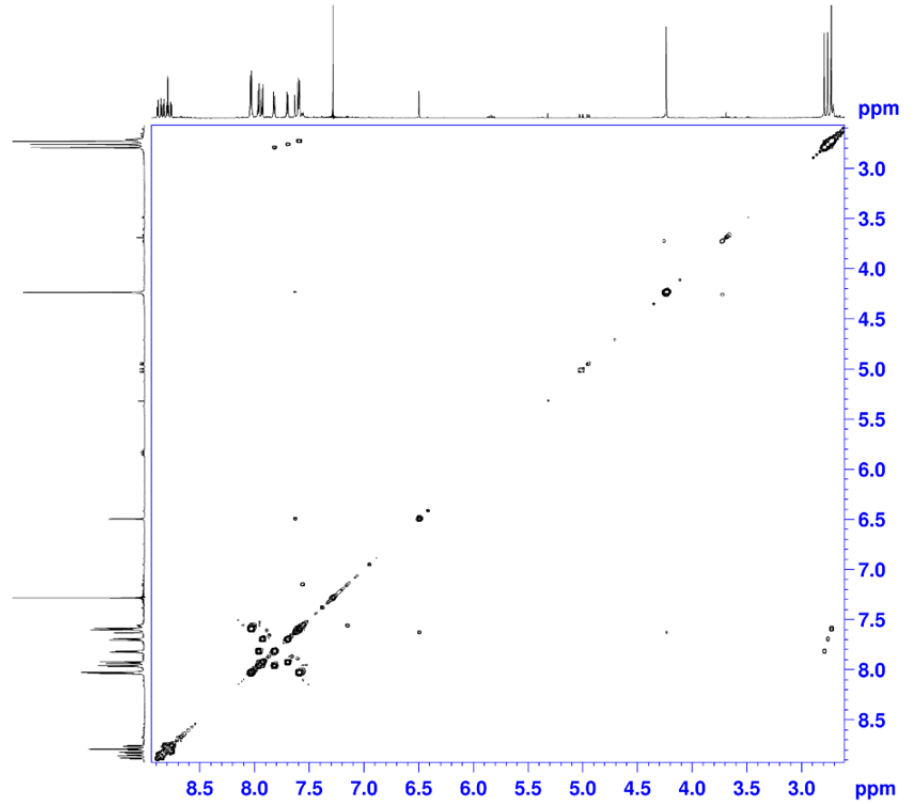

Figure S62. ^{1}H,^{1}H COSY spectrum of [**4b**]I (600 MHz, 300 K, $CDCl_3$).

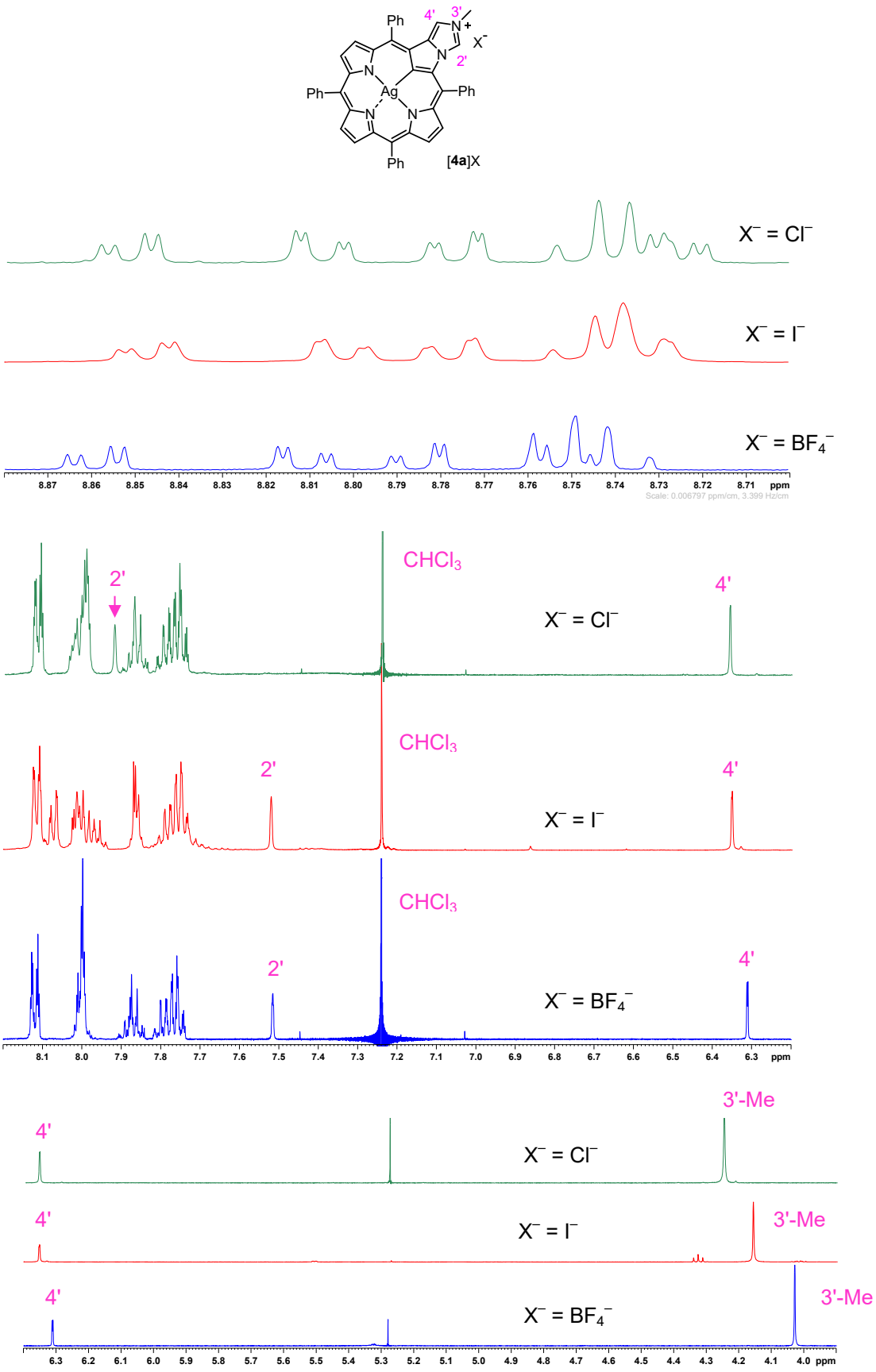

Figure S63. Selected regions of ^{1}H NMR spectra (500 MHz, 300 K, $CDCl_3$) of [**4a**]X (600 MHz, 300 K, $CDCl_3$) with specified counterions.

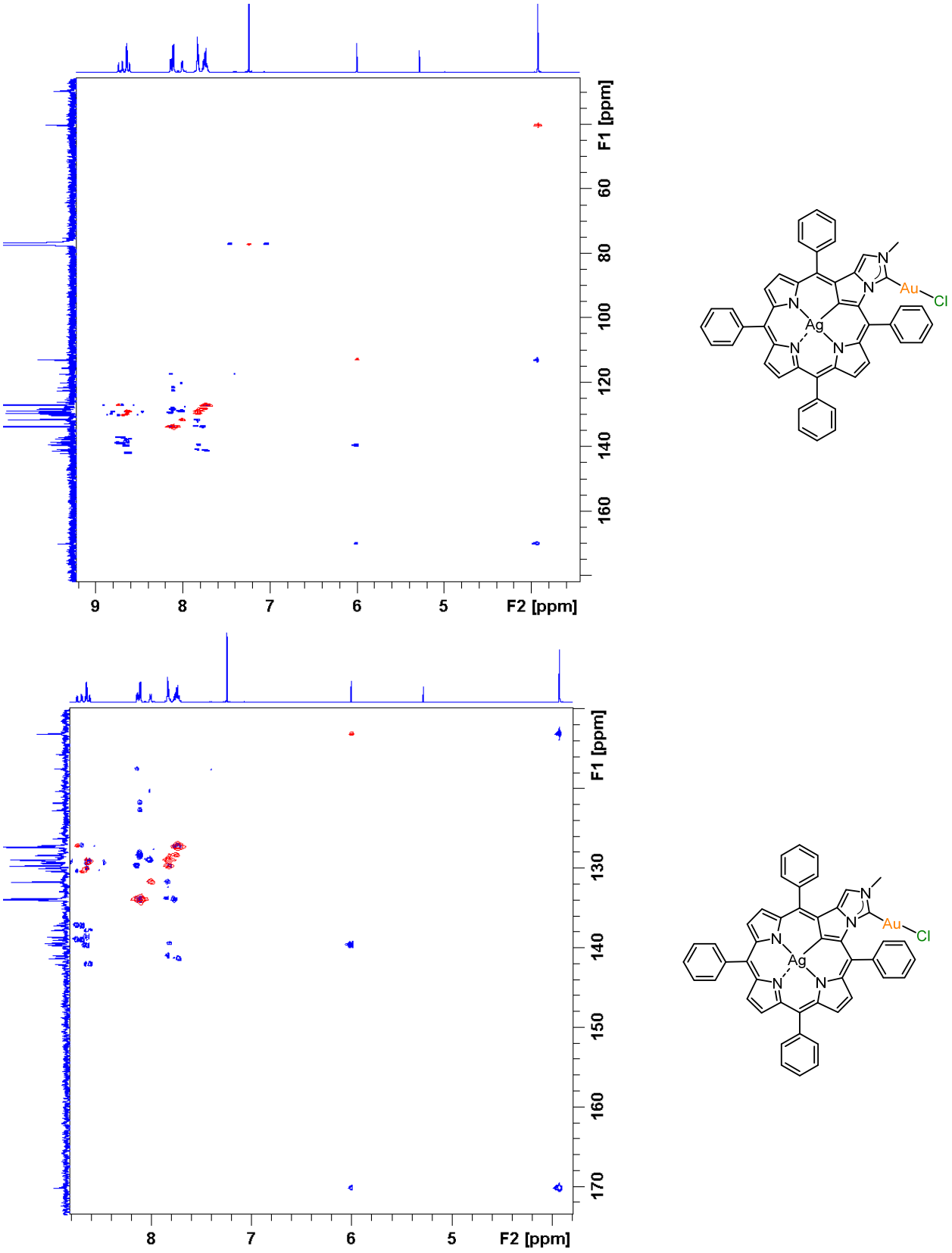

Figure S64. Superimposed ^{1}H,^{13}C HMQC (red spots) and HMBC (blue spots) spectra of **5a** ($CDCl_3$, 300 K) and their down-field region expansions.

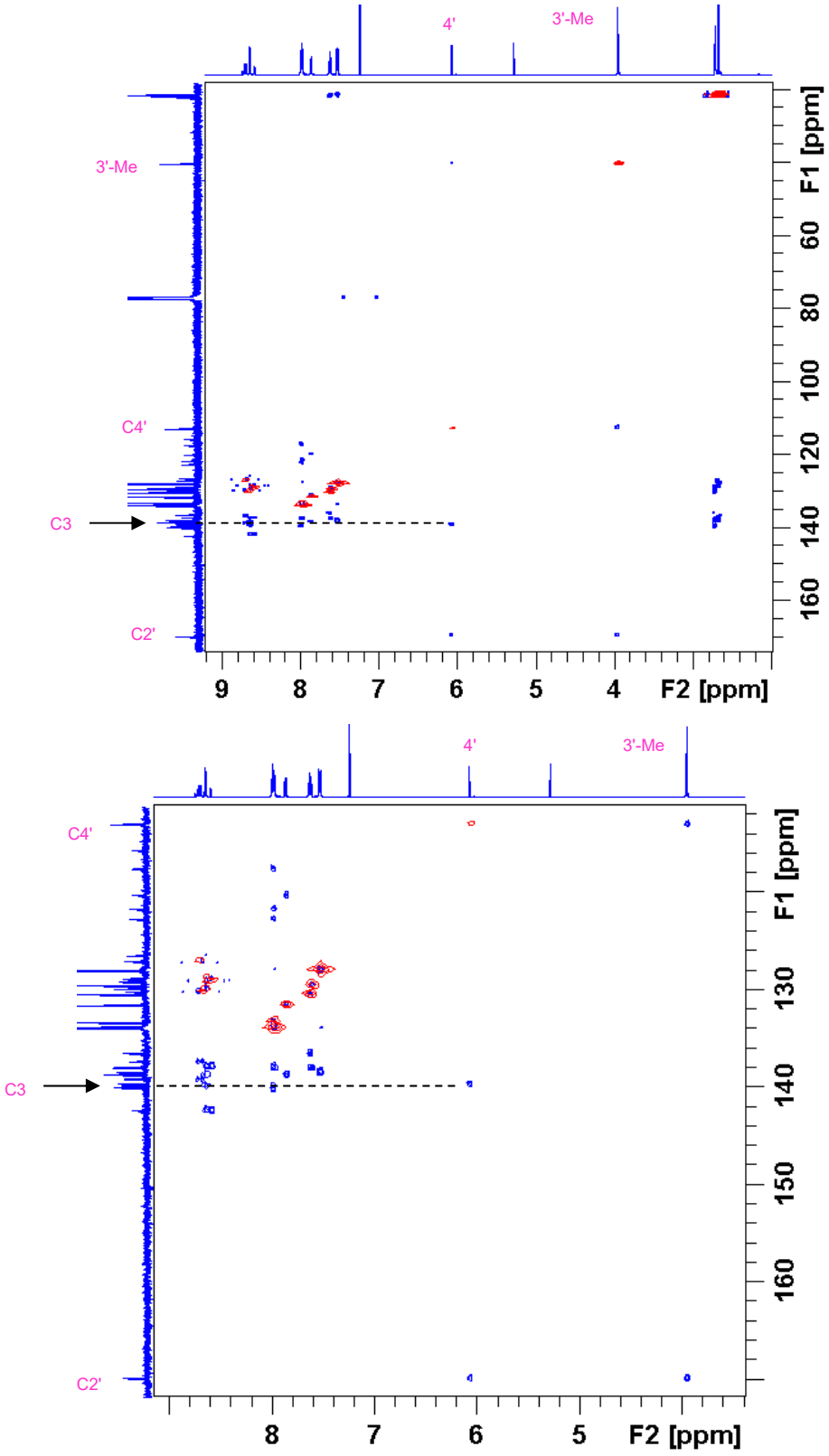

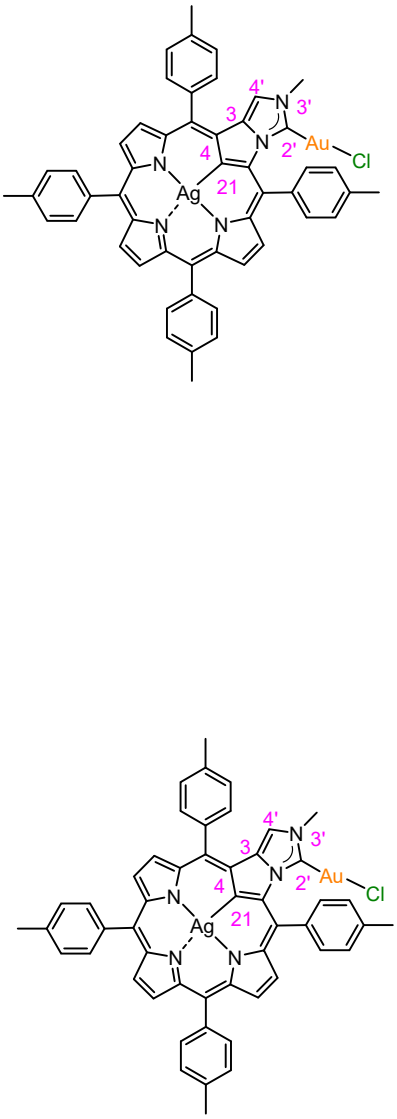

Figure S65. Superimposed $^{1}H,^{13}C$ HMQC (red spots) and HMBC (blue spots) spectra of **5b** ($CDCl_3$, 300 K) and their down-field region expansions.

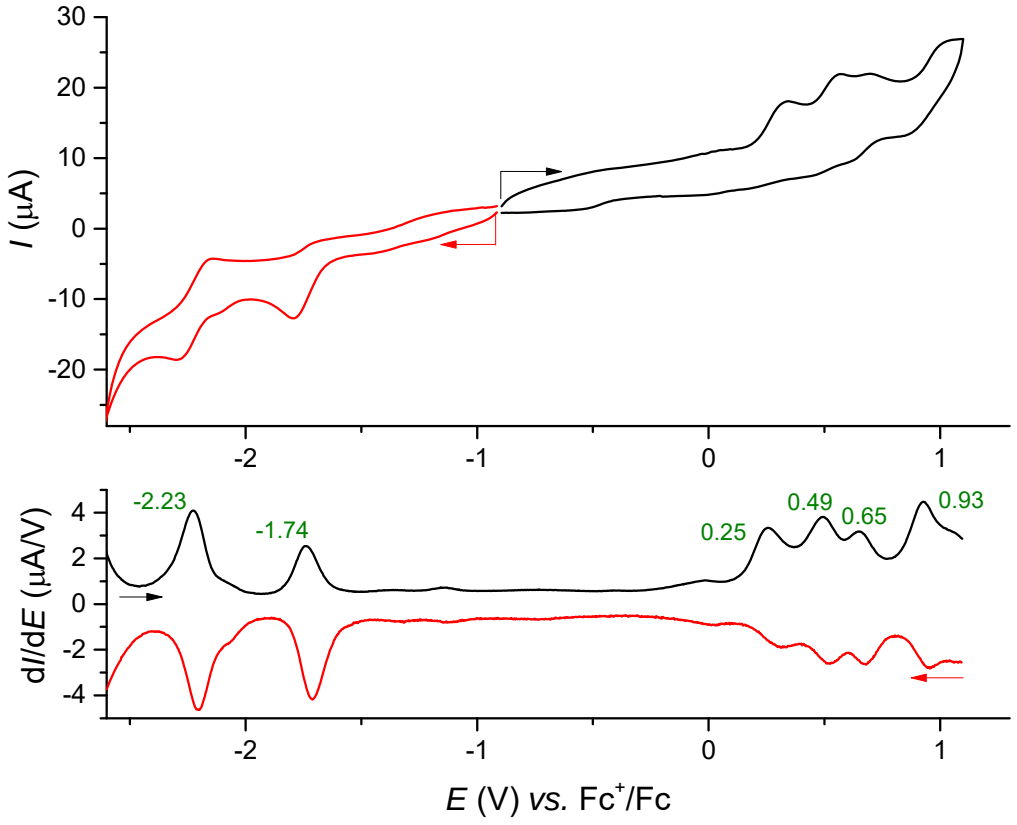

Figure S66. Cyclic voltammograms (top) and differential pulse voltammograms (bottom) for **2a** in DCM. The arrows indicate directions of the electrode potential advancements. Conditions: solvent , DCM; supporting electrolyte, tetrabutylammonium hexafluorophosphate; working electrode, glassy carbon; reference electrode, Ag/AgCl; auxiliary electrode, Pt rod.

Table S3. Electrochemical data for **2a-h**[*]

System	E_{Red1}	E_{Red2}	E_{Ox1}	E_{Ox2}	E_{Ox3}	E_{Ox4}	HLG[a]	Σσ[b]
2a	–1.74	–2.23	0.25	0.49	0.65	0.93	1.99	0
2b	–1.75	–2.25	0.23	0.43	0.55	0.91	1.98	-0.68
2c	–1.76	–2.26	0.24	0.44	0.58	0.97	2.00	-0.56
2d	–1.79	–2.30	0.20	0.40	0.70	n.d.	1.99	-1.08
2e	–1.75	–2.28	0.31	0.52	0.66	1.01	2.06	0.96
2f	–1.76	–2.30	0.30	0.45	0.68	n.d.	2.06	–0.12
2g	–1.67	–2.19	0.32	0.51	0.68	1.00	1.99	0.24
2h	–1.62	–2.13	0.38	0.59	0.77	1.03	2.00	1.8

*Peak potentials in differential pulse voltammograms in volts. [a]Electrochemical HOMO-LUMO gap, HLG = $E_{Ox1} - E_{Red1}$. [b] Sum of the Hammett constants (Hansch, C.; Taft, R. W. A Survey of Hammett Substituent Constants and Resonance and Field Parameters *Chem. Rev.* **1991,** *91*, 165-195.) of the substituents present at the *meso*-aryls.

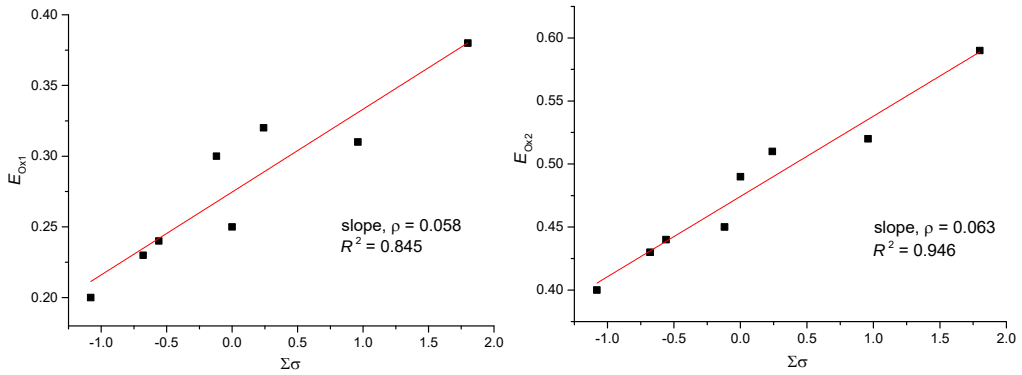

Figure S67. Dependencies of E_{Ox1} (top, left), E_{Ox2} (top, right), and E_{Red1} (bottom) for **2a-h** on the sum of the Hammett constants of the substituents present at the *meso*-aryls.

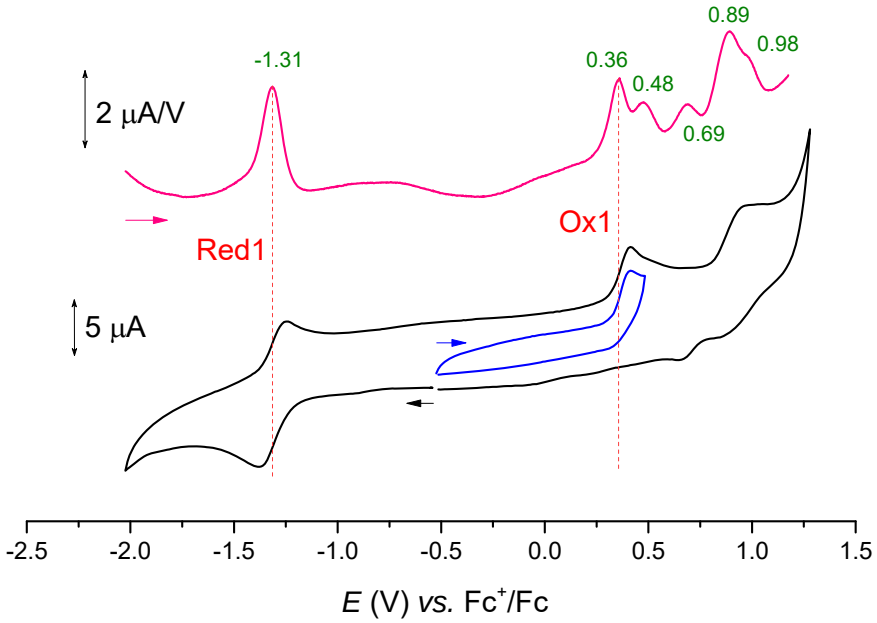

Figure S68. Cyclic voltammograms (bottom) and differential pulse voltammograms (top) for **3a** in DCM. The arrows indicate directions of the electrode potential advancements. The green numbers associated with peaks of the differential pulse voltammogram are electrode potentials in volts. Conditions: solvent, DCM; supporting electrolyte, tetrabutylammonium hexafluorophosphate; working electrode, glassy carbon; pseudoreference electrode, Ag/AgCl; auxiliary electrode, Pt rod.

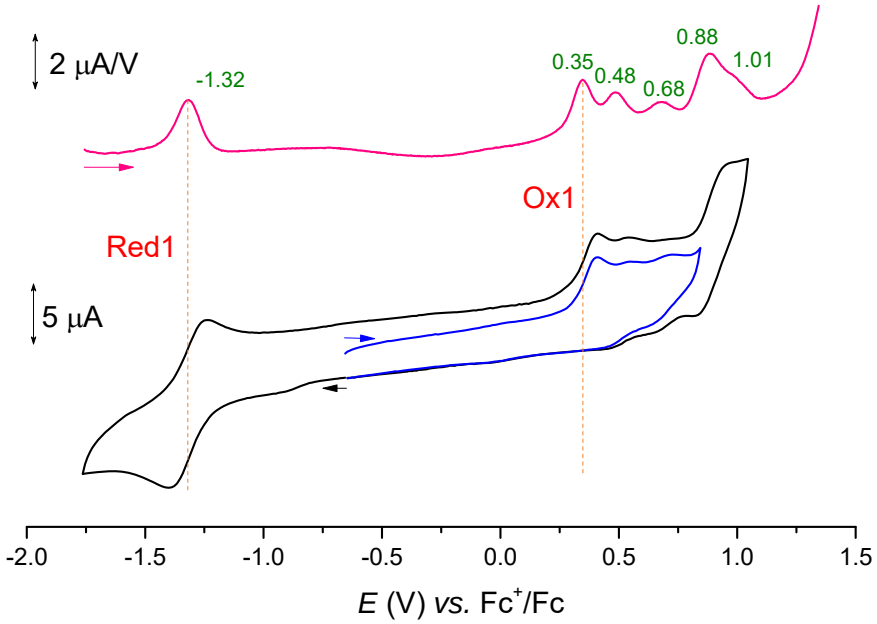

Figure S69. Cyclic voltammograms (bottom) and differential pulse voltammogram (top) for **3b** in DCM. The green numbers associated with peaks of the differential pulse voltammogram are electrode potentials in volts. The arrows indicate directions of the electrode potential advancements. Conditions: solvent, DCM; supporting electrolyte, tetrabutylammonium hexafluorophosphate; working electrode, glassy carbon; pseudoreference electrode, Ag/AgCl; auxiliary electrode, Pt rod.

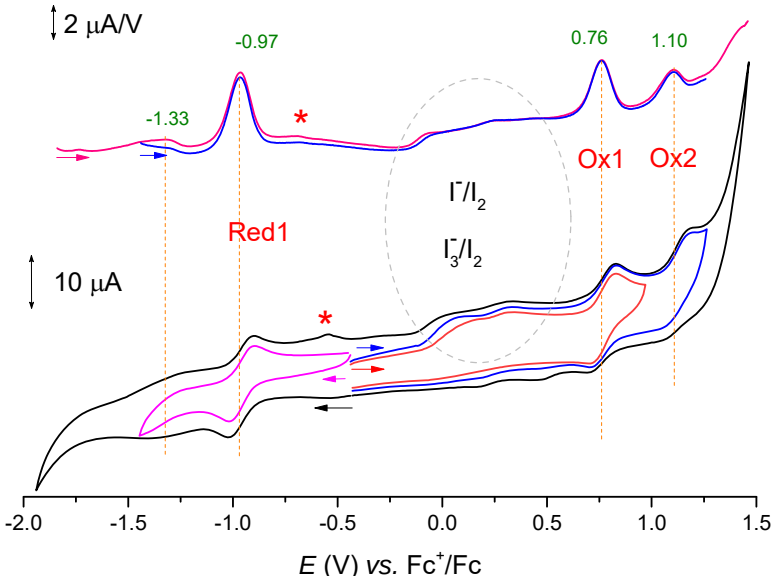

Figure S70. Cyclic voltammograms (bottom) and differential pulse voltammograms (top) for [**4a**]I in DCM. The arrows indicate directions of the electrode potential advancements. The green numbers associated with peaks of the differential pulse voltammogram are electrode potentials in volts. The red asterisks denote re-oxidation of the products of the irreversible second reduction at –1.33 V. The irreversible oxidation of iodide counteranion is marked with dashed ellipsis. Conditions: solvent, DCM; supporting electrolyte, tetrabutylammonium hexafluorophosphate; working electrode, glassy carbon; pseudoreference electrode, Ag/AgCl; auxiliary electrode, Pt rod.

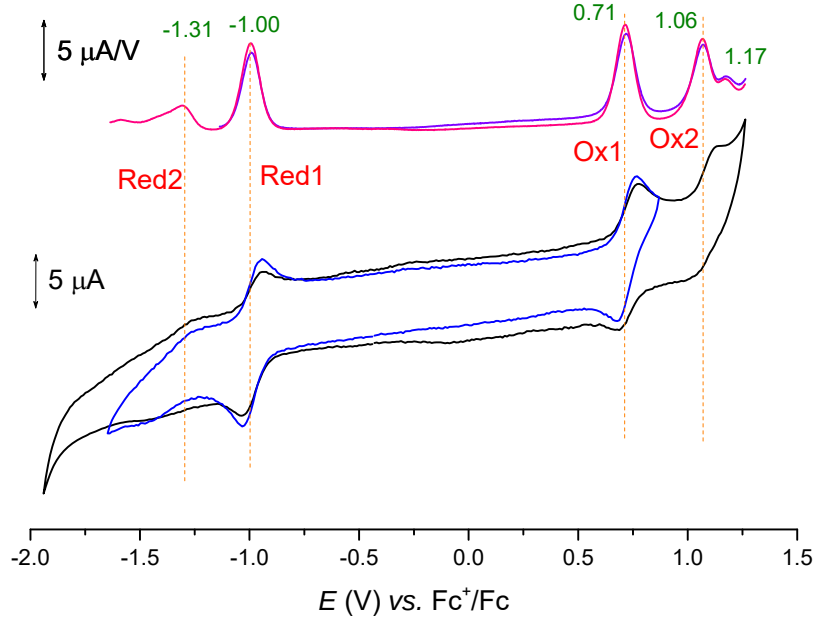

Figure S71. Cyclic voltammograms (bottom) and differential pulse voltammograms (top) for [**4a**]BF_4 in DCM. The green numbers associated with peaks of the differential pulse voltammogram are electrode potentials in volts. Conditions: solvent, DCM; supporting electrolyte, tetrabutylammonium hexafluorophosphate; working electrode, glassy carbon; pseudoreference electrode, Ag/AgCl; auxiliary electrode, Pt rod.

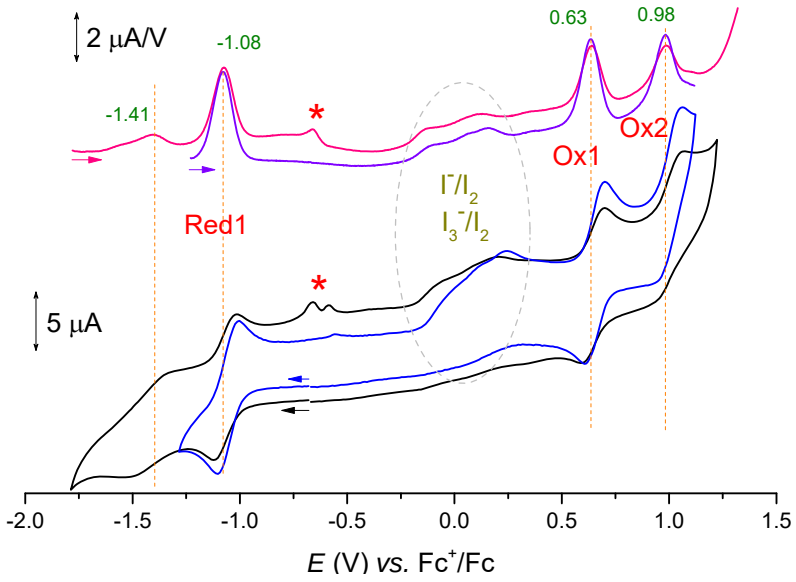

Figure S72. Cyclic voltammograms (bottom) and differential pulse voltammograms (top) for [**4b**]I in DCM. The arrows indicate directions of the electrode potential advancements. The green numbers associated with peaks of the differential pulse voltammogram are electrode potentials in volts. The red asterisks denote re-oxidation of the products of the irreversible second reduction at –1.41 V. The irreversible oxidation of iodide counteranion is marked with dashed ellipsis. Conditions: solvent, DCM; supporting electrolyte, tetrabutylammonium hexafluorophosphate; working electrode, glassy carbon; pseudoreference electrode, Ag/AgCl; auxiliary electrode, Pt rod.

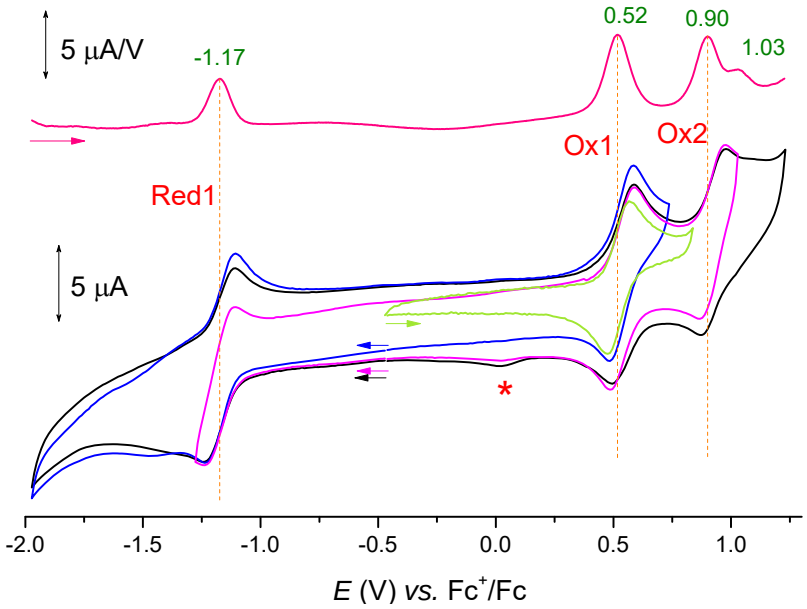

Figure S73. Cyclic voltammograms (bottom) and differential pulse voltammogram (top) for **5a** in DCM. The arrows indicate directions of the electrode potential advancements. The green numbers associated with peaks of the differential pulse voltammogram are electrode potentials in volts. The red asterisks denote re-reduction of the products of the irreversible third oxidation at 1.03 V. Conditions: solvent, DCM; supporting electrolyte, tetrabutylammonium hexafluorophosphate; working electrode, glassy carbon; pseudoreference electrode, Ag/AgCl; auxiliary electrode, Pt rod.

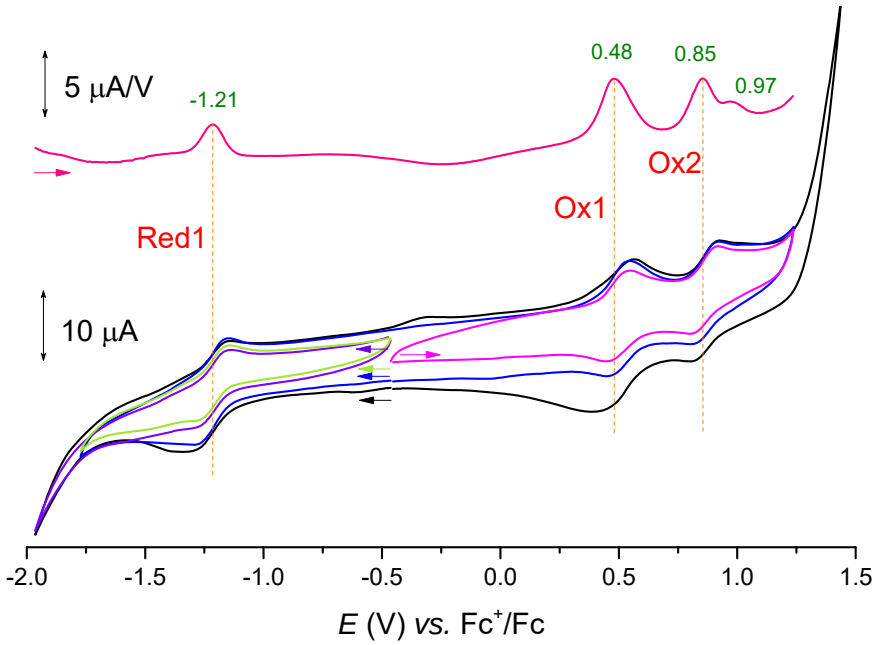

Figure S74. Cyclic voltammograms (bottom) and differential pulse voltammogram (top) for **5b** in DCM. The arrows indicate directions of the electrode potential advancements. The green numbers associated with peaks of the differential pulse voltammogram are electrode potentials in volts. Conditions: solvent, DCM; supporting electrolyte, tetrabutylammonium hexafluorophosphate; working electrode, glassy carbon; pseudoreference electrode, Ag/AgCl; auxiliary electrode, Pt rod.

Table S4. Electrochemical data[*] for silver(III) complexes **3**, **4**, and **5**.

System	E_{Red1}	E_{Red2}	E_{Ox1}	E_{Ox2}	E_{Ox3}	E_{Ox4}	HLG[a]
3a	–1.31	–	0.31[b]	0.48[b]	0.69[b]	0.89[b],0.95[b]	1.67
3b	–1.32	–	0.35[b]	0.48[b]	0.68[b]	0.88[b],1.01[b]	1.67
[**4a**]I[c]	–0.97	–1.33[b]	0.76	1.10	–	–	1.73
[**4a**]BF_4	–1.00	–1.31[b]	0.71	1.06	1.17[b]	–	1.71
[**4b**]I[c]	–1.08	–1.41[b]	0.63	0.98	–	–	1.71
5a	–1.17	–	0.52	0.90	1.03[b]	–	1.69
5b	–1.21	–	0.48	0.85	0.97[b]	–	1.69

*Peak potentials in differential pulse voltammograms in volts. [a] Electrochemical HOMO-LUMO gap, HLG = $E_{Ox1} - E_{Red1}$. [b] Irreversible. [c] Irreversible processes observed at about -0.15 and 0.15 V are related with I^- counteranion oxidation.

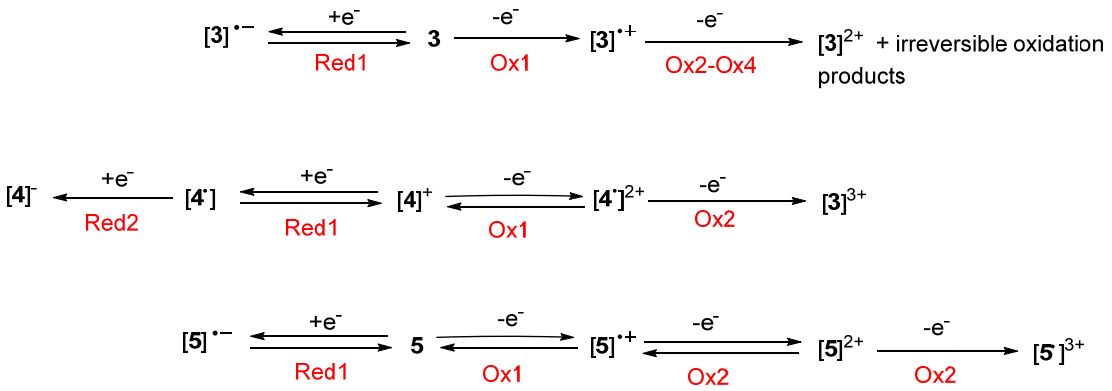

Figure S75 Schematic representations of the electrode reactions for the silver(III) complexes of imidazole-fused carbachlorins **3**, [**4**]$^+$, and **5**.

References

1. Rigaku Oxford Diffraction (2015). CrysAlis PRO. Rigaku Oxford Diffraction, Wrocław, Poland.
2. G. M. Sheldrick, Acta Cryst. 2015, **A71**, 3.
3. G. M. Sheldrick, Acta Cryst. 2015, **C71**, 3.
4. G. R. Geier, III, D. M. Haynes, and J. S. Lindsey, *Org. Lett.*, 1999**, 1**, 1455.